

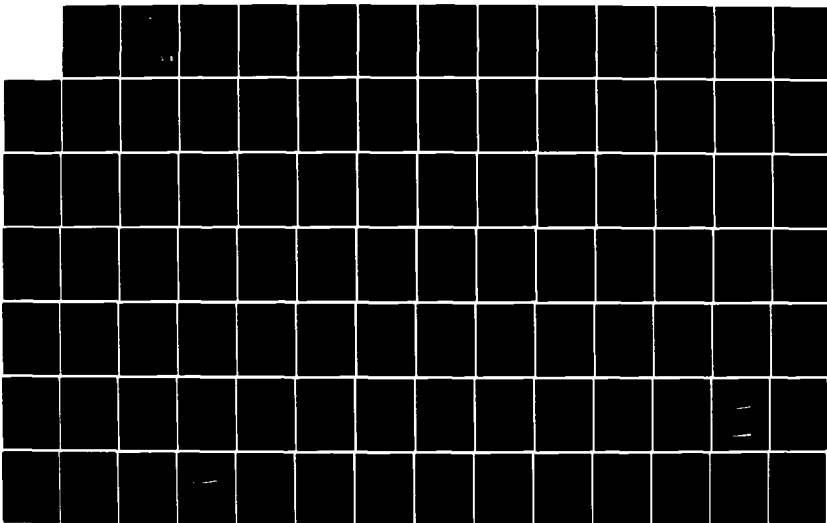
AD-A151 784

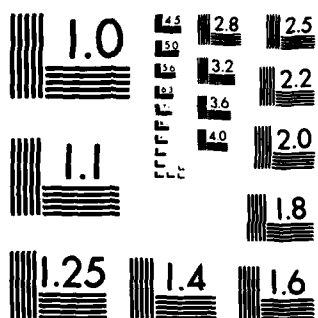
MODEL REDUCTION TECHNIQUES APPLIED TO THE CONTROL OF
LARGE SPACE STRUCTURES(U) AIR FORCE INST OF TECH
WRIGHT-PATTERSON AFB OH SCHOOL OF ENGI... D W VARHOLA
DEC 84 AFIT/GA/AA/84D-11 F/G 14/2

1/2

UNCLASSIFIED

NL





MICROCOPY RESOLUTION TEST CHART
NATIONAL BUREAU OF STANDARDS 1963-A

AD-A151 784

REPRODUCED AT GOVERNMENT EXPENSE

①



MODEL REDUCTION TECHNIQUES APPLIED TO
THE CONTROL OF LARGE SPACE STRUCTURES

THESIS

Dennis W. Varhola
Second Lieutenant, USAF

AETT/GA/AA/84D-11

This document has been approved
for public release and sale; its
distribution is unlimited.

DEPARTMENT OF THE AIR FORCE
AIR UNIVERSITY

AIR FORCE

INSTITUTE OF TECHNOLOGY

Patterson Air Force Base, Ohio

8 03 13 074

DTIC FILE COPY

DTIC
ELECTE
MAR 28 1985
S D E

AFIT/GA/AA/84D-11

MODEL REDUCTION TECHNIQUES APPLIED TO
THE CONTROL OF LARGE SPACE STRUCTURES

THESIS

Dennis W. Varhola
Second Lieutenant, USAF

AFIT/GA/AA/84D-11

DTIC
SELECTED
MAR 28 1965
S E

Approved for public release; distribution unlimited

MODEL REDUCTION TECHNIQUES APPLIED TO
THE CONTROL OF LARGE SPACE STRUCTURES

THESIS

Presented to the Faculty of the School of Engineering
of the Air Force Institute of Technology
Air University
In Partial Fulfillment of the
Requirements for the Degree of
Master of Science in Astronautical Engineering

Dennis W. Varhola, B.S.M.E.
Second Lieutenant, USAF

December 1984



Accession For	
NTIS GRA&I	<input checked="" type="checkbox"/>
DTIC TAB	<input checked="" type="checkbox"/>
Unannounced	<input type="checkbox"/>
Justification	
By	
Distribution/	
Availability Codes	
Dist	Avail and/or Special
A-1	

Approved for public release; distribution unlimited

Acknowledgements

Many thanks are due to those who directly or indirectly helped in this thesis effort. To my thesis adviser Dr. Robert Calico, thank you for your patient guidance and trusting support. To my fellow students, thanks for the humor and commiseration that helped me make it through each day. Thanks to my wife Alice for her help with the typing and unwavering willingness to be there through the bad times. Finally, thanks to my son Jonathan; he's my biggest motivation for being here at all.

Dennis W. Varhola

Table of Contents

	Page
Acknowledgements	ii
List of Figures	iv
Abstract	vi
I. Introduction	1
Model Reduction Problem	2
Levels of Reduction	4
Description of Models Used	5
II. Equations of Motion	9
III. Model Reduction Methods	12
Frequency Truncation	12
Modal Cost Analysis	13
Internal Balancing	19
IV. Control Algorithm	31
State Space Formulation	31
Transformation Technique	37
V. Computer Implementation	43
VI. Investigation and Results	45
VII. Conclusions	85
VIII. Recommendations	86
Bibliography	87
Appendix A: CSDL I and II Data	89
Appendix B: Source Code Listing	99
Vita	116

List of Figures

Figure	Page
1. Model Reduction Process	4
2. CSDL I Model	7
3. CSDL II Model	8
4. Uncontrolled CSDL I response; Typical controlled response	51
5. Internal Balancing Rankings, σ_{BC} & σ_{BH} , CSDL I, 6/6 act/sen	52
6. Modal Cost Rankings, CSDL I, 6/6 act/sen	53
7. Typical CSDL I Eigenvalue Plot	54
8. Frequency Truncation, CSDL I, 6/6 act/sen 2 controlled - 4 suppressed modes	55
9. Time Response - Frequency Truncation, CSDL I 2 controlled - 4 suppressed modes, 6/6 act/sen	56
10. Extended scale time response for case 1	57
11. Internal Balancing, CSDL I, 6/6 act/sen 2 controlled - 4 suppressed modes	58
12. Time Response - Internal Balancing, CSDL I 2 controlled - 4 suppressed modes, 6/6 act/sen	59
13. Extended scale time response for case 2	60
14. Frequency Truncation, CSDL I, 6/6 act/sen 4 controlled - 4 suppressed modes	61
15. Time Response - Frequency Truncation, CSDL I 4 controlled - 4 suppressed modes, 6/6 act/sen	62
16. Internal Balancing, CSDL I, 6/6 act/sen 4 controlled - 4 suppressed modes, 6/6 act/sen	63
17. Time Response - Internal Balancing, CSDL I 4 controlled - 4 suppressed modes; 6/6 act/sen	64

Figure	Page
18. Frequency Truncation, CSDL I, 6/6 act/sen 5 controlled - 3 suppressed modes	65
19. Time Response - Frequency Truncation, CSDL I 5 controlled - 3 suppressed modes; 6/6 act/sen . . .	66
20. Internal Balancing, CSDL I, 6/6 act/sen 5 controlled - 3 suppressed modes	67
21. Time Response - Internal Balancing, CSDL I 5 controlled - 3 suppressed modes; 6/6 act/sen . . .	68
22. Internal Balancing Rankings, σ_{BC} & σ_{BH} CSDL I, 3/6 act/sen	69
23. Modal Cost Rankings, CSDL I, 3/6 act/sen	70
24. Frequency Truncation, CSDL I, 3/6 act/sen 4 controlled - 2 suppressed modes	71
25. Time Response - Frequency Truncation, CSDL I 4 controlled - 2 suppressed modes; 3/6 act/sen . . .	72
26. Extended scale time response for case 7	73
27. Internal Balancing, CSDL I, 3/6 act/sen 4 controlled - 2 suppressed modes	74
28. Time Response - Internal Balancing, CSDL I 4 controlled - 2 suppressed modes; 3/6 act/sen . . .	75
29. Frequency Truncation, CSDL I, 3/6 act/sen 4 controlled - 4 suppressed modes	76
30. Time Response - Frequency Truncation, CSDL I 4 controlled - 4 suppressed modes; 3/6 act/sen . . .	77
31. Extended scale time response for case 9	78
32. Internal Balancing, CSDL I, 3/6 act/sen 4 controlled - 4 suppressed modes	79
33. Time Response - Internal Balancing, CSDL I 4 controlled - 4 suppressed modes; 3/6 act/sen . . .	80
34. Internal Balancing Rankings, σ_{BC} , CSDL II 21/21 act/sen	81
35. Internal Balancing Rankings, σ_{BH} , CSDL II, 21/21 act/sen	82
36. Modal Cost Rankings, CSDL II, 21/21 act/sen	83

Abstract

Three model reduction techniques are examined for their applicability to large lightly damped systems. Frequency truncation, modal cost analysis, and approximate internal balancing methods are applied to the CSDL I and II models. Two actuator/sensor configurations are investigated on the CSDL I. Control of the CSDL I model is implemented through the use of steady state optimal regulator theory, and the effect of various reduced order control models on the structure's time response is detailed. Modal cost analysis and internal balancing yield essentially equivalent results for the cases chosen, although the internal balancing technique provides more information concerning actuator/sensor effectiveness. These methods provide more effective reduced order models for higher order systems than simple frequency truncation.

MODEL REDUCTION TECHNIQUES APPLIED TO
THE CONTROL OF LARGE SPACE STRUCTURES

I. INTRODUCTION

The current state of the art in space flight includes the ability to orbit and manipulate large cargos via the space shuttle system. This capability makes feasible the construction of large structures while in orbit; these structures may take the form of space stations (for commercial, scientific, and military use), large communication antennas, and orbiting observatories, to name a few possibilities. Two common characteristics of many of these structures are:

- 1.) use of low mass structural elements - weight and size restrictions of the payloads will dictate structures designed with thin, lightweight members,
- 2.) low damping - as a consequence of the above constraints, the structures will exhibit low damping to vibrations, especially as the size of the structure increases.

Regardless of their highly flexible nature, these large space structures will be required to support activities dependent on stable platforms. Antennas, lasers, and large optical telescopes are a few examples of systems which will be dependent on precise pointing ability to perform satisfactorily. In general, passive damping achieved by judicious material selection and construction techniques will not be sufficient to

achieve this stringent structural stability. The problem facing the control designer, then, is to damp the unwanted vibrational motion while meeting the required performance objectives.

To achieve the above results, active feedback control methods are required. The structure is first modeled mathematically, and its structural modes and mode shapes are identified from the solution of the undamped, free vibrational problem:

$$\underline{M}\ddot{\underline{q}} + \underline{K}\underline{q} = \underline{0} \quad (1)$$

Finite element methods (NASTRAN) are utilized in this study. Control is achieved through the use of active control techniques applied to a reduced order model. The issue of implementing the required force actuators is not addressed here; they are assumed to exist in a functional form. Measurements of the success of the control are made by strategically placed position and velocity sensors. Using this sensor output, a feedback control law is generated. See section III for further discussion.

Model Reduction Problem

The above control problem is very large. Any real structure has an infinite number of vibrational modes, of which only a relative few are modeled mathematically. Even after this inherent truncation of unmodeled modes, the control of all modeled modes is generally an intractable problem; hundreds of modes may still remain. The computa-

tional burden of controlling such a system would be very high, and its on-line use would be beyond the capabilities of even the present state of the art computers. In addition, it is unnecessary to control modes not significant to the performance objectives.

It is thus desirable to have some scheme to reduce the control model in size. However, the reduced model must retain the significant dynamical characteristics of the entire structure, and give a true picture of the control effectiveness in achieving the desired performance. This thesis considers selective deletion of modes from the control problem while still recognizing their impact on the full mathematical model of the structure. In effect, "a selected set of the differential equations of the system model are discarded" (18).

If the input-output relation of the system can be expressed in terms of a transfer function, the deletion of modes corresponds to eliminating poles. Retained poles are characterized as dominant (those closest to the imaginary axis), and the transfer function of the reduced order model will ideally represent that of the full model with as small an error as possible. However, the representation of a large scale multi-input/multi-output system by matrices of transfer functions is unwieldy; state space methods are typically used, and will be employed here.

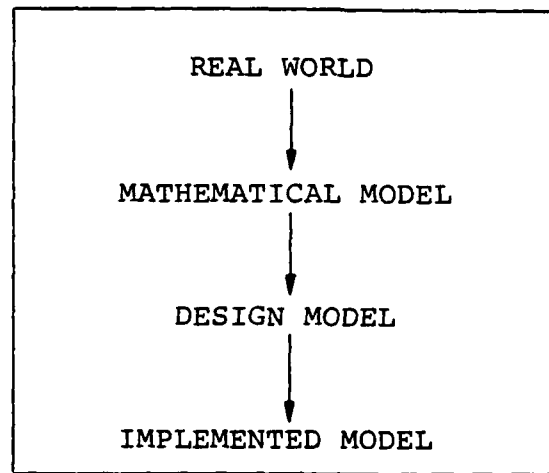


FIGURE 1. Model Reduction Process

Levels of Reduction

The model reduction problem is characterized in Figure 1. An actual structure has an infinite number of vibrational modes. The first reduction occurs in the process of modeling the structure mathematically. Finite element techniques represent the actual structure as a collection of point masses and basic structural elements, often with ideal characteristics. Here the infinite degree of freedom system is reduced to a finite degree of freedom system. Although the subject of some controversy, the assumption in this paper is that the NASTRAN model is a good representation of the true system.

A further step is the reduction of this mathematical model to a tractable size for computational purposes. In this step it must be determined which of the modeled modes are most significant to the control problem at hand. The retained modes at this point constitute the design model.

After the design model control problem is solved, the solution may still be too unwieldy to implement in real time on an actual system. Further truncation of the closed loop system may then be necessary.

This thesis addresses the model reduction process from the finite element mathematical model to the design model. The intent is to identify the modes to be actively controlled in order that the performance objectives are met by the full system mode. Three approaches to the model reduction problem are examined and applied to the structures described below. Based on these reduced models, active feedback control is then utilized to achieve the required pointing objectives, and differences due to the reduction methods are explored.

Description of Models Used

In order to facilitate comparisons between various controller design methods, several standardized structures have been developed by the Charles Stark Draper Laboratory. Two of these models are utilized in this thesis.

The CSDL I model (Figure 2) is a basic tetrahedral structure supported by six legs attached to ground. Such a tetrahedral arrangement is considered to be a fundamental building block for larger assemblies. The NASTRAN analysis utilizes ideal massless truss members which transmit axial forces only; no torsional or bending moments are modeled. Point masses are lumped at grid points one through

four, the intersections of the tetrahedral arms. Each mass exhibits three degrees of freedom, yielding a total of twelve for the structure. Six co-located actuator/sensor pairs are nominally located on the structure's legs. The performance index is considered to be the displacement of node 1, which simulates a pointing line-of-sight requirement. The typical criterion for a successful control design is to reduce the x and y displacements to less than 0.0004 radians and 0.00025 radians respectively in 20 seconds, given specified initial conditions with no additional disturbances. This study uses the displaced radius from a zero position of node 1 for time response comparisons.

The CSDL II model (Figure 3) represents a non-trivial approximation to a three mirror optical space system. Structural members include bending, axial, and torsional stiffnesses in the finite element model. The total structure is nearly 28 meters high and has a mass of 9300 kg; twenty-one co-located actuators and sensors and two sinusoidal disturbances complete the model. This model was used in a multiple controller investigation by Calico and Aldridge (1) and in an application of direct output feedback methods by Calico and Thyfault (23). Here it is used primarily to exercise the model reduction schemes of interest for a large scale system. Control implementation and system time responses were not achieved.

Further configuration details for the two models and the major NASTRAN analysis results are given in Appendix A.

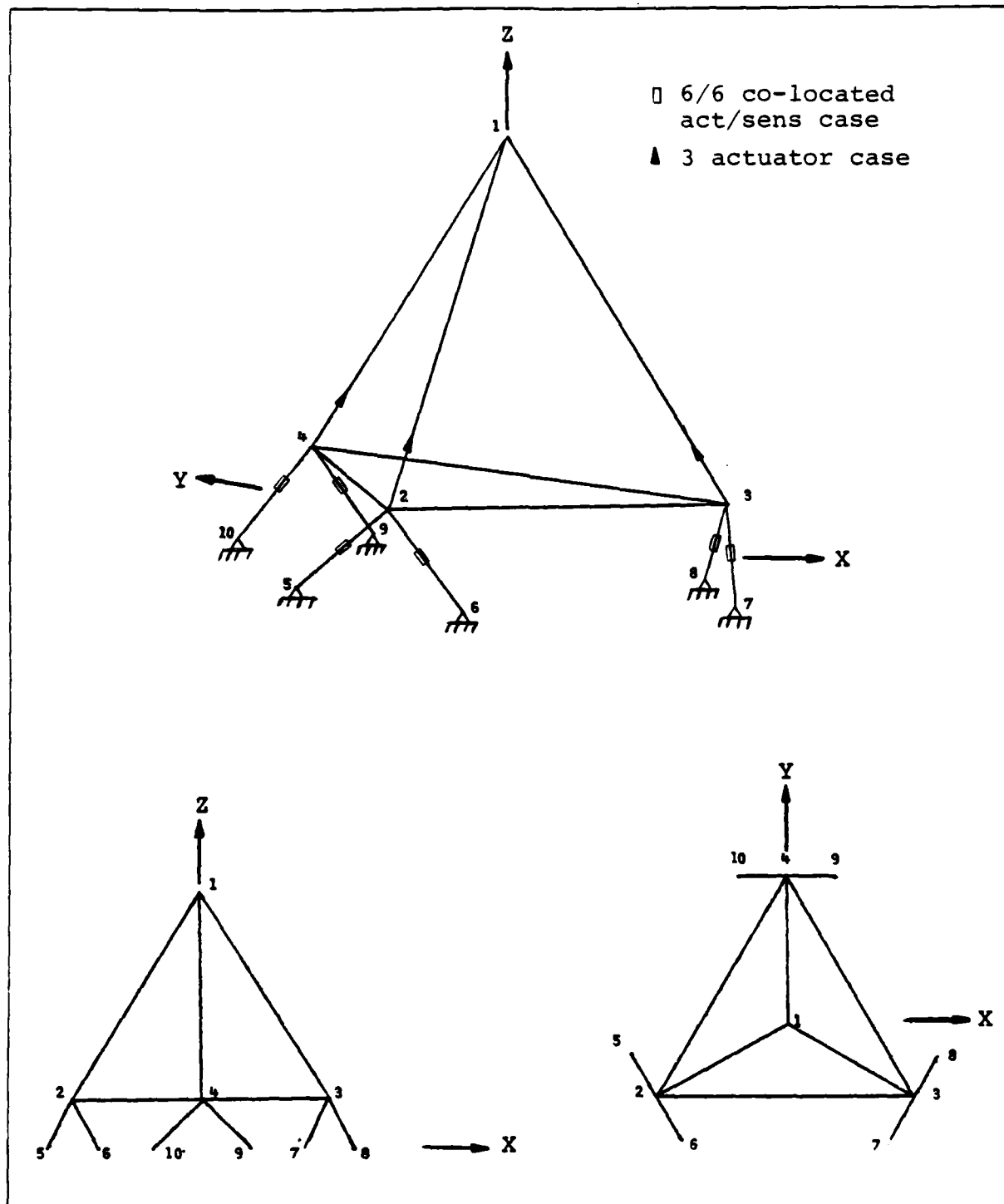


FIGURE 2. CSDL I Model

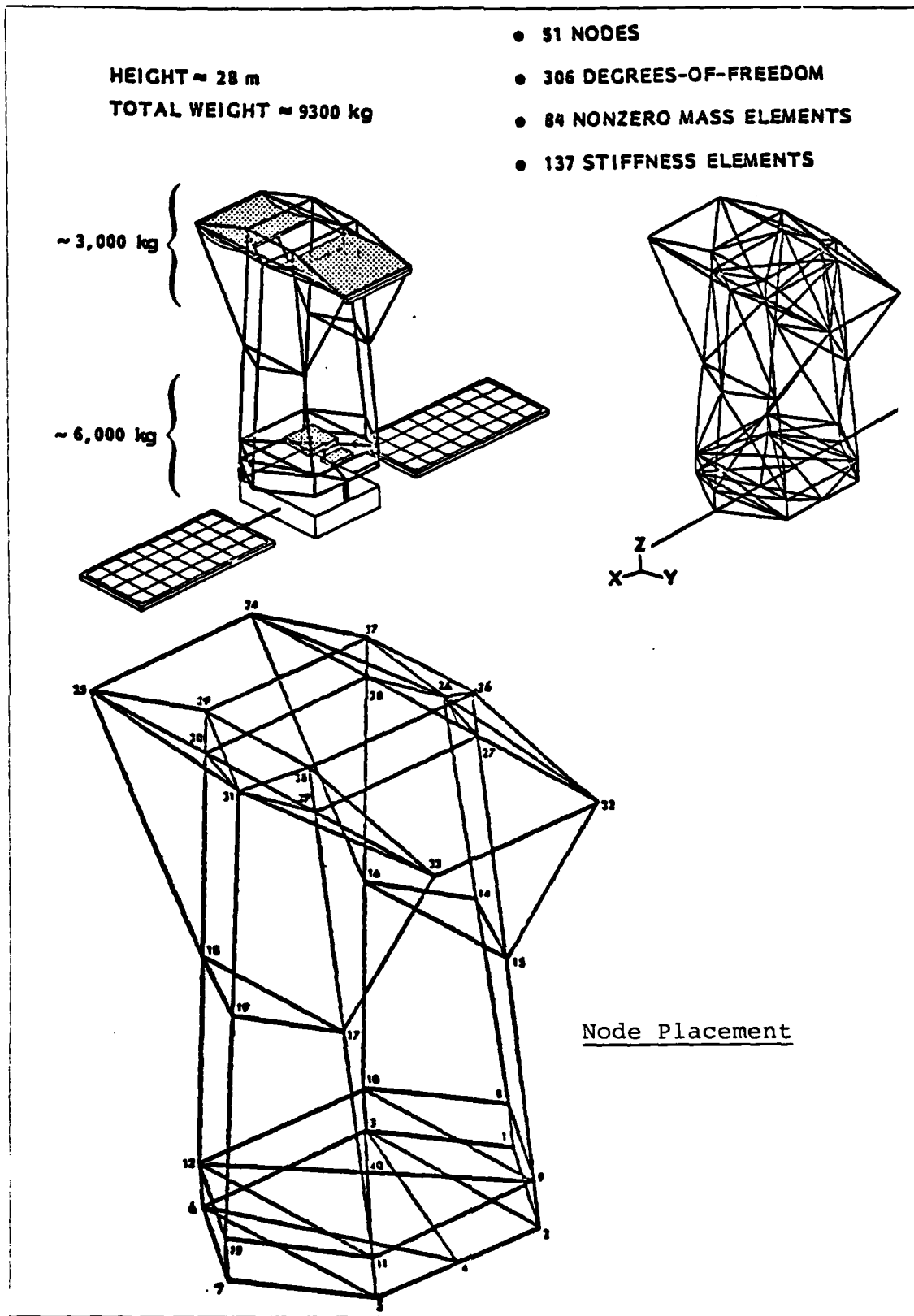


FIGURE 3. CSDL II Model

II. EQUATIONS OF MOTION

The following relationships hold for the systems of interest in this study. For a large structure, the vibrational equations of motion can be expressed as

$$\underline{M}\ddot{\underline{q}} + \underline{E}\dot{\underline{q}} + \underline{K}\underline{q} = \underline{D}\underline{u} + \underline{R}\underline{w} \quad (2)$$

where

$\underline{M} \equiv$ nxn mass matrix $\underline{R} \equiv$ rxr disturbance map matrix

$\underline{E} \equiv$ nxn damping matrix

$\underline{K} \equiv$ nxn stiffness matrix

$\underline{D} \equiv$ nxm actuator map matrix

$\underline{q} \equiv$ nx1 physical coordinate vector

$\underline{u} \equiv$ mx1 control force vector

$\underline{w} \equiv$ rx1 disturbance vector with statistics

$$E\{\underline{w}(t)\} = \underline{0} \quad E\{\underline{w}(t)\underline{w}(\tau)^T\} = \underline{W}\delta(t-\tau) \quad (3)$$

$\underline{W} \equiv$ rxr noise strength matrix

Solving the undamped free vibration problem

$$\underline{M}\ddot{\underline{q}} + \underline{K}\underline{q} = \underline{0} \quad (4)$$

yields the system natural frequencies ω_i , $i=1\dots n$, and the nxn modal matrix $\underline{\phi}$ such that

$$\underline{q} = \underline{\phi}\underline{\eta} \quad (5)$$

where $\underline{\eta}$ is the nx1 vector of modal coordinates and the columns of $\underline{\phi}$ are the eigenvectors \underline{u} of $[\underline{M}\omega_i^2 - \underline{K}]\underline{u}_i = \underline{0}$.

Substituting (5) in (2) and premultiplying by $\underline{\phi}^T$ gives

$$\underline{\phi}^T \underline{M} \underline{\phi} \ddot{\underline{\eta}} + \underline{\phi}^T \underline{E} \underline{\phi} \dot{\underline{\eta}} + \underline{\phi}^T \underline{K} \underline{\phi} \underline{\eta} = \underline{\phi}^T \underline{D} \underline{u} + \underline{\phi}^T \underline{R} \underline{w} \quad (6)$$

which, due to the properties of $\underline{\phi}$, is

$$\ddot{\underline{\eta}} + \left[2\zeta_i \omega_i \right] \dot{\underline{\eta}} + \left[\omega_i^2 \right] \underline{\eta} = \underline{\phi}^T \underline{D} \underline{u} + \underline{\phi}^T \underline{R} \underline{w} \quad (7)$$

Note that the damped case does not in general present a diagonal damping matrix in modal coordinates. However, when the damping values ζ_i are small, as they are here, the off-diagonal terms can be considered as second-order terms and a diagonal approximation may be achieved by discarding them (12).

Now consider an "output" or index of performance,

$$\underline{y} = \underline{C}_p \underline{q} + \underline{C}_v \dot{\underline{q}} \quad (8)$$

where

$\underline{C}_p \equiv$ pxn displacement matrix

$\underline{C}_v \equiv$ vxn velocity matrix

such that \underline{y} is some linear combination of states of interest. In the problem at hand, \underline{y} represents the line of sight deviation from nominal.

A similar relation is the measurement vector of sensor output

$$\underline{z} = \underline{H}_p \underline{q} + \underline{H}_v \dot{\underline{q}} \quad (9)$$

where \underline{H}_p and \underline{H}_v are position and velocity sensor map matrices.

Again, substitution of (5) yields

$$\underline{y} = \begin{bmatrix} \underline{C}_p \phi \end{bmatrix} \underline{n} + \begin{bmatrix} \underline{C}_v \phi \end{bmatrix} \dot{\underline{n}} \quad (10)$$

$$\underline{z} = \begin{bmatrix} \underline{H}_p \phi \end{bmatrix} \underline{n} + \begin{bmatrix} \underline{H}_v \phi \end{bmatrix} \dot{\underline{n}} \quad (11)$$

In state space form, the system equations become

$$\dot{\underline{x}} = \underline{A}\underline{x} + \underline{B}\underline{u} + \underline{G}\underline{w} \quad (12)$$

$$\underline{y} = \underline{C}\underline{x} \quad (13)$$

$$\underline{z} = \underline{H}\underline{x} \quad (14)$$

where

$$\underline{x} = \begin{bmatrix} \underline{n} \\ \dot{\underline{n}} \end{bmatrix} = \begin{bmatrix} \phi^T \underline{Q} \\ \vdots \\ \phi^T \underline{Q} \end{bmatrix} \quad (15)$$

$$\underline{A} = \begin{bmatrix} \underline{0} & \vdots & \underline{I} \\ \vdots & \ddots & \vdots \\ -\omega^2 & \vdots & -2\zeta\omega \end{bmatrix} \quad \underline{B} = \begin{bmatrix} \underline{0} \\ \vdots \\ \phi^T \underline{D} \end{bmatrix} \quad \underline{G} = \begin{bmatrix} \underline{0} \\ \vdots \\ \phi^T \underline{R} \end{bmatrix} \quad (16)$$

$$\underline{C} = \begin{bmatrix} \underline{C}_p \phi \\ \vdots \\ \underline{C}_v \phi \end{bmatrix} \quad \underline{H} = \begin{bmatrix} \underline{H}_p \phi \\ \vdots \\ \underline{H}_v \phi \end{bmatrix} \quad (17)$$

These equations form the basis for the following development.

III. MODEL REDUCTION METHODS

Many model reduction methods exist, and are typically grouped into the categories of parameter optimization, polynomial approximation, and component truncation (18). In the first, a quadratic error criterion is minimized by determination of the parameters of a system through non-linear mathematical programming. The second group attempts to approximate the system's frequency response over a given range of frequencies, or alternatively tries to truncate an expanded version of the matrix transfer function to arrive at a reduced model. The third category endeavors to retain a select set of the differential equations of the system (the "components") while truncating the rest. Three methods that belong to this third group are frequency truncation, modal cost analysis, and internal balancing; these techniques will be investigated here. Their selection was based on 1) ease of applicability to large scale multiple input, multiple output systems, and 2) compatibility with the finite element representation of the structures of interest.

Frequency Truncation

The simplest method involves merely truncating the higher order modes. For many control problems this is adequate; the low frequency modes contribute most to the performance objectives, and the higher frequency modes are essentially outside the required response bandwidth. An example is an aircraft control problem that may require a

designer to account for effects due to low frequency bending modes; higher modes, through, simply do not impact the control problem.

A different situation exists for large lightly damped structures. First, these assemblies are much less stiff as a whole; finite element analysis reveals a cluster of vibrational modes within the bandwidth of the controllers and sensors. Second, the pointing requirements of onboard systems may be much more stringent, making the consideration of the effects of higher modes imperative. A simple truncation may still leave a large number of modes to be dealt with. Even so, one tends to favor the retention of lower frequency modes when possible since the model is known more accurately at low frequencies, a lower sampling rate on the control law will be possible, and the actuators and sensors do have a finite bandwidth (16).

Modal Cost Analysis

Modal cost analysis is a model reduction technique developed principally by Skelton (7,18,19,20,21) and is a special application of his more general component cost analysis (18). Essentially, a cost function is established detailing the weighted contributions of each component of a system to an output relationship. The individual contributions of each component are assessed, and

their ranking provides a basis for model reduction. In a vibrations application, the structural modes play the part of "components," and the summed contributions of all modes make up the value of the total system response.

Consider the matrix second order system in Eq (2) and its state space formulation. In the case of small damping, Eq (7) represents a set of dynamically uncoupled modal equations in the open loop sense. If \underline{u} is a function of state, as in feedback control, these equations do not uncouple (20). For this reason, the modal cost analysis techniques are split into open and closed loop forms. This paper will deal principally with the open loop case.

In the open loop case, the feedback control $\underline{u} = \underline{0}$ and we are interested in the contribution of each mode to the output \underline{y} (open loop control can be applied, but for the purposes here the modeling of open loop disturbance inputs only is most productive). A cost function is defined as

$$V = \lim_{t \rightarrow \infty} E\{\underline{y}^T \underline{Q} \underline{y}\} = \sum_{i=1}^n V_i \quad (18)$$

that is, V is the expected mean square response weighted by the matrix \underline{Q} , and is made up of the sum of the contributions from each of n system modes. Note that \underline{y} here is some system output or performance criterion of interest; in the case at hand, \underline{y} represents the deviation from a desired pointing constraint, a quantity that we wish to control.

The eigenvalues of the damped, unforced system

$$\ddot{\eta} + \left[2\zeta_i \omega_i \right] \dot{\eta} + \left[\omega_i^2 \right] \eta = 0 \quad i=1 \dots n \quad (19)$$

are given by the roots of the characteristic equation

$$\det \left\{ \lambda^2 \left[I \right] + \lambda \left[2\zeta_i \omega_i \right] + \left[\omega_i^2 \right] \right\} = 0 \quad (20)$$

and correspond to the eigenvalues of the matrix \underline{A} in Eq (12).

Their form is given by

$$\lambda_i, \bar{\lambda}_i = -\zeta_i \omega_i \pm j\omega_i \sqrt{1-\zeta_i^2} \approx -\zeta_i \omega_i \pm j\omega_i \quad (21)$$

where the approximation holds for small damping, $\zeta_i \rightarrow 0$ $i=1 \dots n$.

In addition, the eigenvalue problem

$$\underline{A}\underline{E} = \underline{E}\underline{\Lambda} \quad \underline{\Lambda} = \begin{bmatrix} \lambda_i \end{bmatrix} \quad i=1, \dots, 2n \quad \begin{matrix} \text{for} \\ \text{all} \\ \text{complex} \\ \text{eigenvalues} \end{matrix} \quad (22)$$

yields the matrix \underline{E} whose columns are the so-called "right" eigenvectors of \underline{A} corresponding to λ_i :

$$\underline{E} = \begin{bmatrix} \underline{e}_1 & \underline{e}_2 & \dots & \underline{e}_{2n} \end{bmatrix} \quad (23)$$

Here, with \underline{A} as in Eq (16), \underline{E} takes the form

$$\underline{E} = \begin{bmatrix} I_n & \vdots & I_n \\ \vdots & \ddots & \vdots \\ \lambda_i & \vdots & \bar{\lambda}_1 \end{bmatrix} \quad i=1, \dots, n \quad (24)$$

The "left" eigenvectors of \underline{A} are found from

$$\underline{F}\underline{A} = \underline{\Lambda}\underline{F} \quad (25)$$

and correspond to the rows of

$$\underline{F} = \underline{E}^{-1} = \begin{bmatrix} \underline{f}_1^T \\ \dots \\ \underline{f}_2^T \\ \vdots \\ \dots \\ \underline{f}_{2n}^T \end{bmatrix} \quad (26)$$

Now define an "observability" vector:

$$\underline{o}_i = \underline{C}\underline{e}_i = \left[\underline{C}_p \phi \right]_k + \lambda_i \left[\underline{C}_v \phi \right]_k \quad \begin{matrix} i=1, \dots, 2n \\ k=1, \dots, n \\ \text{columns} \end{matrix} \quad (27)$$

It is shown in (19,20) that the individual modal cost for the open loop case of Eq (12), $\underline{u} = \underline{0}$, can be expressed as

$$V_i = - \sum_{j=1}^n \left\{ \left[(\underline{o}_i^T \underline{Q} \underline{o}_j) \underline{f}_j^T (\underline{G} \underline{W} \underline{G}^T) \underline{f}_i \right] / (\bar{\lambda}_i + \lambda_j) \right\} \quad (28)$$

where \underline{Q} is the weighting matrix from the cost function,

Eq (18), and \underline{W} is the noise strength matrix from Eq (3).

Note that if the disturbances can be considered independent and uncorrelated, \underline{W} is a diagonal matrix whose elements are the mean square values of $\underline{w}(t)$.

To show this, the cost V may be written in terms of

the initial condition covariance as

$$V = E \int_0^{\infty} (\underline{y}^T Q \underline{y}) dt = \text{tr}(\underline{K} \underline{P}_0) \quad (29)$$

where

$$\underline{K} = \int_0^{\infty} e^{\underline{A}^T t} \underline{C}^T Q \underline{C} e^{\underline{A} t} dt \quad (30)$$

$$\underline{P}_0 = E \left[\underline{x}(0) - \bar{\underline{x}}(0) \right] \left[\underline{x}(0) - \bar{\underline{x}}(0) \right]^T \quad (31)$$

Transforming to modal coordinates in the damped system, Eq (19), the elements of \underline{K} become, in terms of the previous "observability" vectors

$$\begin{aligned} K_{ij} &= \left[\underline{E}^T \underline{K} \underline{E} \right]_{ij} = \underline{o}_i^T \underline{Q} \underline{o}_j \int_0^{\infty} e^{(\bar{\lambda}_i + \lambda_j)t} dt \\ &= -1 / (\bar{\lambda}_i + \lambda_j) (\underline{o}_i^T \underline{Q} \underline{o}_j) \end{aligned} \quad (32)$$

\underline{P}_0 transforms as $\underline{P}_0 = \underline{E} \underline{P} \underline{E}^T$, and, from Eq (29),

$$\begin{aligned} V &= \text{tr}(\underline{K} \underline{P}_0) = \text{tr}(\underline{E}^{-T} \underline{K} \underline{E}^{-1} \underline{E} \underline{P} \underline{E}^T) = \text{tr}(\underline{K} \underline{P}) \\ &= \sum_{j=1}^n \underline{k}_{i-i}^T \underline{p}_i \quad i = i^{\text{th}} \text{ column} \end{aligned} \quad (33)$$

so that

$$V_i = \underline{k}_{i-i}^T \underline{p}_i = - \sum_{j=1}^n \left\{ (\underline{o}_i^T \underline{Q} \underline{o}_j) (\underline{E}_i^{-1} \underline{P}_0 \underline{E}_j^{-T}) / (\bar{\lambda}_i + \lambda_j) \right\} \quad (34)$$

where, for example, \underline{E}_i^{-1} denotes the i^{th} column of \underline{E}^{-1} . Substituting $\underline{f}_i^T = \underline{E}_i^{-1}$ in Eq (34), and considering the disturbance statistics rather than the initial condition statistics ($\underline{P}_0 \rightarrow \underline{G} \underline{W} \underline{G}^T$) yields Eq (28).

It is evident from Eq (28) that in the general case the cost due to an individual mode is the result of the direct excitation of that mode plus the coupling effects of all other modes. However, in the case of small damping, it can be shown (20) that the term resulting from $i=j$ dominates the summation to the extent that the other terms may be neglected. This is equivalent to the statement following Eq (7) regarding decoupling of a lightly damped system in modal coordinates.

Combining the cost due to a mode and its conjugate in Eq (28) leads to the simplified expression

$$V_i = \left[(\underline{O}_i^T \underline{Q} \underline{O}_i) \underline{f}_i^T (\underline{G} \underline{W} \underline{G}^T) \underline{f}_i \right] / (\zeta_i \omega_i) \quad (35)$$

Denoting the i th column of $\underline{C}_p \underline{\Phi}$ by $(\underline{C}_p \underline{\Phi})_i$, the terms of the above equation become

$$\underline{O}_i^T \underline{Q} \underline{O}_i = (\underline{C}_p \underline{\Phi})_i^T \underline{Q} (\underline{C}_p \underline{\Phi})_i + \omega_i^2 (\underline{C}_v \underline{\Phi})_i^T \underline{Q} (\underline{C}_v \underline{\Phi})_i + 0 / (\zeta_i) \quad (36)$$

$$\underline{f}_i^T \underline{G} \underline{W} \underline{G}^T \underline{f}_i = (\underline{\Phi}^T \underline{R} \underline{W} \underline{R}^T \underline{\Phi})_i / (4 \omega_i^2) \quad (37)$$

so that the modal costs become

$$V_i = \left\{ \left[(\underline{C}_p \underline{\Phi})_i^T \underline{Q} (\underline{C}_p \underline{\Phi})_i + \omega_i^2 (\underline{C}_v \underline{\Phi})_i^T \underline{Q} (\underline{C}_v \underline{\Phi})_i \right] (\underline{\Phi}^T \underline{R} \underline{W} \underline{R}^T \underline{\Phi})_i \right\} / 4 \zeta_i \omega_i^3 \quad (38)$$

in terms of explicitly known quantities in the original system.

In the study here, only output position variables were necessary, so $\underline{C}_v = \underline{0}$ and the expression further simplifies to

$$V_i = (\underline{C}_p \underline{\Phi})_i^T \underline{Q} (\underline{C}_p \underline{\Phi})_i (\underline{\Phi}^T \underline{R} \underline{W} \underline{R}^T \underline{\Phi})_i / (4\zeta_i \omega_i^3) \quad (39)$$

Thus, based on the system model and its computed natural frequencies and mode shapes, the individual modal contributions to an "output" can be assessed and ranked. Presumably, modes having a small contribution could be truncated from a control model whose purpose was to minimize the "output."

A similar expression can be developed for a closed loop system with $\underline{u} \neq \underline{0}$ in Eq (7). However, this case involves feedback gains which must be computed first for the high order model; closed loop modes may then be truncated. The computation of feedback gains for a high order model is computationally unwieldy, to say the least. An alternative approach is: first apply the open loop method to the high order model, compute the feedback gains for a truncated control system, and then apply the closed loop version of the model cost equation for further model reduction. No closed loop applications were attempted here.

Internal Balancing

A third model reduction technique applicable to large systems is based on the work of Moore (14).

Essentially, Moore proposes that a system representation which has been transformed to an "internally balanced" coordinate system (Grammian - balanced) may be state - truncated in that coordinate system to produce a reduced order model. The truncation is accomplished based on the relative controllability/observability of the system states. This method is advantageous in that it incorporates information about sensor/actuator location that is not done in modal cost analysis; in addition, any chosen subset of the transformed system model is guaranteed to be stable. Unfortunately, for a general multi-input, multi-output system, a different coordinate basis is required for each input-output pair. However, in the case where damping is very small, it can be shown that modal coordinates and balanced coordinates are approximately equivalent (4,9). Hence the technique's applicability to the problem at hand.

The controllability and observability Grammians (Gram matrices) derived from the system of Eqs (12), (13), and (14) with \underline{A} asymptotically stable and time-invariant are

$$\underline{W}_C = \int_0^{\infty} e^{\underline{A}t} \underline{B} \underline{B}^T e^{\underline{A}^T t} dt \quad (40)$$

$$\underline{W}_O = \int_0^{\infty} e^{\underline{A}^T t} \underline{H}^T \underline{H} e^{\underline{A}t} dt \quad (41)$$

The steady state \underline{W}_C and \underline{W}_O satisfy the Lyapunov matrix equations:

$$\underline{A}\underline{W}_C + \underline{W}_C\underline{A}^T + \underline{B}\underline{B}^T = \underline{0} \quad (42)$$

$$\underline{A}^T\underline{W}_O + \underline{W}_O\underline{A} + \underline{C}^T\underline{C} = \underline{0} \quad (43)$$

The eigenvalues of \underline{W}_C can be considered to be a qualitative measure of the controllability of the system states in a given coordinate system (17). The smaller an eigenvalue of \underline{W}_C , the more difficult it is to affect the related state by an application of control energy; i.e., it is less controllable. The observability Grammian is the dual of \underline{W}_C , and hence similar properties can be identified in \underline{W}_O .

It is desired to find a coordinate system wherein these attributes can be exploited most advantageously. Note that the Grammians are not invariant under coordinate transformations; the thrust here is to find a transformation that will leave the Grammians equal and diagonal.

The system of Eqs (12), (13), and (14) transforms to this new coordinate frame through the transformation \underline{T} as

$$\begin{aligned} \underline{x} &= \underline{T}\hat{\underline{x}} & \hat{\underline{A}} &= \underline{T}^{-1}\underline{A}\underline{T} & \hat{\underline{B}} &= \underline{T}^{-1}\underline{B} & \hat{\underline{D}} &= \underline{T}^{-1}\underline{D} \\ & & \hat{\underline{C}} &= \underline{C}\underline{T} & \hat{\underline{H}} &= \underline{H}\underline{T} \end{aligned} \quad (44)$$

so that the system in the transformed frame is:

$$\begin{aligned}\hat{\underline{x}} &= \hat{\underline{A}}\hat{\underline{x}} + \hat{\underline{B}}\underline{u} + \hat{\underline{D}}\underline{w} \\ \underline{y} &= \hat{\underline{C}}\hat{\underline{x}} \\ \underline{z} &= \hat{\underline{H}}\hat{\underline{x}}\end{aligned}\tag{45}$$

The Grammians transform as

$$\hat{\underline{W}}_C = \underline{T}^{-1}\underline{W}_C\underline{T}^{-T} \quad \hat{\underline{W}}_O = \underline{T}^T\underline{W}_O\underline{T}\tag{46}$$

Now, using the notation of (9,11), the controllability Grammian can be expressed as

$$\underline{W}_C = \underline{U}_C \underline{\Sigma}_C \underline{U}_C^T\tag{47}$$

where

$\underline{\Sigma}_C$ = diagonal matrix of eigenvalues of \underline{W}_C

\underline{U}_C = matrix whose columns are eigenvectors of \underline{W}_C

A transformation $\underline{T}^* = \underline{U}_C \underline{\Sigma}_C^{\frac{1}{2}}$ transforms the Grammians as

$$\begin{aligned}\underline{W}_C &\xrightarrow{\underline{T}^*} \underline{I} \\ \underline{W}_O &\xrightarrow{\underline{T}^*} \underline{W}_O^* = \underline{\Sigma}_C^{\frac{1}{2}} \underline{U}_C^T \underline{W}_O \underline{U}_C \underline{\Sigma}_C^{\frac{1}{2}} = \underline{H}^T \underline{H}\end{aligned}\tag{48}$$

where

$$\underline{H} = \underline{\Sigma}_O^{\frac{1}{2}} \underline{U}_O^T \underline{U}_C \underline{\Sigma}_C^{\frac{1}{2}}$$

bearing in mind that \underline{U}_C is an orthogonal matrix so that $\underline{U}_C^{-1} = \underline{U}_C^T$. This new matrix \underline{W}_O^* decomposes as

$$\underline{W}_O^* = \underline{H}^T \underline{H} = \underline{U}_O^* \underline{\Sigma}^{*2} \underline{U}_O^{*T} \quad (49)$$

where

$$\underline{\Sigma}^{*2} = \begin{bmatrix} \sigma_1^2 & & \\ & \ddots & \\ & & \sigma_n^2 \end{bmatrix} \quad (50)$$

σ^2 = eigenvalues of \underline{W}_O^*

\underline{U}_O^* = matrix whose columns are eigenvectors of \underline{W}_O^*

It is shown in (9) that the transformation

$$\underline{T} = \underline{U}_C \underline{\Sigma}^{*1/2} \underline{U}_O^{*T} \underline{\Sigma}^{*-1/2} \quad (51)$$

operates on \underline{W}_C and \underline{W}_O such that

$$\hat{\underline{W}}_C = \hat{\underline{W}}_O = \underline{\Sigma}^* \quad (52)$$

that is, the controllability and observability Grammians are equal and diagonal in the new state space. As well, the diagonal elements of $\underline{\Sigma}^{*2}$ are the eigenvalues of $\underline{W}_O \underline{W}_C$, and the elements of

$$\underline{\Sigma}^* = \begin{bmatrix} \sigma_1 & & \\ & \ddots & \\ & & \sigma_n \end{bmatrix} \quad (53)$$

are singular values of \underline{H} in Eq (48). A system in this form, $\hat{\underline{W}}_C = \hat{\underline{W}}_O = \underline{\Sigma}^*$, is internally balanced.

Essentially, then, the best model truncation decisions based on controllability and observability can be made by rank ordering the σ_i and keeping only the modes corresponding to the higher values. In the case of Eq (45), transformed to balanced coordinates and partitioned as

$$\begin{aligned} \begin{bmatrix} \dot{\underline{x}}_1 \\ \dot{\underline{x}}_2 \end{bmatrix} &= \begin{bmatrix} \underline{A}_{11} & \underline{A}_{12} \\ \underline{A}_{21} & \underline{A}_{22} \end{bmatrix} \begin{bmatrix} \underline{x}_1 \\ \underline{x}_2 \end{bmatrix} + \begin{bmatrix} \underline{B}_1 \\ \underline{B}_2 \end{bmatrix} \underline{u} \\ \underline{y} &= \begin{bmatrix} \underline{C}_1 & \underline{C}_2 \end{bmatrix} \underline{x} \\ \underline{z} &= \begin{bmatrix} \underline{H}_1 & \underline{H}_2 \end{bmatrix} \underline{x} \\ \underline{\Sigma}^* &= \begin{bmatrix} \underline{\Sigma}_1^* & 0 \\ 0 & \underline{\Sigma}_2^* \end{bmatrix} \quad \begin{aligned} \underline{\Sigma}_1^* &= \text{diag}[\sigma_1 \dots \sigma_k] \\ \underline{\Sigma}_2^* &= \text{diag}[\sigma_{k+1} \dots \sigma_n] \end{aligned} \end{aligned} \quad (54)$$

with $\sigma_k \gg \sigma_{k+1}$, then input \underline{u} affects \underline{x}_2 less than it affects \underline{x}_1 , and output \underline{y} is affected by \underline{x}_2 less than by \underline{x}_1 (4). Note that additional relationships can be examined by using \underline{D} in Eq (40) or \underline{H} in Eq (41) and considering the "disturbability" and "measureability" Grammians.

An explicit form of this transformation \underline{T} is given in (4). For Eqs (12) and (14) with $\underline{w} = \underline{0}$, written for each mode as

$$\dot{\underline{x}}_i = \underline{A}_i \underline{x}_i + \underline{B}_i \underline{u} \quad i=1 \dots n \quad (55)$$

$$\underline{z}_k = \sum_{i=1}^n \underline{H}_i \underline{x}_i \quad \text{for } k\text{th sensor} \quad (56)$$

that is,

$$\dot{\underline{x}}_i = \begin{bmatrix} \dot{\eta}_i \\ \ddot{\eta}_i \end{bmatrix} = \begin{bmatrix} 0 & 1 \\ -\omega_i^2 & -2\zeta_i\omega_i \end{bmatrix} \begin{bmatrix} \eta_i \\ \dot{\eta}_i \end{bmatrix} + \begin{bmatrix} 0 \\ \underline{b}_i \end{bmatrix} \underline{u} \quad (57)$$

$$\underline{z}_k = \sum_{i=1}^n \left[(\underline{h}_{pi})_k \quad (\underline{h}_{vi})_k \right] \begin{bmatrix} \eta_i \\ \dot{\eta}_i \end{bmatrix} \quad \begin{array}{l} k=1\dots s \\ s \equiv \text{number of} \\ \text{sensors} \end{array} \quad (58)$$

where

$\underline{b}_i \equiv$ ith row of $\underline{\Phi}^T \underline{D}$

$\underline{h}_{pi}, \underline{h}_{vi} \equiv$ ith column of $\underline{H}_p \underline{\Phi}, \underline{H}_v \underline{\Phi}$

$k \equiv$ kth element of a column

the balancing transformation is

$$\underline{T}_i = \left[(\underline{b}_i \underline{b}_i^T) / (4\zeta_i \omega_i) \right]^{\frac{1}{2}} \begin{bmatrix} \omega_i^{-1} & 0 \\ 0 & 1 \end{bmatrix} \underline{V}_i \begin{bmatrix} \sigma_{1i}^{-\frac{1}{2}} & 0 \\ 0 & \sigma_{2i}^{-\frac{1}{2}} \end{bmatrix} \quad (59)$$

$$\sigma_{1i} = (\underline{b}_i \underline{b}_i^T)^{\frac{1}{2}} / (4\zeta_i \omega_i) \left[\underline{h}_{vi}^T \underline{h}_{vi} + \omega_i^{-2} \underline{h}_{pi}^T \underline{h}_{pi} (1 - 2\zeta_i \gamma_i - 2\zeta_i (1 + \gamma_i^2)^{\frac{1}{2}}) \right]^{\frac{1}{2}} \quad (60)$$

$$\sigma_{2i} = (\underline{b}_i \underline{b}_i^T)^{\frac{1}{2}} / (4\zeta_i \omega_i) \left[\underline{h}_{vi}^T \underline{h}_{vi} + \omega_i^{-2} \underline{h}_{pi}^T \underline{h}_{pi} (1 - 2\zeta_i \gamma_i + 2\zeta_i (1 + \gamma_i^2)^{\frac{1}{2}}) \right]^{\frac{1}{2}} \quad (61)$$

$$\underline{v}_i = \begin{bmatrix} v_{1i} & v_{2i} \\ -v_{2i} & v_{1i} \end{bmatrix} \quad \begin{aligned} v_{1i} &= \left[(1 + \gamma_i)/2 \right]^{\frac{1}{2}} \\ v_{2i} &= \left[(1 - \gamma_i)/2 \right]^{\frac{1}{2}} \end{aligned} \quad (62)$$

$$\gamma_i = \text{sgn}(\gamma_i) (1 + \gamma_i^{-2})^{-\frac{1}{2}} \quad (63)$$

$$\gamma_i = \omega_i \underline{h}_{pi}^T \underline{h}_{vi} / (\underline{h}_{pi}^T \underline{h}_{pi}) - \zeta_i \quad (64)$$

Applying this transformation yields a balanced subsystem with balanced Grammians

$$\underline{\Sigma}_i^* = \begin{bmatrix} \sigma_{1i} & 0 \\ 0 & \sigma_{2i} \end{bmatrix} \quad (65)$$

In the case of small damping, $\zeta_i \ll 1$, then Eqs (60) and (61) reduce to $\sigma_{1i} \approx \sigma_{2i} = \sigma_i$, and the approximate balanced system is

$$\tilde{\underline{\Sigma}}_i^* = \sigma_i \underline{I} \quad (66)$$

$$\hat{\dot{\underline{x}}}_i = \tilde{\underline{A}}_i \hat{\underline{x}}_i + \tilde{\underline{B}}_i \underline{u} \quad i=1 \dots n \quad (67)$$

$$\underline{z} = \tilde{\underline{H}}_i \hat{\underline{x}}_i \quad (68)$$

where

$$\underline{x}_i = \tilde{\underline{A}}_i \hat{\underline{x}}_i \quad \tilde{\underline{B}}_i = \underline{T}_i^{-1} \underline{B}_i \quad \tilde{\underline{H}}_i = \underline{H}_i \underline{T}_i \quad (69)$$

$$\tilde{\underline{\Sigma}}_i^* = \underline{T}_i^{-1} \underline{W}_{ci} \underline{T}_i^{-T} = \underline{T}_i^T \underline{W}_{oi} \underline{T}_i \quad (70)$$

The major result here (4) is:

- 1) if damping is small, $\zeta_i \ll 1$, then the i th subsystem of Eqs (66) - (68) is approximately internally balanced with

$$\sigma_i = (4\zeta_i \omega_i)^{-1} \left[\underline{b}_i \underline{b}_i^T (\underline{h}_{vi}^T \underline{h}_{vi} + \omega_i^{-2} \underline{h}_{pi}^T \underline{h}_{pi}) \right]^{1/2} \quad (71)$$

- 2) if all modal damping is small and the modal natural frequencies are sufficiently distinct, i.e. if

$$\max(\zeta_i, \zeta_j) \max(\omega_i, \omega_j) / |\omega_i - \omega_j| \ll 1, \quad i \neq j \quad (72)$$

then the entire model is approximately internally balanced with

$$\underline{\Sigma}^* \approx \tilde{\underline{\Sigma}}^* = \begin{bmatrix} \sigma_1 & & \\ & \ddots & \\ & & \sigma_n \end{bmatrix} \quad i=1 \dots n \quad (73)$$

Furthermore, in the cases of position or velocity sensors only, that is, $\underline{H}_p = \underline{0}$ or $\underline{H}_v = \underline{0}$, the above balanced coordinates are a special case of modal coordinates. In other words, no transformation is needed from the system of Eqs (12) - (14), yet the above results still apply. As position sensors only are utilized in this study, this conclusion is valid.

Several cases of modal ranking may now be investigated, depending on the system matrices used in the Grammian definitions, Eqs (40) and (41).

Actuators to Output. Being consistent with the system matrices as defined, the Grammians of interest in this case are

$$\underline{W}_C = \int_0^{\infty} e^{\underline{A}t} \underline{B} \underline{B}^T e^{\underline{A}^T t} dt \quad (74)$$

$$\underline{W}_O = \int_0^{\infty} e^{\underline{A}^T t} \underline{C}^T \underline{C} e^{\underline{A}t} dt \quad (75)$$

The balancing approximation yields rankings of σ_{BC_i} , that is, the degree to which actuators can affect the i th mode's contribution to the output.

Disturbances to Output. One may consider the disturbance propagation through the system to the output by replacing \underline{B} with \underline{G} in Eq (74). The resulting σ_{GC_i} rankings indicate the modes that are most necessary to control in order that the effects of disturbances on performance is minimized.

Disturbances to Sensors. Similarly, replacing \underline{C} by \underline{H} in Eq (75) results in a modal ranking of the relative observability of the disturbance inputs.

Actuators to Sensors. Using the \underline{B} and \underline{H} matrices in Eq (74) and (75) yields a ranking of the ability of the actuator/sensor configuration to sense and respond to a given mode. The configuration may be able to powerfully influence a mode, but if this mode has little contribution to the performance, this ability is not useful.

Utilizing these four rankings, one may analyze the modal mechanism of the disturbance propagation and the corresponding ability of the given actuator/sensor configuration to sense and eliminate these disturbance effects. This provides a straightforward method for selective truncation of the high order mathematical model to the low order control design model.

A relationship exists between the modal costs of Eq (38) and the internal balancing disturbance/output ranking given by

$$\sigma_{GC_i} = (4\zeta_i\omega_i)^{-1} \left[\underline{g}_i \underline{g}_i^T (\underline{c}_{vi}^T \underline{c}_{vi} + \omega_i^{-2} \underline{c}_{pi} + \underline{c}_{pi}) \right]^{1/2} \quad (76)$$

Assuming disturbances characterized as zero mean white noises of unit strength, then

$$V_i = 4\zeta_i\omega_i Q_i \sigma_{GC_i}^2 \quad (77)$$

Approximation Error. The internal balancing approximation is valid for cases that satisfy Eq (72), which involves modal damping ratios and natural frequencies. In this study, damping is assumed uniform for all modes and equal to .005. The remaining condition requires a sufficient separation of modal natural frequencies. For the case of $\zeta = .005$, a frequency difference of 5% results in an approximation error of less than 5% (4). Frequency differences of less than this result in significantly higher

errors. In the case of a high order model, modal natural frequencies may in fact be quite close together, and the approximation error may be unacceptable. However, the subset of modes that do meet the error criterion still provides useful information in the model reduction process; this situation will be discussed in connection with the CSDL II structure.

IV. CONTROL ALGORITHM

Once an open loop reduced order model has been achieved, the next step is the implementation of some form of closed loop (feedback) control technique. In this study, the method utilized is that developed by Calico and associated students (1,3,8,23). The basic methodology is presented in (8), and will be summarized here.

State Space Formulation

The deterministic feedback control system is

$$\dot{\underline{x}} = \underline{A}\underline{x} + \underline{B}\underline{u} \quad \underline{u} = \underline{G}_c \underline{x} \quad (78)$$

$$\underline{y} = \underline{C}\underline{x} \quad (79)$$

$$\underline{z} = \underline{H}\underline{x} \quad (80)$$

This system is in the form of the mathematical model of Figure 1, that is, it is a finite dimensional representation of the infinite dimensional true system. The modes which have been eliminated in this inherent truncation are known as unmodeled modes; they are typically very high frequency and do not significantly impact the control problem. The modes that make up the mathematical model of Eqs (78)-(80) are the modeled modes.

The modeled modes are identified as either controlled, suppressed, or residual. The controlled modes, \underline{x}_c , are those selected by the model reduction techniques that must be directly controlled in order for the system to meet the

performance objectives. The remaining modeled but uncontrolled modes will be affected by the application of control to \underline{x}_c even though they themselves are not directly controlled; this phenomenon (see Eq (105)) is known as control spillover, and may result in poor performance or even closed loop instabilities if not remedied. The uncontrolled modes whose reaction to this spillover must be suppressed are designated \underline{x}_s , suppressed modes. The remaining modeled, uncontrolled modes that are relatively insensitive to the spillover effect are termed residual modes. The design level controller is unaware of the existence of these residual modes, however they do contribute to the performance of the reduced order control model; hence their inclusion in the final system.

The system of Eqs (78)-(80) may be separated into the states corresponding to the controlled, suppressed, and residual modes as

$$\dot{\underline{x}}_c = \underline{A}_c \underline{x}_c + \underline{B}_c \underline{u} \quad \underline{u} = \underline{G}_c \underline{x}_c \quad (81)$$

$$\dot{\underline{x}}_s = \underline{A}_s \underline{x}_s + \underline{B}_s \underline{u} \quad (82)$$

$$\dot{\underline{x}}_r = \underline{A}_r \underline{x}_r + \underline{B}_r \underline{u} \quad (83)$$

$$\underline{y} = \underline{C}_c \underline{x}_c + \underline{C}_s \underline{x}_s + \underline{C}_r \underline{x}_r \quad (84)$$

$$\underline{z} = \underline{H}_c \underline{x}_c + \underline{H}_s \underline{x}_s + \underline{H}_r \underline{x}_r \quad (85)$$

The unknown quantity here is the feedback gain matrix \underline{G}_C . This is found by the application of steady state optimal regulator theory (10), where a quadratic cost function to be minimized is

$$J_C = \int_0^{\infty} \left[\underline{x}_C^T \underline{Q}_C \underline{x}_C + \underline{u}^T \underline{R}_C \underline{u} \right] dt \quad (86)$$

$\underline{Q}_C \equiv n_C \times n_C$ state weighting matrix (pos. semi-definite)

$\underline{R}_C \equiv m \times m$ control penalty weighting matrix (pos. def.)

Here, \underline{R}_C is assumed to be the unit diagonal. The optimum gain \underline{G}_C to minimize the cost J_C is known to be

$$\underline{G}_C = -\underline{R}_C^{-1} \underline{B}_C^T \underline{S} \quad (87)$$

where \underline{S} is the solution to the steady state matrix Riccati equation

$$\underline{S} \underline{A}_C + \underline{A}_C^T \underline{S} - \underline{S} \underline{B}_C \underline{R}_C^{-1} \underline{B}_C^T \underline{S} + \underline{Q}_C = 0 \quad (88)$$

However, in order to form $\underline{u} = \underline{G}_C \underline{x}_C$, the state \underline{x}_C is required. This is normally not known explicitly, but only as an integral part of the measurement vector \underline{z} in Eq (85). It is therefore necessary to estimate the states of interest. In this deterministic treatment, a Luenberger observer is introduced, of the form

$$\hat{\underline{x}}_C = \underline{A}_C \hat{\underline{x}}_C + \underline{B}_C \underline{u} + \underline{K}_C (\underline{z} - \hat{\underline{z}}) \quad (89)$$

$$\hat{\underline{x}}_C(0) = \underline{0} \quad (90)$$

$$\hat{\underline{z}} = \underline{H}_C \hat{\underline{x}}_C \quad (91)$$

where the hat notation denotes an estimate. Eq (89) results in an estimate of the state whose error

$$\underline{e}_C = \hat{\underline{x}}_C - \underline{x}_C \quad (92)$$

approaches zero as $t \rightarrow \infty$ if the gain \underline{K}_C is chosen so that the observer is asymptotically stable. By combining Eqs (81), (85), (89), and (91), the estimator can be written in terms of the error states as

$$\dot{\underline{e}}_C = (\underline{A}_C - \underline{K}_C \underline{H}_C) \underline{e}_C + \underline{K}_C (\underline{H}_S \underline{x}_S + \underline{H}_R \underline{x}_R) \quad (93)$$

In order to insure the desired stability, we concentrate on finding the observer gain matrix \underline{K}_C such that the eigenvalues of $\underline{A}_C - \underline{K}_C \underline{H}_C$ in

$$\dot{\underline{e}}_C = (\underline{A}_C - \underline{K}_C \underline{H}_C) \underline{e}_C \quad (94)$$

retain negative real parts in the closed loop system. To be sure, the suppressed and residual terms in Eq (93) still impact the observer and are termed observation spillover (see Eq (105)); the method of suppressing these effects will be addressed in the next section.

In order to determine the gain \underline{K}_C , a problem analogous to Eq (94) is posed as

$$\dot{\underline{w}} = (\underline{A}_C - \underline{K}_C \underline{H}_C)^T \underline{w} \quad (95)$$

or
$$\dot{\underline{w}} = \underline{A}_C^T \underline{w} - \underline{H}_C^T \underline{g} \quad (96)$$

where
$$\underline{g} = \underline{K}_C^T \underline{w} \quad (97)$$

Since the eigenvalues of a matrix equal the eigenvalues of its transpose, a gain matrix \underline{K}_C that insures stability of Eq (95) will also satisfy the requirements for Eq (94). Eqs (96) and (97) respond to an application of steady state optimal regulator theory as before. A quadratic observer cost function to be minimized is

$$J_O = \int_0^\infty \left[\underline{w}^T \underline{Q}_O \underline{w} + \underline{g}^T \underline{R}_O \underline{g} \right] dt \quad (98)$$

with \underline{Q}_O and \underline{R}_O defined in a manner similar to those in Eq (86). These weighting matrices should be chosen so that the observer error in Eq (94) exhibits a rapid exponential decay. The optimal gain solution of Eq (97) is

$$\underline{K}_C^T = +\underline{R}_O^{-1} \underline{H}_C^T \underline{P} \quad (99)$$

where \underline{P} is the solution to the steady state matrix Riccati equation

$$\underline{P} \underline{A}_C^T + \underline{A}_C \underline{P} - \underline{P} \underline{H}_C^T \underline{R}_O^{-1} \underline{H}_C \underline{P} + \underline{Q}_O = 0 \quad (100)$$

The state equations (81), (82), and (83), may now be written in terms of the gain and error states as

$$\dot{\underline{x}}_c = (\underline{A}_c + \underline{B}_c \underline{G}_c) \underline{x}_c + \underline{B}_c \underline{G}_c \underline{e}_c \quad (101)$$

$$\dot{\underline{x}}_s = \underline{A}_s \underline{x}_s + \underline{B}_s \underline{G}_c \underline{x}_c + \underline{B}_s \underline{G}_c \underline{e}_c \quad (102)$$

$$\dot{\underline{x}}_r = \underline{A}_r \underline{x}_r + \underline{B}_r \underline{G}_c \underline{x}_c + \underline{B}_r \underline{G}_c \underline{e}_c \quad (103)$$

Forming the augmented state vector \underline{z} as

$$\underline{z} = \begin{bmatrix} \underline{x}_c \\ \dots \\ \underline{e}_c \\ \dots \\ \underline{x}_s \\ \dots \\ \underline{x}_r \end{bmatrix} \quad (104)$$

allows the expression of the closed loop system as

$$\dot{\underline{z}} = \begin{bmatrix} (\underline{A}_c + \underline{B}_c \underline{G}_c) & \underline{B}_c \underline{G}_c & \underline{0} & \underline{0} \\ \underline{0} & (\underline{A}_c - \underline{K}_c \underline{H}_c) & \underline{K}_c \underline{H}_s & \underline{K}_c \underline{H}_r \\ \underline{B}_s \underline{G}_c & \underline{B}_s \underline{G}_c & \underline{A}_s & \underline{0} \\ \underline{B}_r \underline{G}_c & \underline{B}_r \underline{G}_c & \underline{0} & \underline{A}_r \end{bmatrix} \underline{z} \quad (105)$$

Note that the application of control gains \underline{G}_C affects not only the \underline{x}_C modes but also the uncontrolled modes through the control spillover terms $\underline{B}_S \underline{G}_C$ and $\underline{B}_r \underline{G}_C$. Likewise, the presence of the suppressed and residual modes impacts the observer through the observation spillover terms $\underline{K}_C \underline{H}_S$ and $\underline{K}_C \underline{H}_r$. The effect of these spillover terms may be small; on the other hand, as control and observation gains \underline{G}_C and \underline{K}_C are increased in an effort to control the \underline{x}_C terms more precisely, the spillover terms may in fact cause overall system instabilities.

Transformation Technique

In light of the above mentioned potential for instabilities, a method is desired to eliminate or suppress the spillover effects. Eq (105) represents the full mathematical system model; the representation of only those modes which require active intervention, either through direct control or spillover suppression, is

$$\dot{\underline{z}} = \begin{bmatrix} (\underline{A}_C + \underline{B}_C \underline{G}_C) & \underline{B}_C \underline{G}_C & \underline{0} \\ \underline{0} & (\underline{A}_C - \underline{K}_C \underline{H}_C) & \underline{K}_C \underline{H}_S \\ \underline{B}_S \underline{G}_C & \underline{B}_S \underline{G}_C & \underline{A}_S \end{bmatrix} \underline{z} \quad (106)$$

where

$$\underline{z} = \begin{bmatrix} \underline{x}_C \\ \dots \\ \underline{e}_C \\ \dots \\ \underline{x}_S \end{bmatrix} \quad (107)$$

If the system eigenvalues of Eq (106) can be guaranteed to have negative real parts, then this system will be stable. Now the diagonal blocks of Eq (106) have stable eigenvalues: $(\underline{A}_C + \underline{B}_C \underline{G}_C)$ and $(\underline{A}_C - \underline{K}_C \underline{H}_C)$ because the gains have been formulated so that this is so, and \underline{A}_S due to the natural modal damping. Since the eigenvalues of a block triangular matrix are equal to the eigenvalues of its diagonal blocks, a block triangularization of the matrix of Eq (106) would produce the desired stability. Causing $\underline{B}_S \underline{G}_C = \underline{0}$ or $\underline{K}_C \underline{H}_S = \underline{0}$ and rearranging accomplishes this triangularization. Here, a transformation is sought such that $\underline{K}_C \underline{H}_S = \underline{0}$.

An obvious solution is $\underline{K}_C = \underline{0}$; however, this also renders $\underline{K}_C \underline{H}_C = \underline{0}$, disrupting the observer stability. What is needed is a transformation such that

$$\underline{K}_C \underline{H}_S = \underline{0} \quad (108)$$

while $\underline{K}_C \underline{H}_C \neq \underline{0} \quad (109)$

or, in the form convenient to the following development

$$\underline{H}_S^T \underline{K}_C^T = \underline{0} \quad (110)$$

$$\underline{H}_C^T \underline{K}_C^T \neq \underline{0} \quad (111)$$

A transformation \underline{T} would accomplish this if

$$\underline{H}_S^T \underline{T} = \underline{0} \quad (112)$$

$$\underline{H}_C^T \underline{T} \neq \underline{0} \quad (113)$$

Assuming such a transformation exists, we define a vector

$$\underline{g} = \underline{T} \underline{v} \quad (114)$$

such that its substitution into Eq (96) yields

$$\dot{\underline{w}} = \underline{A}_C^T \underline{w} - \underline{H}_C^T \underline{T} \underline{v} \quad (115)$$

or
$$\dot{\underline{w}} = \underline{A}_C^T \underline{w} - \underline{H}_C^{*T} \underline{v} \quad (116)$$

with
$$\underline{H}_C^{*T} = \underline{H}_C^T \underline{T} \quad (117)$$

and
$$\underline{v} = \underline{K}_C^{*T} \underline{w} \quad (118)$$

where the * denotes "transformed" quantities. Comparing Eqs (115) and (118) to Eq (96), we find

$$\underline{K}_C^T = \underline{T} \underline{K}_C^{*T} \quad (119)$$

However, as \underline{T} is not in general a square matrix, the new observer gain \underline{K}_C^* is found as before from the solution to the steady state optimal regulator problem:

$$\underline{K}_C^{*T} = \underline{R}_O^{*-1} \underline{H}_C^* \underline{P} \quad (120)$$

with \underline{p} generated from the steady state matrix Riccati equation

$$\underline{p}\underline{A}_C^T + \underline{A}_C\underline{p} - \underline{p}\underline{H}^*{}^T\underline{R}_O^{*-1}\underline{H}^*\underline{p} + \underline{Q}_O^* = \underline{0} \quad (121)$$

where

$$\underline{R}_O^* = \underline{T}^T \underline{R}_O \underline{T} \quad (122)$$

Substituting Eq (119) into Eq (110) demonstrates that the gain matrix \underline{K}_C^* in fact suppresses the observer spillover terms if the \underline{T} matrix can be found that satisfies Eqs (112) and (113). This \underline{T} matrix is found by a singular value decomposition of \underline{H}_S^T .

For a general real matrix $\underline{A} \in \mathbb{R}^{m \times n}$, the following is true (22):

$$\underline{V}^T \underline{A} \underline{U} = \begin{bmatrix} \underline{\Sigma} & \underline{0} \\ \underline{0} & \underline{0} \end{bmatrix} \quad (123)$$

$$\underline{\Sigma} \equiv \text{diag}(\sigma_1, \sigma_2, \dots, \sigma_q)$$

$\sigma_1 \dots$ \equiv singular values of \underline{A} arranged in descending order
(square roots of the non-zero eigenvalues of $\underline{A}^T \underline{A}$)

$\underline{U} \equiv$ nxn matrix whose columns are right singular vectors
of \underline{A} (eigenvectors of $\underline{A}^T \underline{A}$)

$\underline{V} \equiv$ mxm matrix whose columns are left singular vectors
of \underline{A} (eigenvectors of $\underline{A} \underline{A}^T$)

$q \equiv$ rank of \underline{A}

Thus, the number of non-zero singular values equals the rank of \underline{A} . Partitioning \underline{U} and \underline{V} to isolate the eigenvectors

associated with the non-zero singular values,

$$\underline{U} = \begin{bmatrix} \underline{U}_q & : & \underline{U}_{n-q} \end{bmatrix} \quad (124)$$

$$\underline{V} = \begin{bmatrix} \underline{V}_q & : & \underline{V}_{m-q} \end{bmatrix} \quad (125)$$

From Eq (117),

$$\underline{A} = \underline{V}_q \underline{\Sigma} \underline{U}_q^T \quad (126)$$

Since \underline{U} is an orthogonal matrix,

$$\underline{U}_q^T \underline{U}_{n-q} = \underline{0} \quad (127)$$

so that

$$\underline{A} \underline{U}_{n-q} = \underline{V}_q \underline{\Sigma} \underline{U}_q^T \underline{U}_{n-q} = \underline{0} \quad (128)$$

In the problem at hand, where $\underline{A} \equiv \underline{H}_s^T$, comparing Eq (104) and Eq (122), the required transformation is

$$\underline{T} = \underline{U}_{p-q} \quad (129)$$

where

$\underline{U} \equiv$ matrix whose columns are the eigenvectors of $\underline{H}_s \underline{H}_s^T$
associated with its zero singular values

$p \equiv$ number of sensors

$q \equiv$ rank of \underline{H}_s^T

Assuming \underline{H}_s to be a full rank matrix with dimensions $p \times n_s$

in the case of position sensors only, then its rank will be the minimum of p or n_s . Eq (129) shows that in order that \underline{T} be other than the trivial solution $\underline{T} = \underline{0}$, p must be greater than q ; that is, the number of sensors p must be greater than the number of suppressed modes n_s .

A parallel development to eliminate control spillover terms $\underline{B}_s \underline{G}$ is given in (1), (8).

V. COMPUTER IMPLEMENTATION

Although the generation of a working computer algorithm was an extremely time consuming portion of the thesis process, its description here will be limited to brief comments. A source code listing and flow diagram may be found in Appendix B.

The computer implementation of the model reduction techniques was fairly straightforward. The code was designed to be compatible with data files created for the controller design algorithm. Input consists of the pertinent finite element analysis results for the model of interest; output is in the form of ranked modes from the internal balancing scheme and from the modal cost analysis scheme. In addition, a check is made of the appropriateness of the approximate internal balancing method for the case at hand.

The controller design and spillover suppression algorithm used is a scaled version of the code developed by Aldridge (1). In its original form the code was designed for the investigation of multiple controller systems. Here it was modified for use with one controller only, as the variable of interest in this study is the reduced order model and not the control scheme. In addition, corrections were made to the time response portion implemented by Baker (3) so that true system output versus time may be observed.

Plotting routines and the use of procedure files allow the output of eigenvalue or time response plots via the CDC Cyber NOS interactive system with only one user input system command.

VI. INVESTIGATION AND RESULTS

The CSDL I model was used as the principle test case for the study. Various situations were investigated involving the different model reduction schemes, different combinations of controlled and suppressed modes, and different actuator/sensor combinations. Eigenvalue plots were generated for each case; in addition, plots depicting the time response of node one under the action of the various feedback control configurations allowed observation of the physical reactions to each arrangement. These time response plots track the radius of deflection from the undeflected position subject to the initial conditions given in Appendix A. In all cases the sampling rate is 20 Hz.

Figure 4 shows the uncontrolled response and the effects of controlling the first four modes with a cost function weighting of 20. It is desired that motion due to the initial conditions be effectively damped in 20 seconds; this time region will be examined in subsequent plots.

Two actuator/sensor configurations were investigated:

- 1) six co-located actuator/sensor pairs on the "legs" of the structure, and
- 2) three actuators on the "arms" of the tetrahedron, 6 sensors on the "legs" (see Figure 2).

Experimentation determined that a control weighting of 20 made the residual modes sufficiently sensitive to spillover to be observed while maintaining reasonable stability in the unsup-

pressed control case. Thus, differences due to the model reduction were sought in the unsuppressed case; often, though, such differences were not apparent until suppression was applied.

Application of the internal balancing and modal cost analysis methods yields modal rankings for the CSDL I as given in Figure 5 and 6. As exactly known initial conditions, not disturbances, are considered for the CSDL I, zero mean white noise disturbances were considered to be applied at the actuator locations to generate the modal cost rankings. Weighting the output variables equally, the modal cost rankings are essentially the same as internal balancing except for the inversion of modes 1 and 2. The rankings suggested by Figure 5 indicate, for example, that although mode 6 is highly controllable/observable for the 6/6 co-located actuator/sensor case, its usefulness in achieving the desired performance objective is minimal. Thus it is ranked last in terms of modes to be controlled.

Figure 7 is included as an aid to interpreting the eigenvalue plots. In all cases, weightings for the controlled mode and associated observer states are equal; under this condition the observer eigenvalues will typically "shadow" those of the controlled modes. The uncontrolled modes remain in the vicinity of their naturally damped position, disturbed only by the previously discussed spillover

effects. Note that mode seven is driven close to instability by this effect, while the damping of mode eight is actually improved. Application of the suppression technique of Section IV to modes 6, 7, and 8 removes this spillover; however, the tradeoff required is evident in the consequent reduced damping of the controlled modes. Note that mode 6 is typically unaffected by spillover, and, although easily controlled, has minimal effect on the line-of-sight performance.

Figures 8 thru 21 depict various controlled/suppressed mode arrangements chosen according to frequency truncation and internal balancing. In cases exhibiting instability caused by spillover, extended scale time responses are included to show the long term system behavior. These instabilities are often minimal and, in concert with the well damped modes, result in an essentially steady state motion as shown in Figure 10. More severe instabilities are obvious in Figures 31 and 33. The degree of instability for a given case is governed by the cost function weightings of Eq (86) and (98). Thus, an attempt to improve the output response by simply adding more control energy to the controlled modes may have the opposite effect.

Unsuppressed time response differences brought about solely due to the choice of model reduction schemes are not significant until the case of 5 controlled modes in Figures 18 and 20. Here, the best performance before application of suppression was achieved by controlling 5 modes according to the balancing selection process as in Figure 20.

Suppression actually degraded the performance somewhat, as the damping of mode 3 had been enhanced by the spillover; elimination of this spillover reduced the damping and diverted control energy from the controlled modes to accomplish this.

A conclusion that might be reached is that one could examine the controlled, unsuppressed eigenvalues and suppress only those modes whose damping was degraded by spillover. However, a test case of suppressing only mode 9 in Figure 20 resulted in poorer performance, as mode 3 was driven unstable in the process. A predictable relationship between spillover and mode stability is elusive.

In addition, there are situations when the balancing algorithm chooses a mode to be suppressed that has been driven unstable by spillover, whereas simple frequency truncation does not. This is true when controlling only the two most critical modes as shown in Figures 8 thru 13; time responses after suppression reflect this difference.

A second actuator/sensor configuration was examined consisting of three actuators located on the tetrahedron arms and six sensors on the legs. Such a setup represents a possible controller designed to reduce hardware complexity and computation requirements. Corresponding internal balancing rankings and modal costs are given in Figures 22 and 23. Figures 29 thru 33 illustrate some representative controller behaviors for frequency truncated and internally balanced reduced models. An interesting effect is demon-

strated in the unsuppressed time responses of Figures 25 and 28. Although both are unstable, the balancing model is much more so, illustrating the fact that the choice of a reduced order model by the one criterion of actuator/output modal ranking does not predict what the closed loop behavior will be. Here, the balancing algorithm does not anticipate the instability introduced by the spillover effect on mode 4. When suppression is incorporated, however, the balanced model outperforms that generated by frequency truncation.

Internal balancing modal rankings for the first thirty-three modes of the CSDL II model are given in Figures 34 and 35. Assuming unit intensity white noise disturbances at the actuator locations, modal costs in Figure 36 yield identical rankings. The first three modes are attitude rigid body modes; they are immediately included in any controller design. The modal observability/controllability given by the actuator/sensor ranking matches reasonably well with the modes most significant to the output; it can be expected from this that the actuator/sensor configuration would be able to damp those modes most critical to the performance. Time responses for the CSDL II model were not generated in this study.

As discussed previously, for higher order models the distinctness of the natural frequencies may present a problem. Modes for which the approximate internal balancing algorithm is seriously in error are given in Table 1. For the most significant modes as ranked in Figures 34 and 35, only mode 6

does not meet the distinctness requirement for a valid approximate balanced model. Thus, deletion of all the modes in Table 1 still leaves a usable ranking of modes most critical to the control of the CSDL II line-of-sight pointing error.

NODE ONE TIME RESPONSE

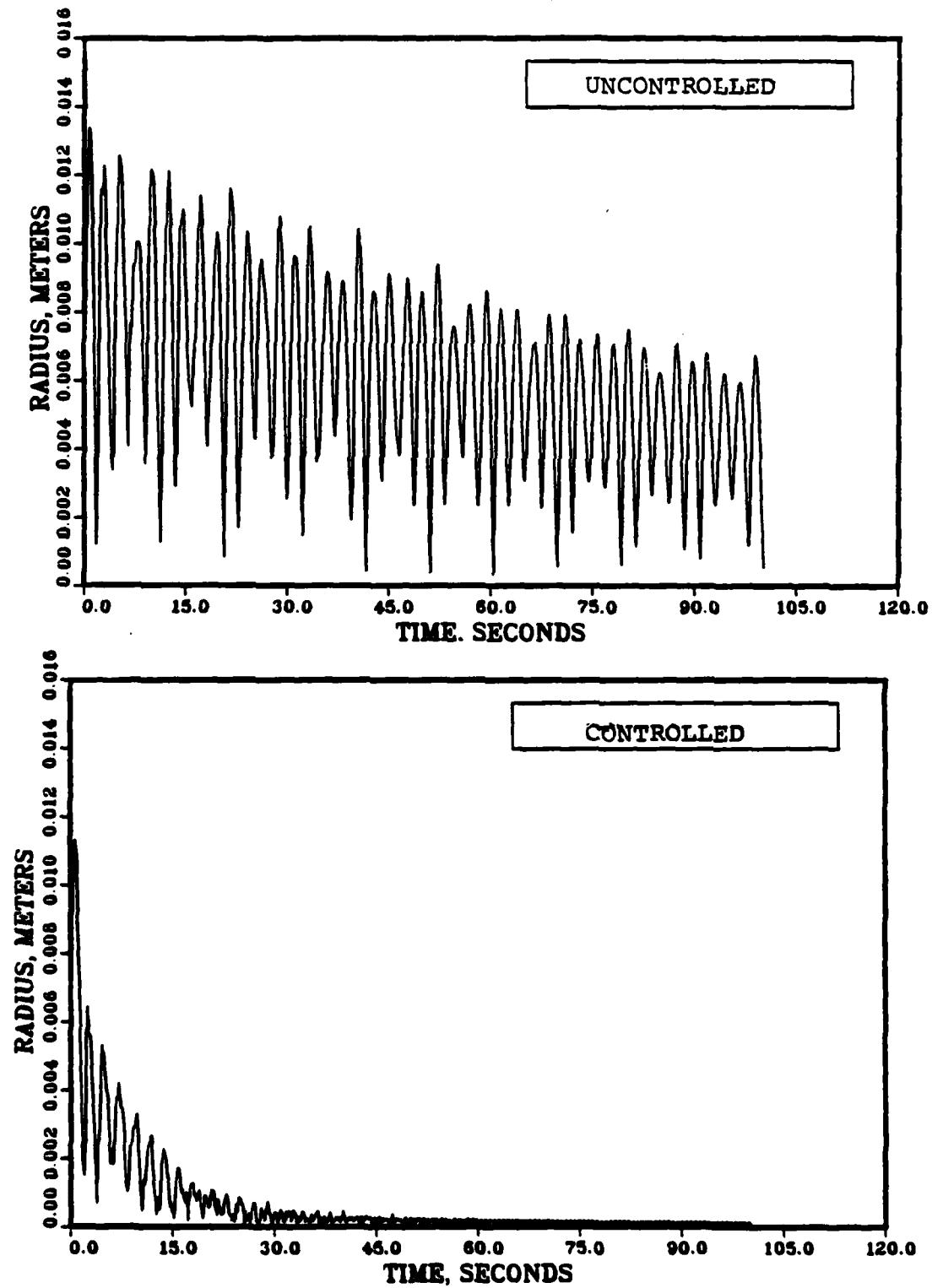
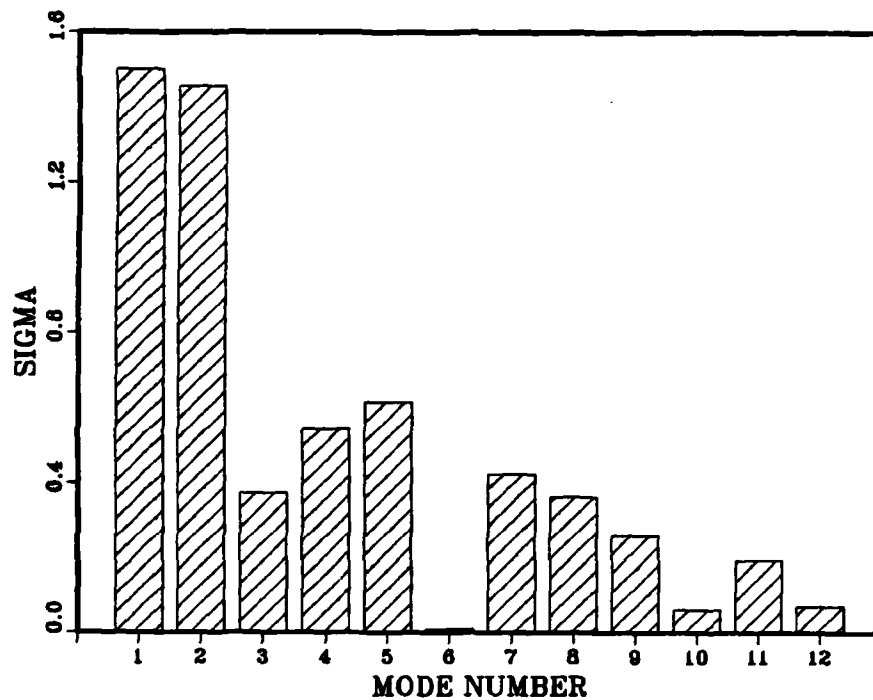


FIGURE 4. Uncontrolled CSDL I response;
Typical controlled response

MODAL RANKINGS, ACTUATOR/OUTPUT



MODAL RANKINGS, ACTUATOR/SENSOR

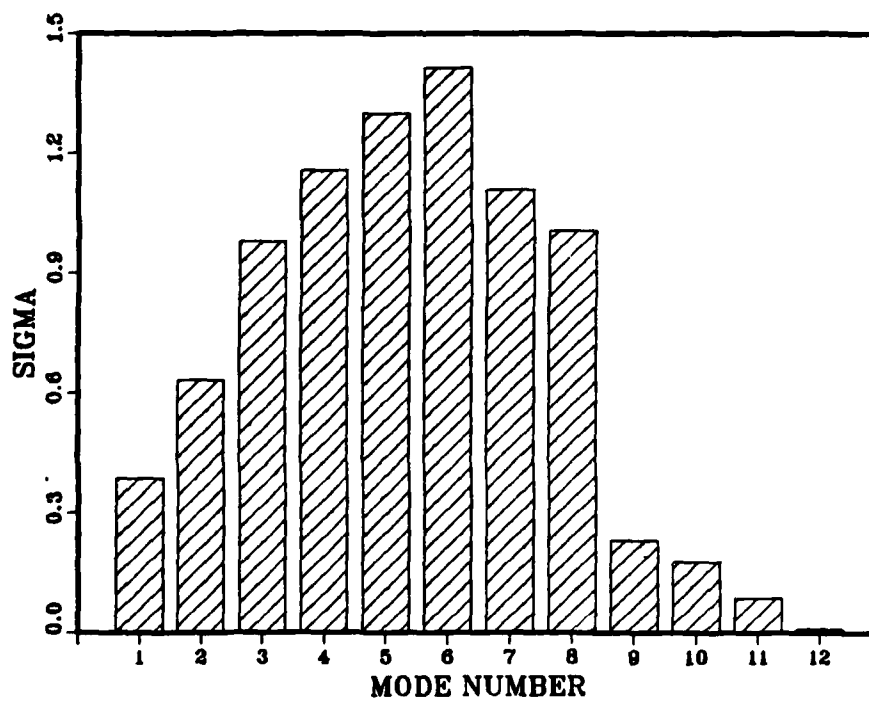


FIGURE 5. Internal Balancing Rankings, σ_{BC} & σ_{BH}
CSDL I, 6/6 act/sen

MODAL COST

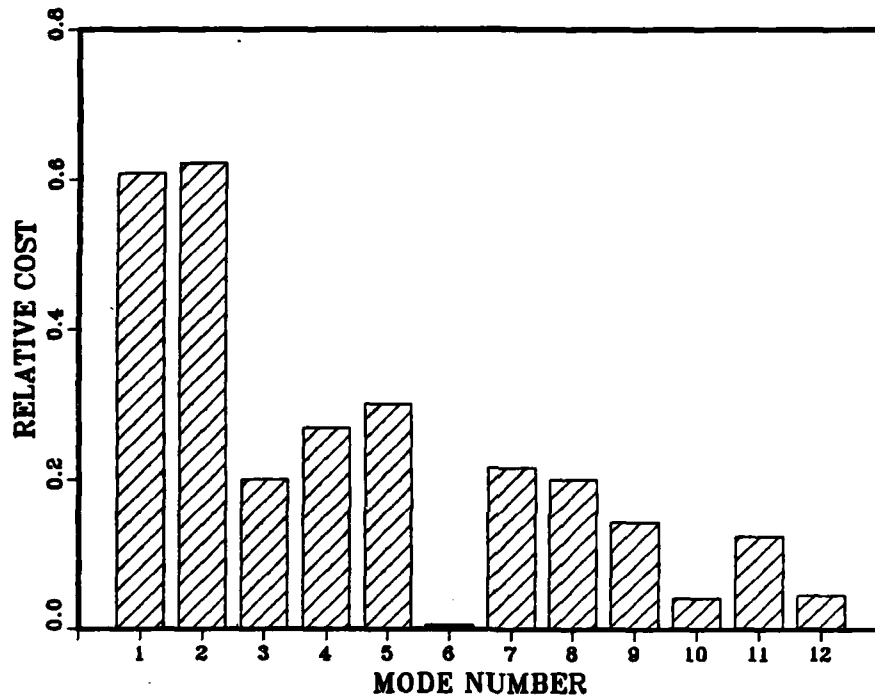


FIGURE 6. Modal Cost Rankings, CSDL I, 6/6 act/sen

CONTROLLED SYSTEM EIGENVALUES

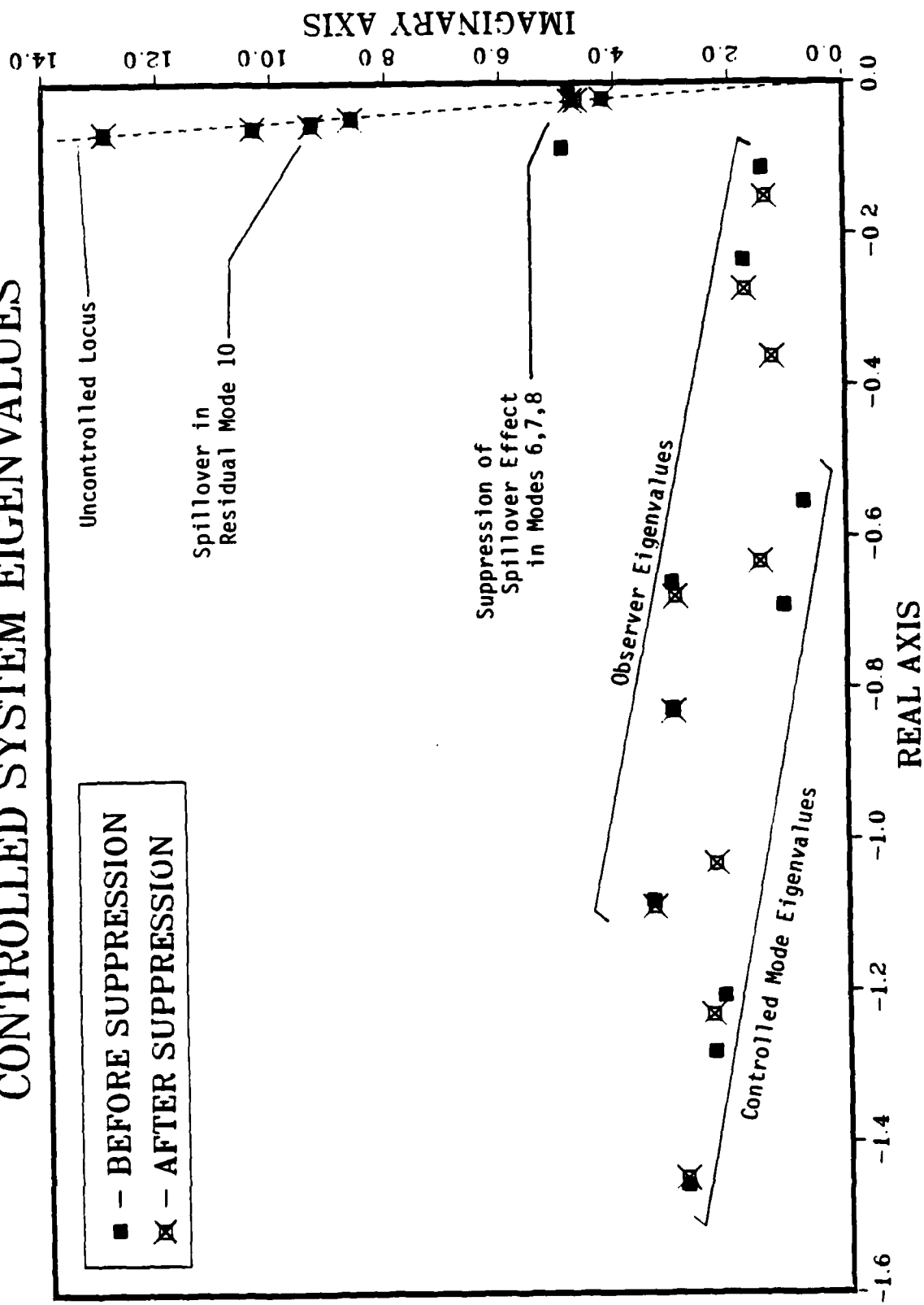
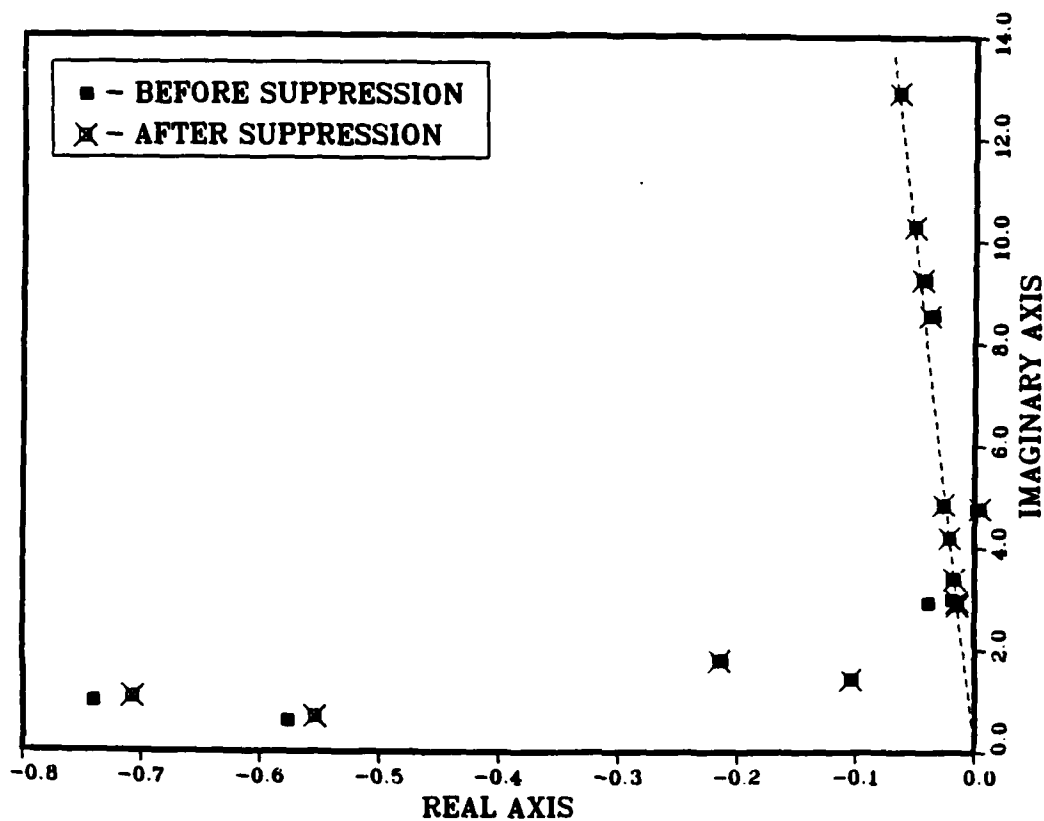


FIGURE 7. Typical CSDL I Eigenvalue Plot

CONTROLLED SYSTEM EIGENVALUES (CASE 1)



CONTROLLED MODES : 1 2	ZETA = 0.005
SUPPRESSED MODES : 3 4 5 6	WEIGHTING = 20.00
RESIDUAL MODES : 7 8 9 10 11 12	

FIGURE 8. Frequency Truncation, CSDL I, 6/6 act/sen
2 controlled - 4 suppressed modes

NODE ONE TIME RESPONSE (CASE 1)

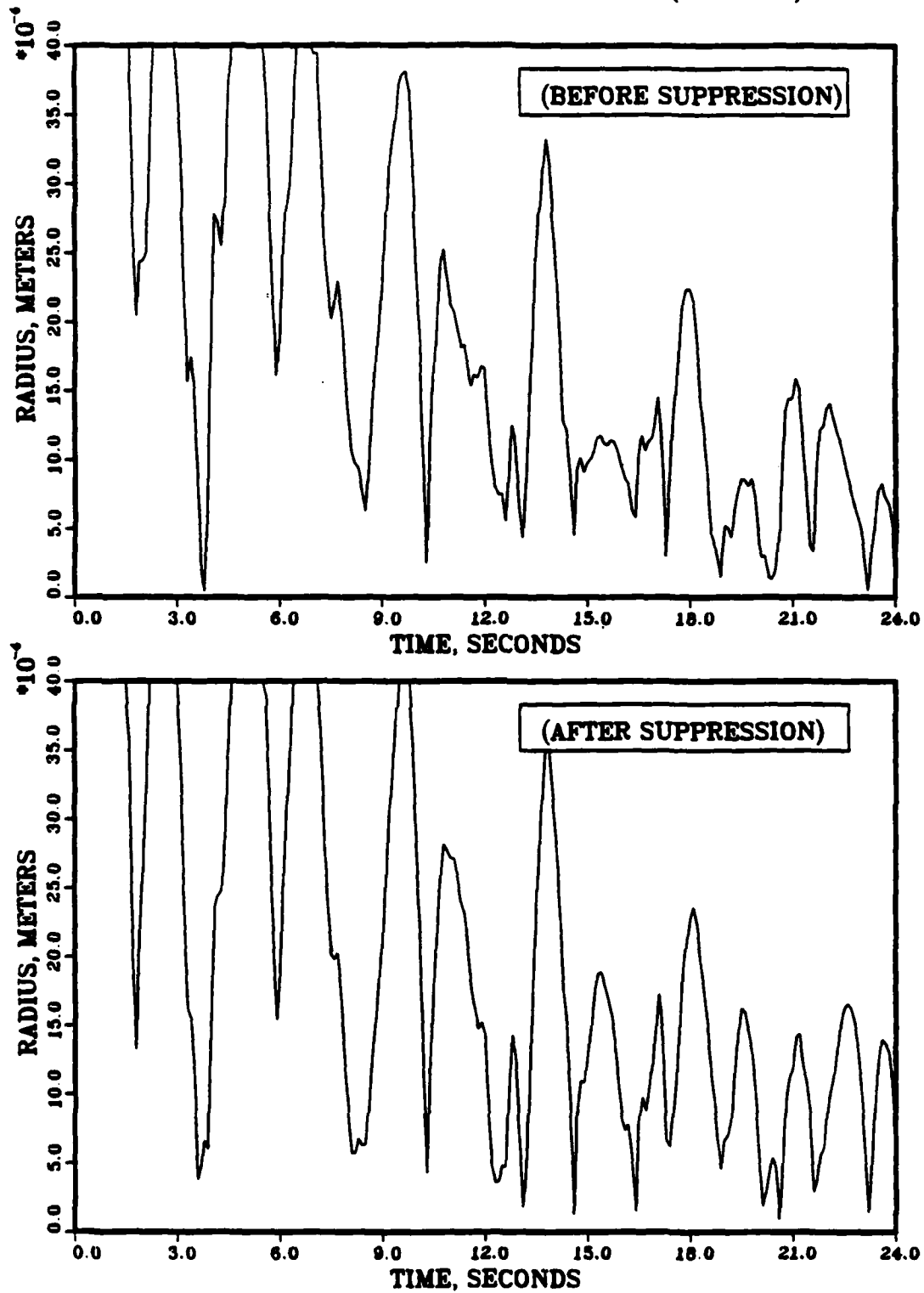


FIGURE 9. Time Response - Frequency Truncation, CSDL I
2 controlled - 4 suppressed modes, 6/6 act/sen

NODE ONE TIME RESPONSE (CASE 1)

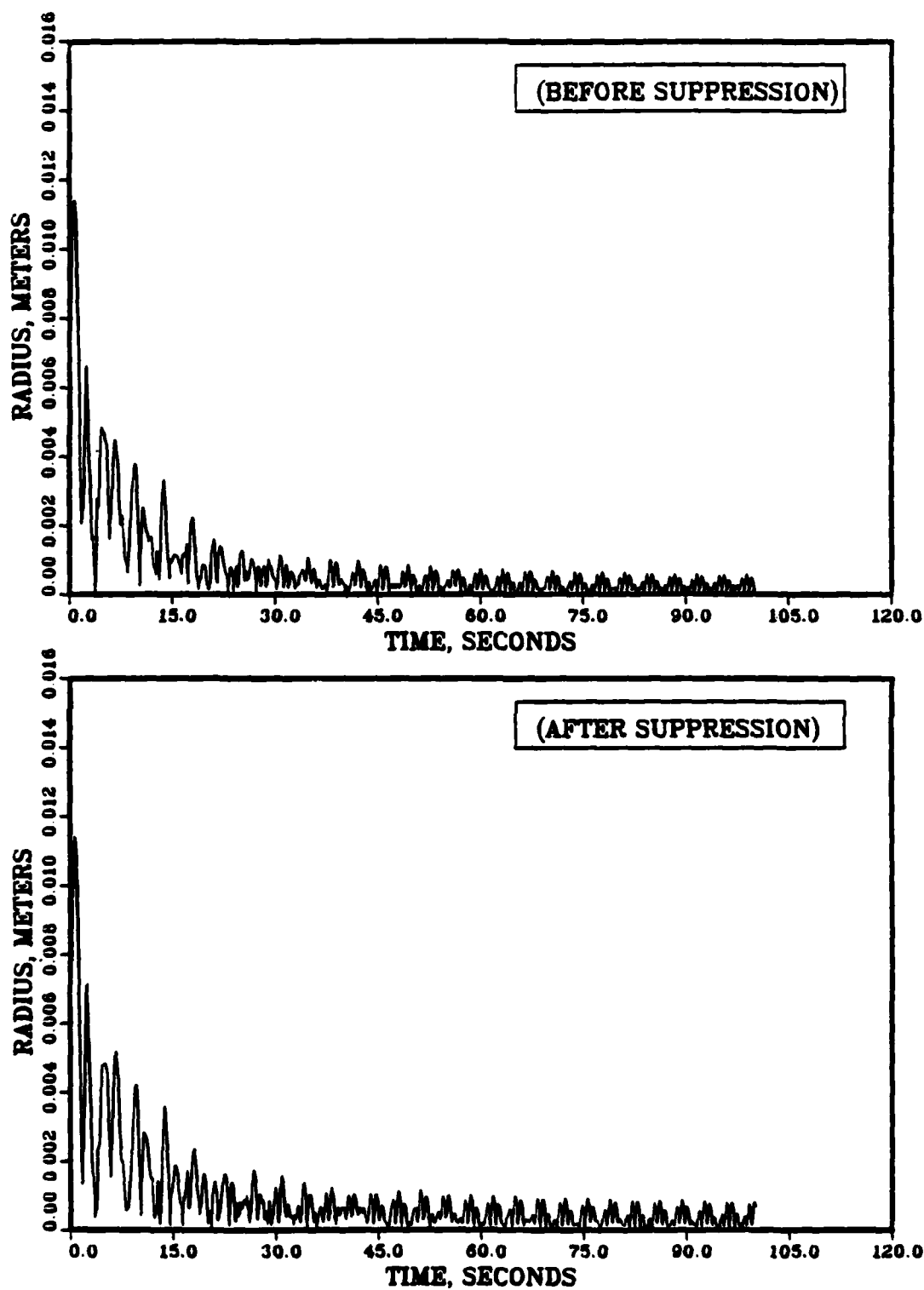
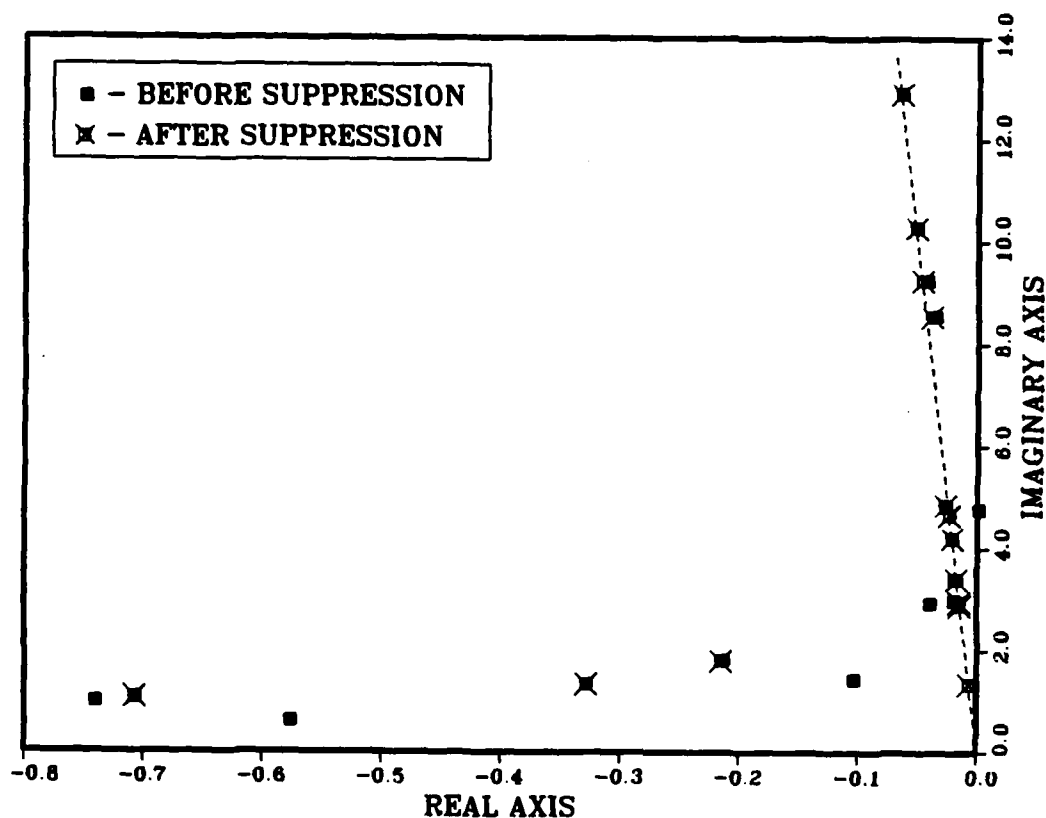


FIGURE 10. Extended scale time response for case 1

CONTROLLED SYSTEM EIGENVALUES (CASE 2)



CONTROLLED MODES : 1 2

SUPPRESSED MODES : 5 4 7 3

RESIDUAL MODES : 8 9 11 12 10 6

ZETA = 0.005

WEIGHTING = 20.00

FIGURE 11. Internal Balancing, CSDL I, 6/6 act/sen
2 controlled - 4 suppressed modes

NODE ONE TIME RESPONSE (CASE 2)

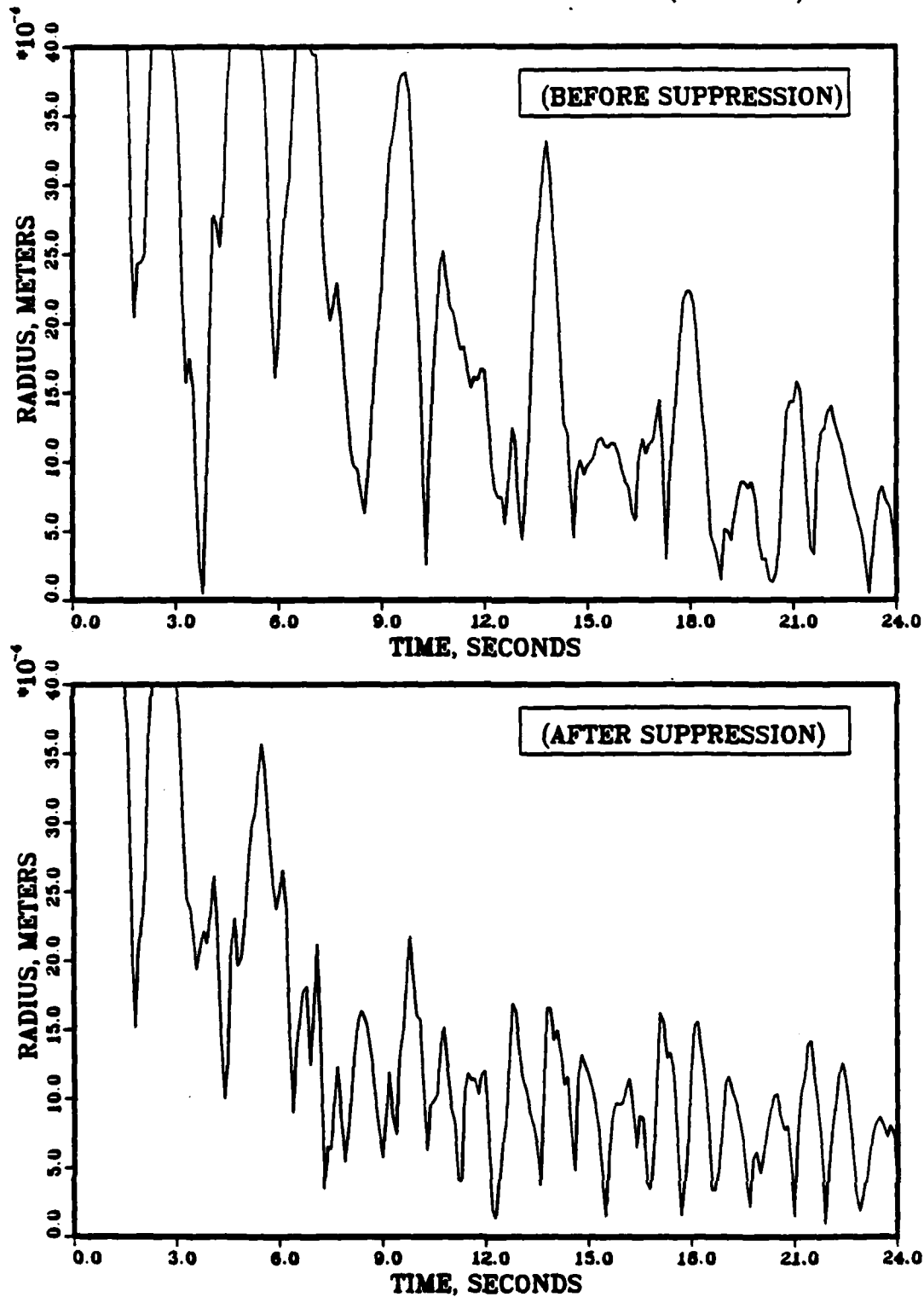


FIGURE 12. Time Response - Internal Balancing, CSDL I
2 controlled - 4 suppressed modes, 6/6 act/sen

NODE ONE TIME RESPONSE (CASE 2)

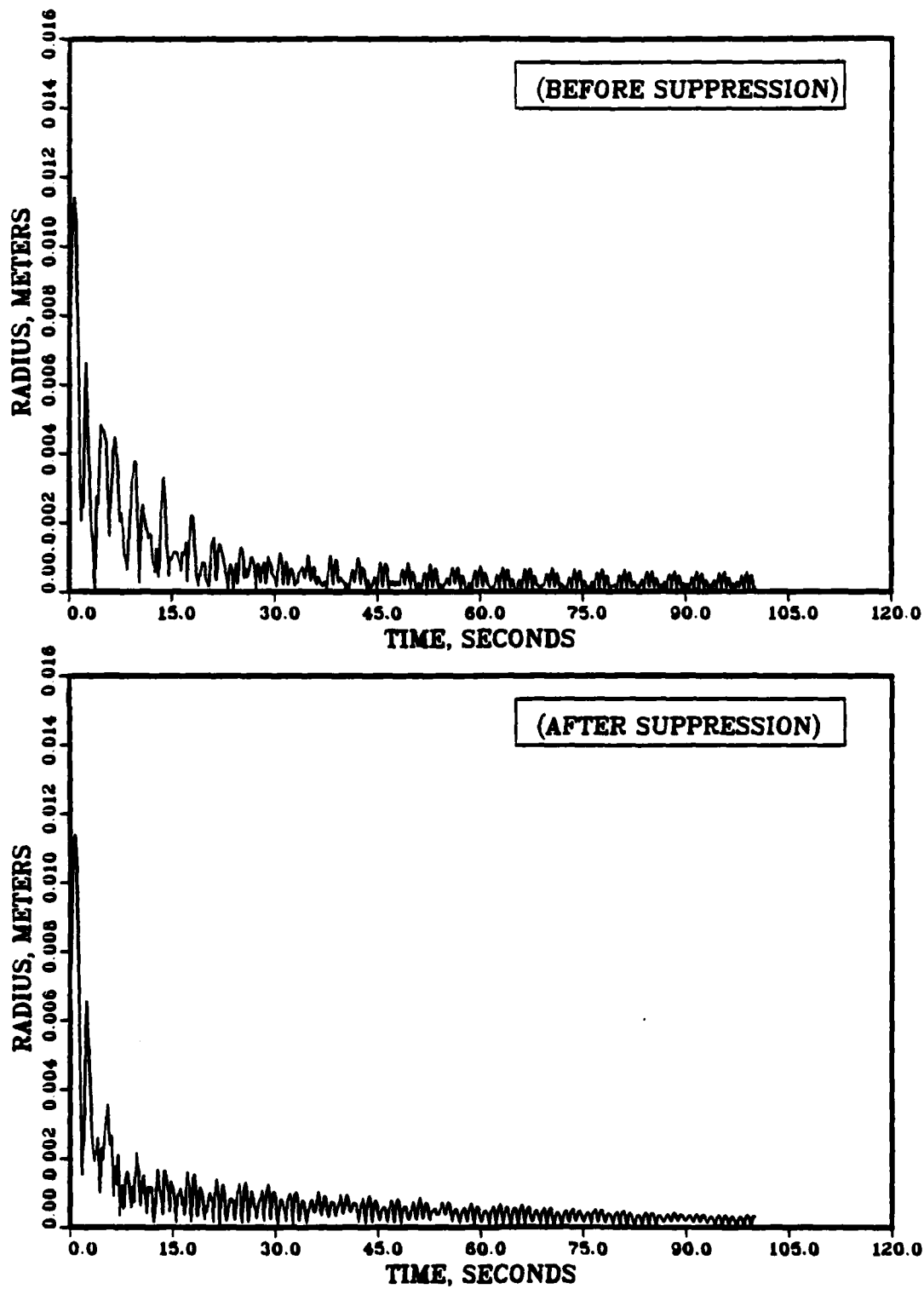
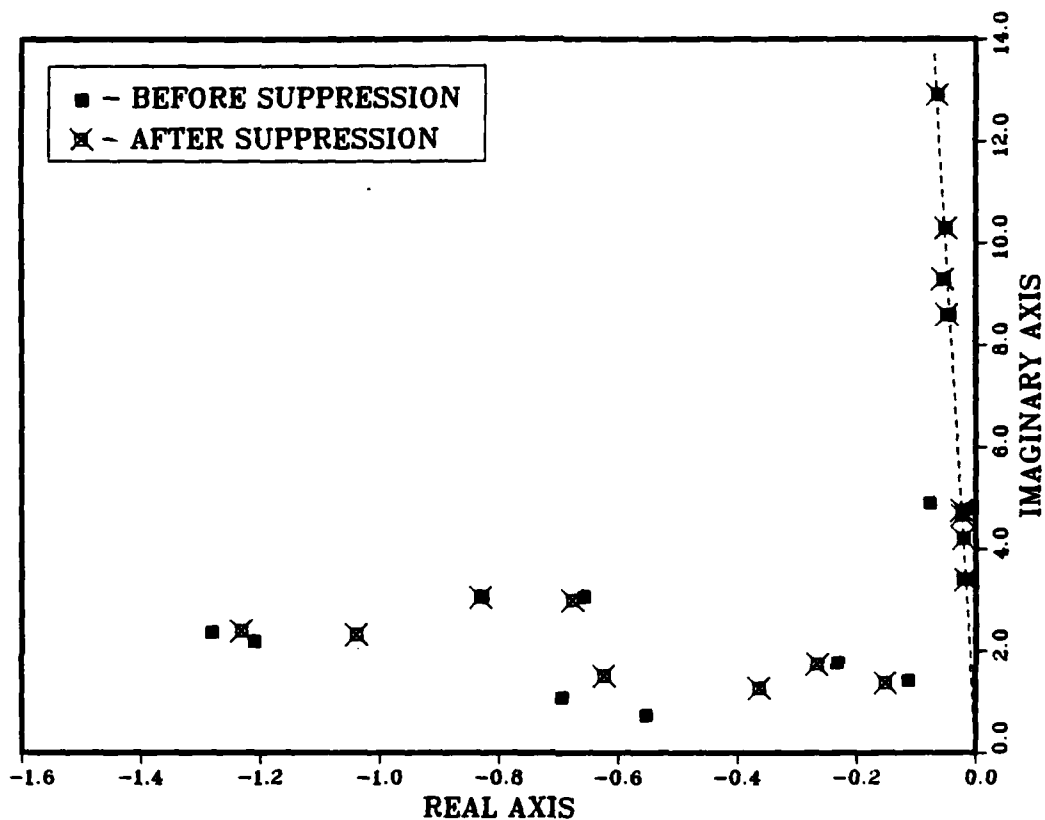


FIGURE 13. Extended scale time response for case 2

CONTROLLED SYSTEM EIGENVALUES (CASE 3)



CONTROLLED MODES : 1 2 3 4
 SUPPRESSED MODES : 5 6 7 8
 RESIDUAL MODES : 9 10 11 12

ZETA = 0.005
 WEIGHTING = 20.00

FIGURE 14. Frequency Truncation, CSDL I, 6/6 act/sen
 4 controlled - 4 suppressed modes

NODE ONE TIME RESPONSE (CASE 3)

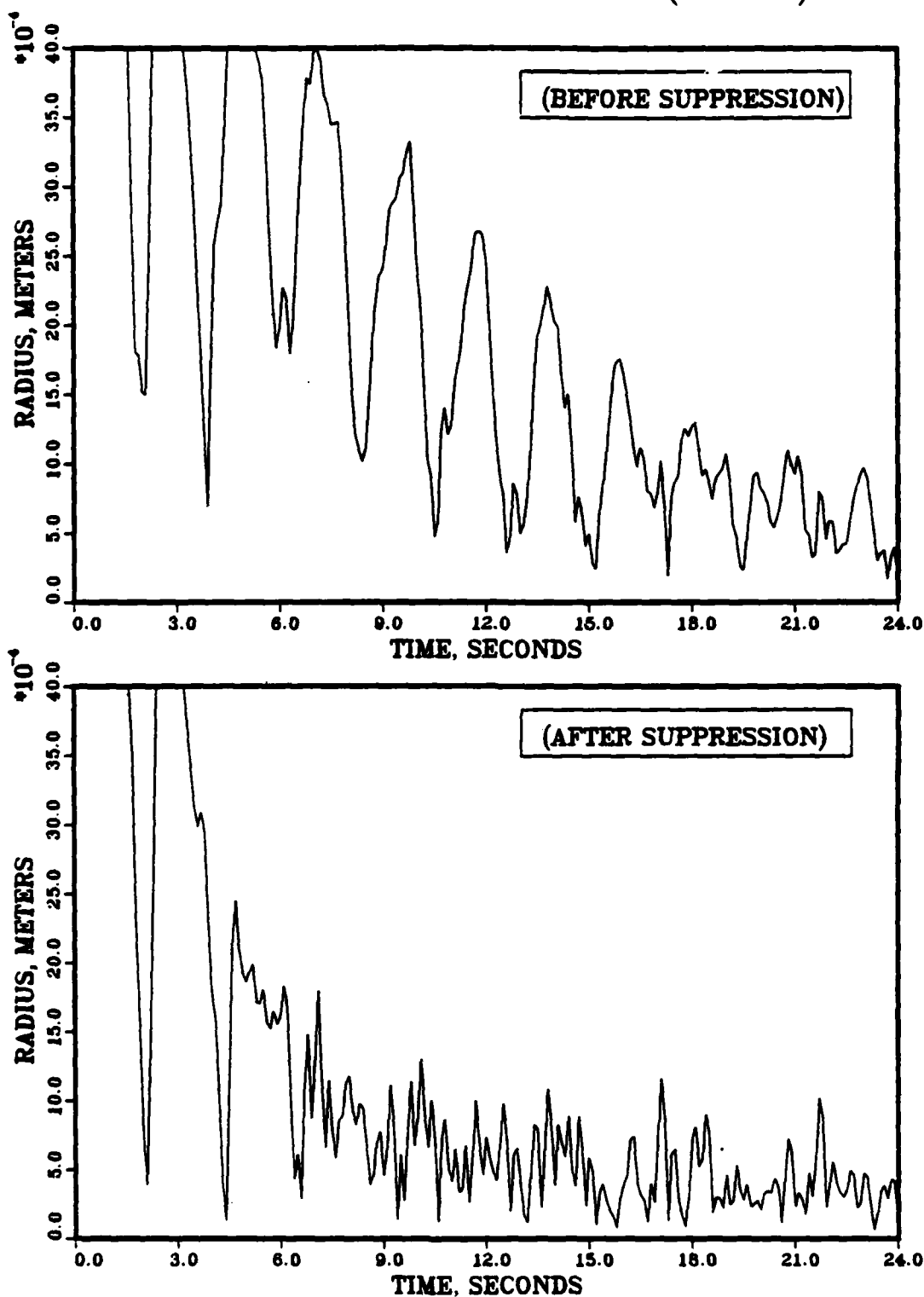
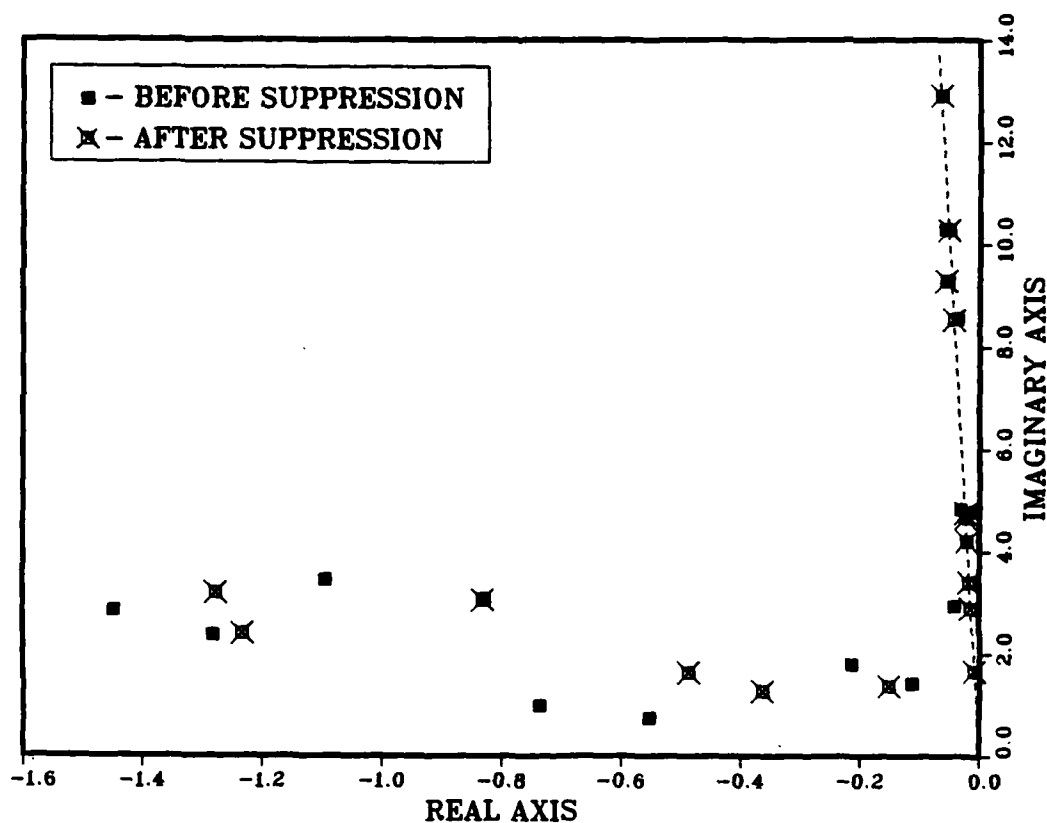


FIGURE 15. Time Response - Frequency Truncation, CSDL I
4 controlled - 4 suppressed modes, 6/6 act/sen

CONTROLLED SYSTEM EIGENVALUES (CASE 4)



CONTROLLED MODES : 1 2 5 4
 SUPPRESSED MODES : 7 3 8 9
 RESIDUAL MODES : 11 12 10 6

ZETA = 0.005
 WEIGHTING = 20.00

FIGURE 16. Internal Balancing, CSDL I, 6/6 act/sen
 4 controlled - 4 suppressed modes

NODE ONE TIME RESPONSE (CASE 4)

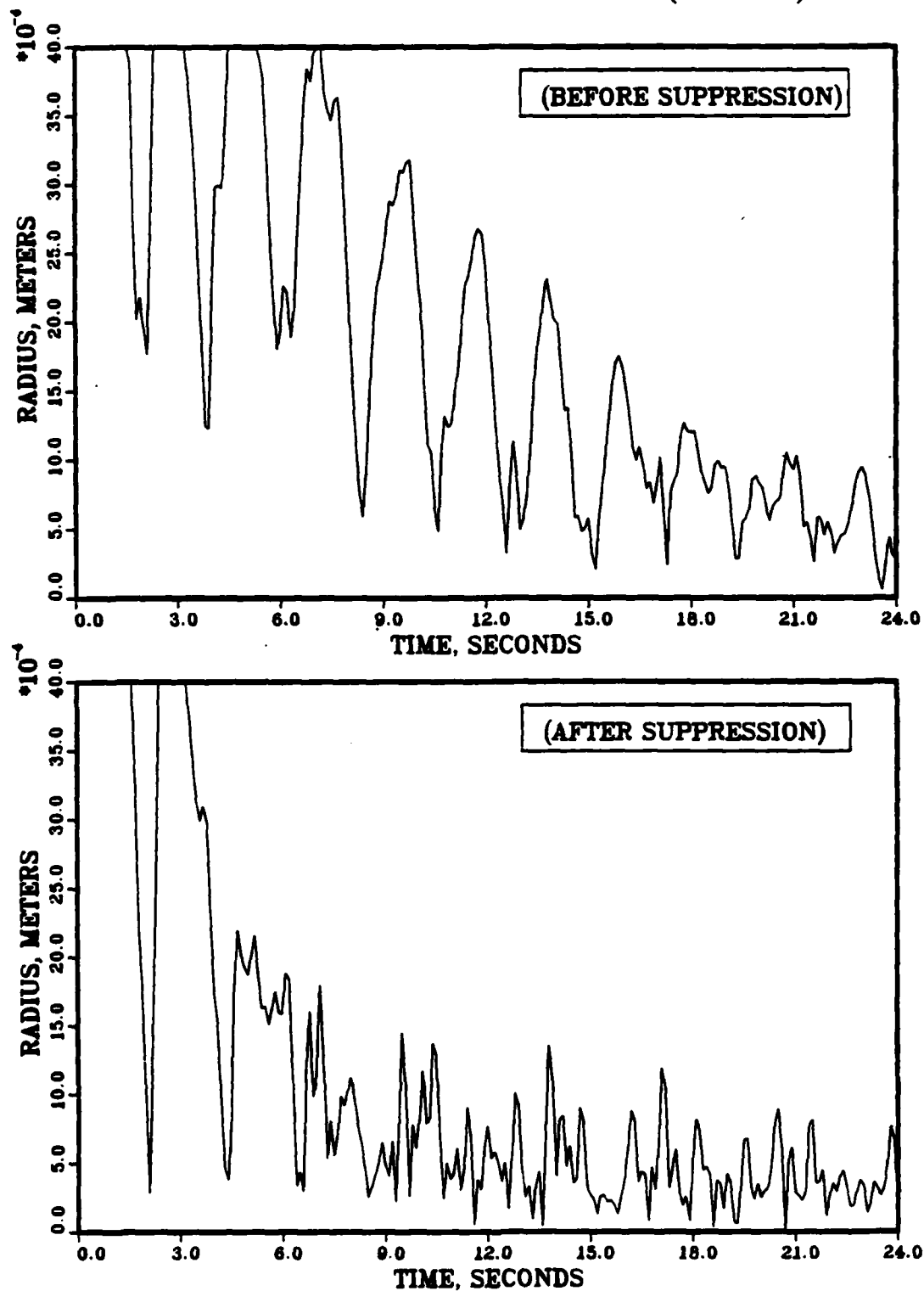
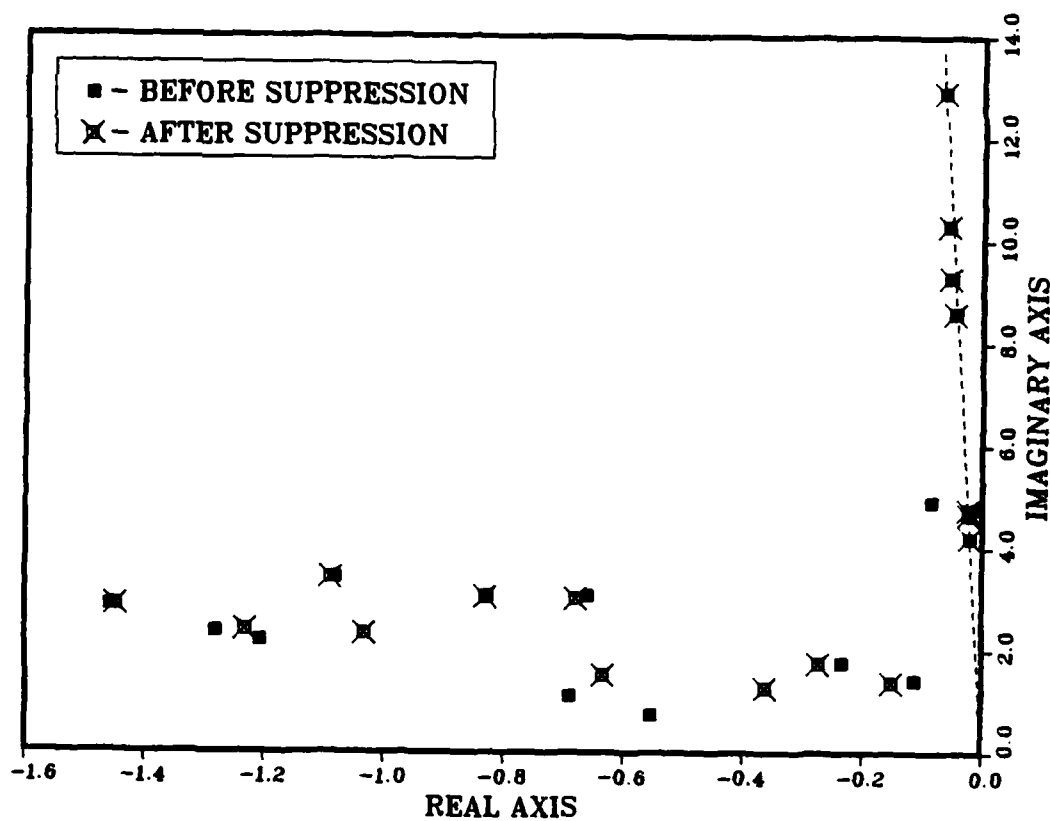


FIGURE 17. Time Response - Internal Balancing, CSDL I
4 controlled - 4 suppressed modes; 6/6 act/sen

CONTROLLED SYSTEM EIGENVALUES (CASE 5)



CONTROLLED MODES : 1 2 3 4 5
 SUPPRESSED MODES : 6 7 8
 RESIDUAL MODES : 9 10 11 12

ZETA = 0.005
 WEIGHTING = 20.00

FIGURE 18. Frequency Truncation, CSDL I, 6/6 act/sen
 5 controlled - 3 suppressed modes

NODE ONE TIME RESPONSE (CASE 5)

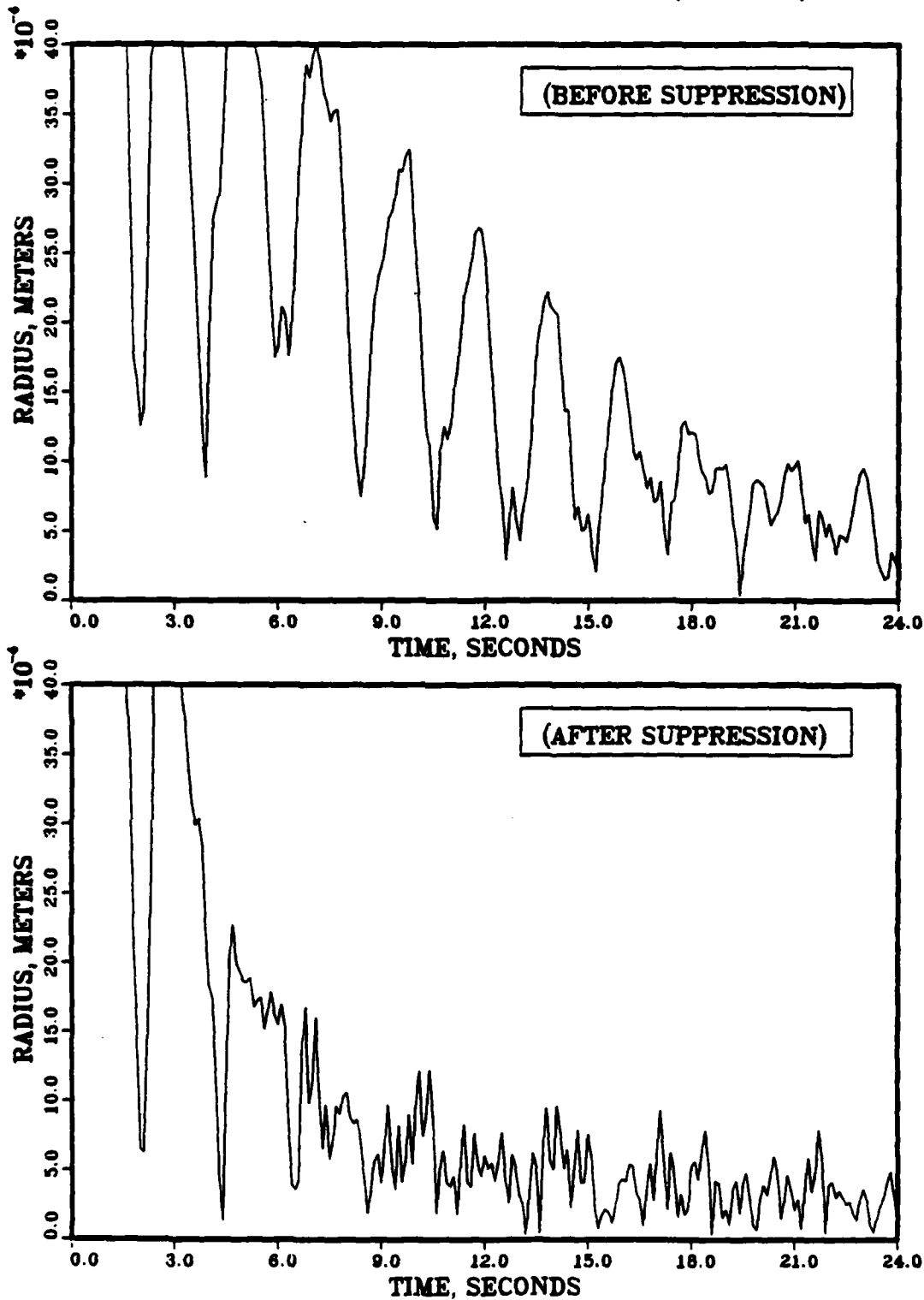
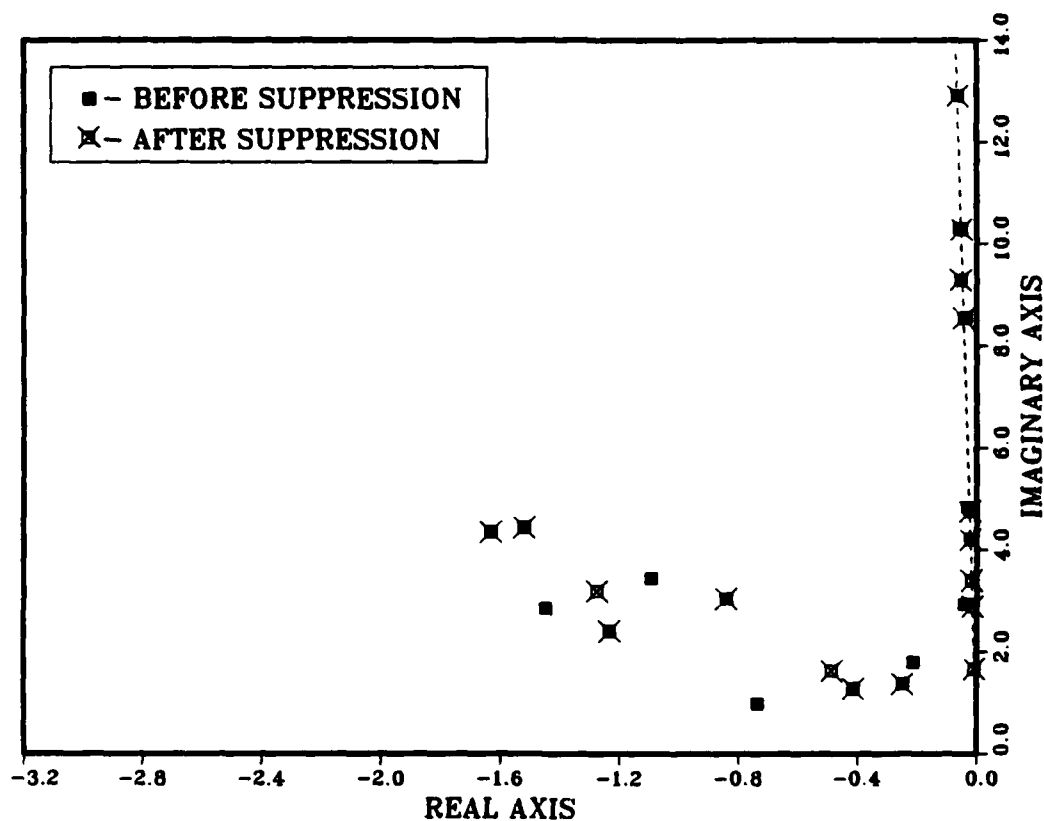


FIGURE 19. Time Response - Frequency Truncation, CSDL I
5 controlled - 3 suppressed modes; 6/6 act/sen

CONTROLLED SYSTEM EIGENVALUES (CASE 6)



CONTROLLED MODES : 1 2 5 4 7
 SUPPRESSED MODES : 3 8 9
 RESIDUAL MODES : 11 12 10 6

ZETA = 0.005
 WEIGHTING = 20.00

FIGURE 20. Internal Balancing, CSDL I, 6/6 act/sen
 5 controlled - 3 suppressed modes

NODE ONE TIME RESPONSE (CASE 6)

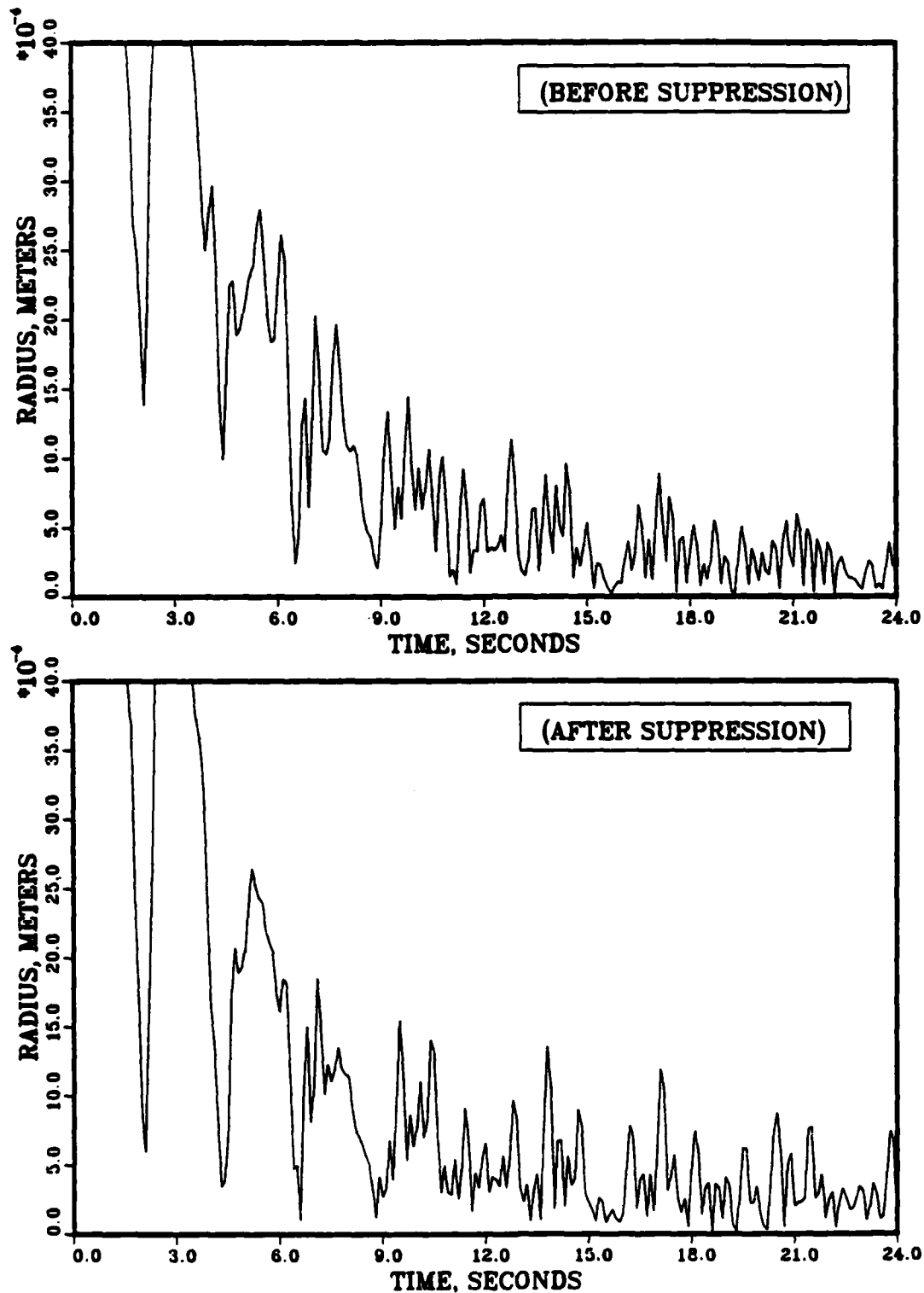
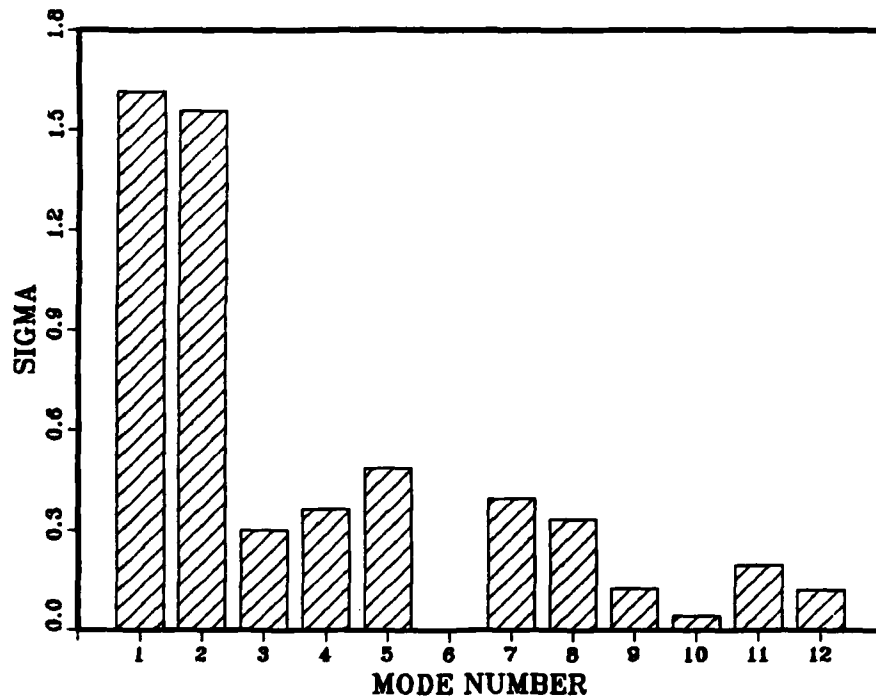


FIGURE 21. Time Response - Internal Balancing, CSDL I
5 controlled - 3 suppressed modes; 6/6 act/sen

MODAL RANKINGS, ACTUATOR/OUTPUT



MODAL RANKINGS, ACTUATOR/SENSOR

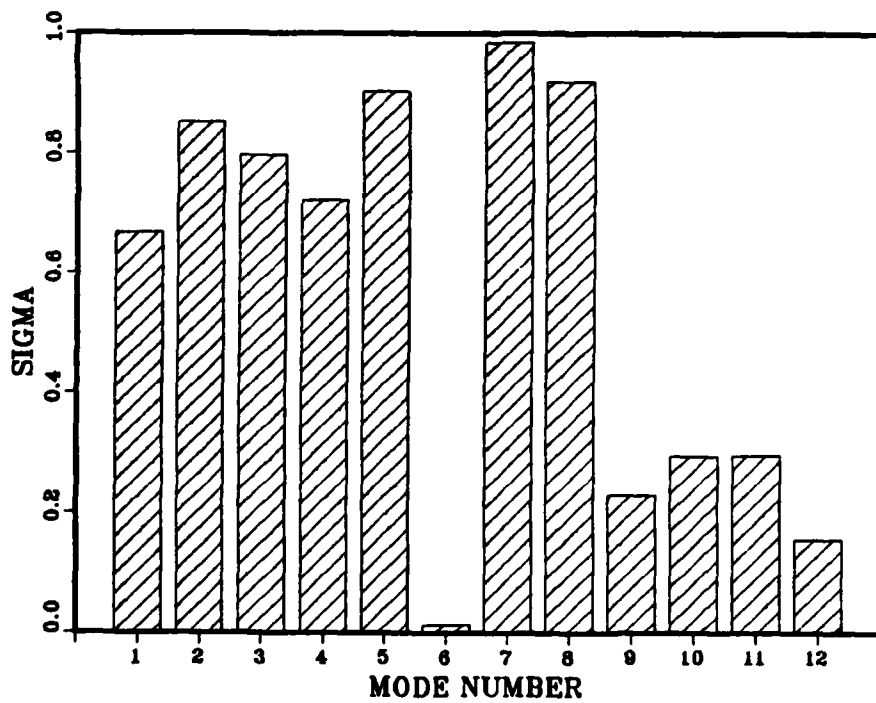


FIGURE 22. Internal Balancing Rankings, σ_{BC} & σ_{BH}
CSDL I, 3/6 act/sen

MODAL COST

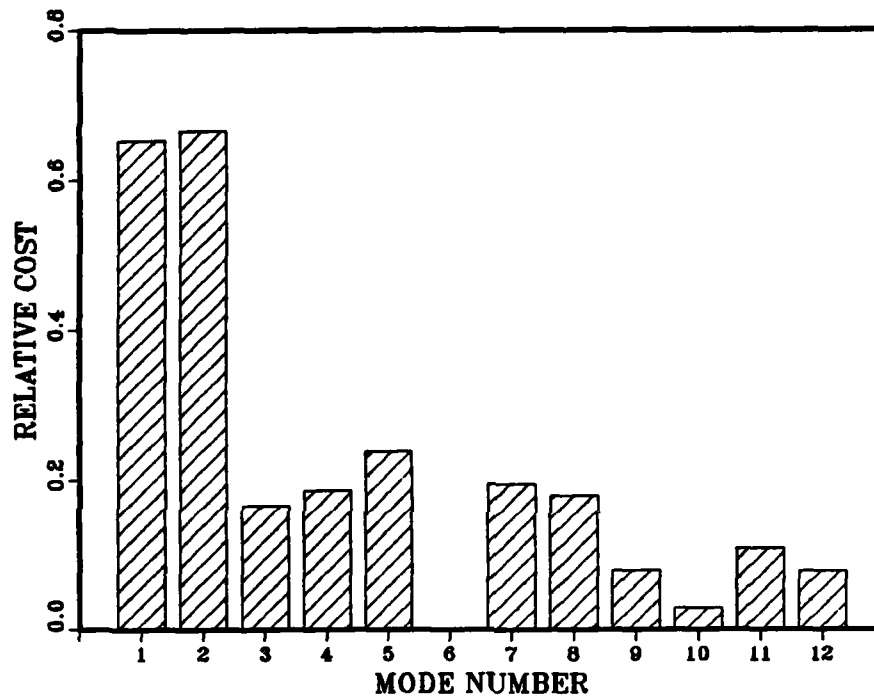
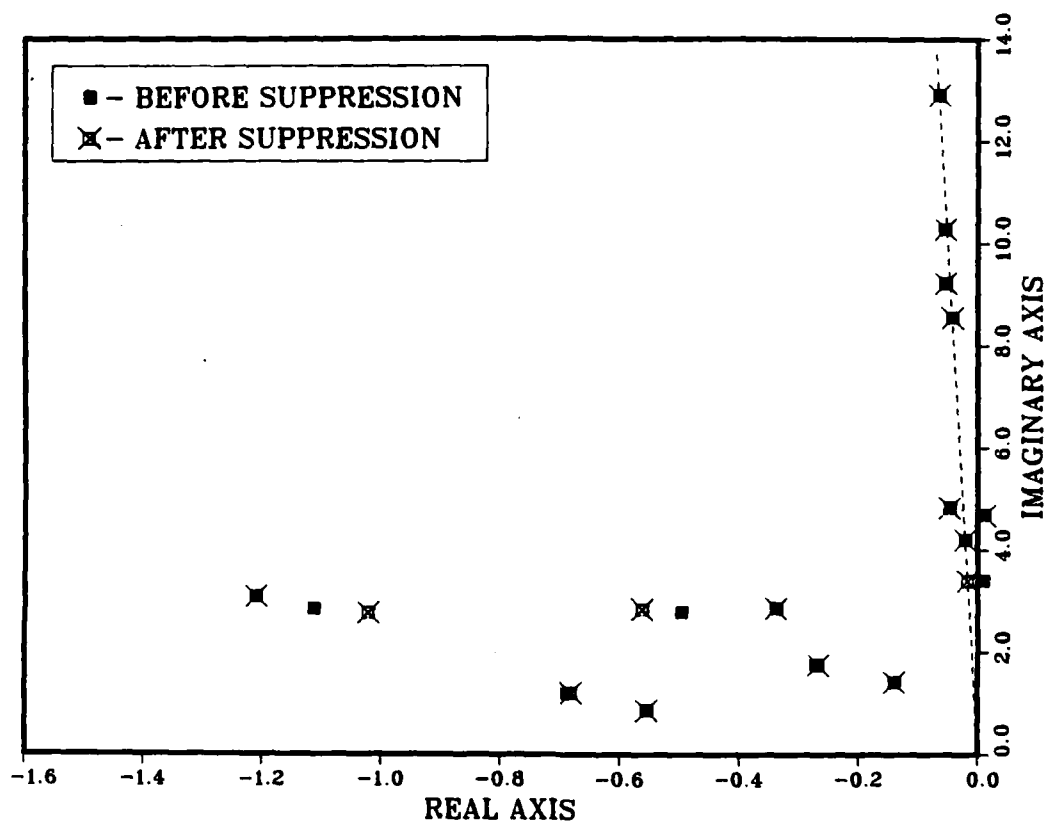


FIGURE 23. Modal Cost Rankings, CSDL I, 3/6 act/sen

CONTROLLED SYSTEM EIGENVALUES (CASE 7)



CONTROLLED MODES : 1 2 3 4

SUPPRESSED MODES : 5 6

RESIDUAL MODES : 7 8 9 10 11 12

ZETA = 0.005

WEIGHTING = 20.00

FIGURE 24. Frequency Truncation, CSDL I, 3/6 act/sen
4 controlled - 2 suppressed modes

NODE ONE TIME RESPONSE (CASE 7)

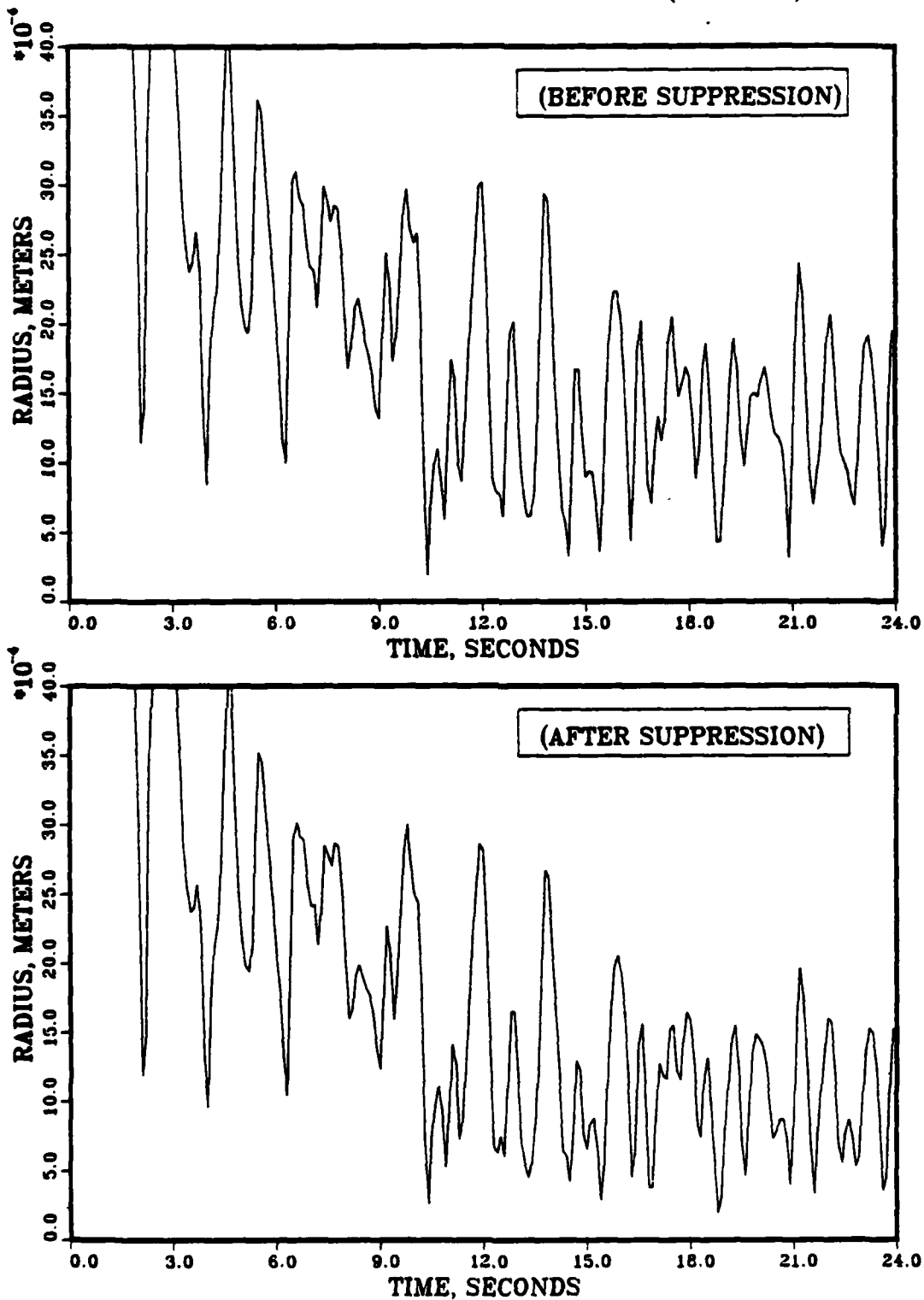


FIGURE 25. Time Response - Frequency Truncation, CSDL I
4 controlled - 2 suppressed modes; 3/6 act/sen

NODE ONE TIME RESPONSE (CASE 7)

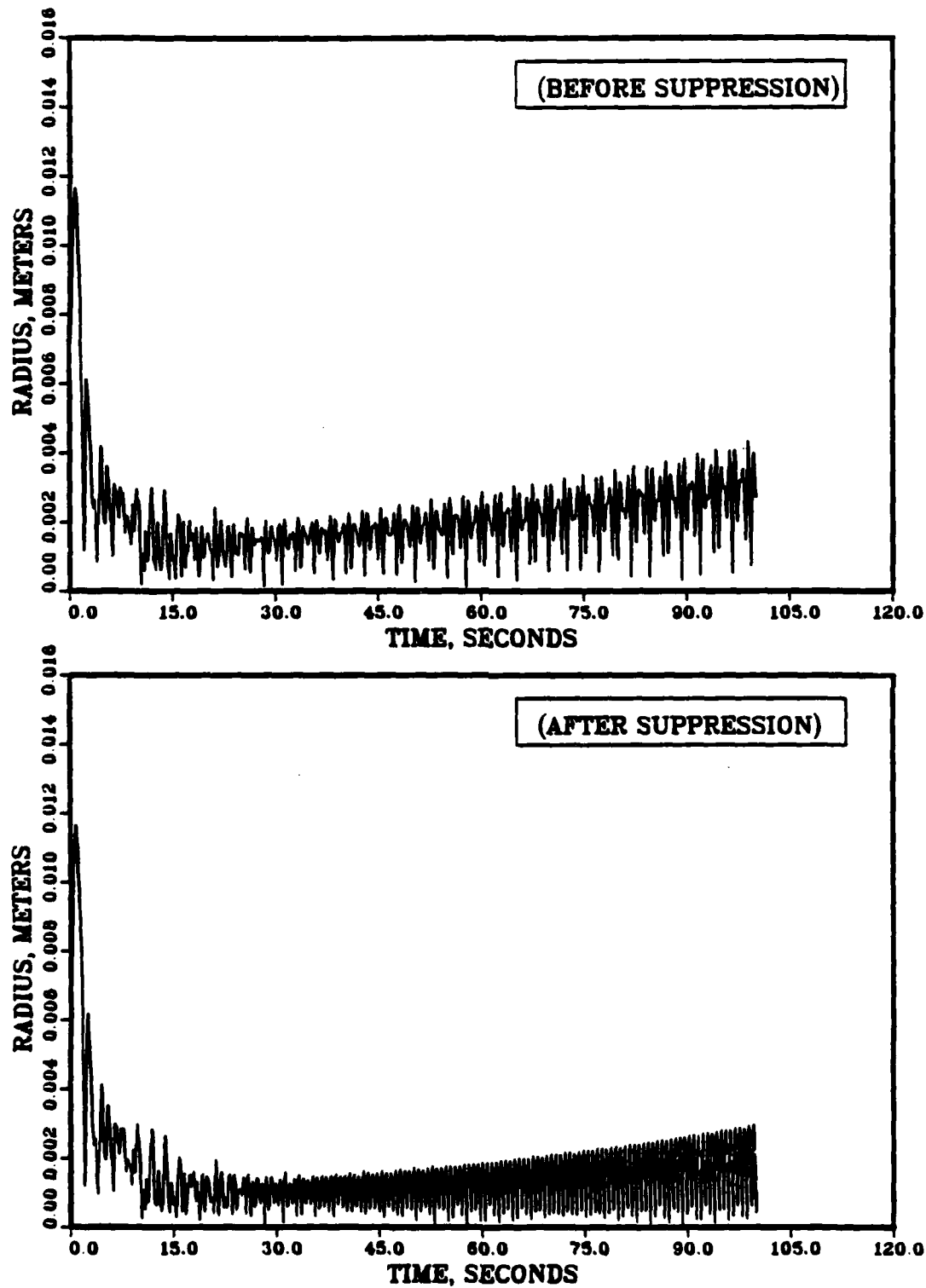
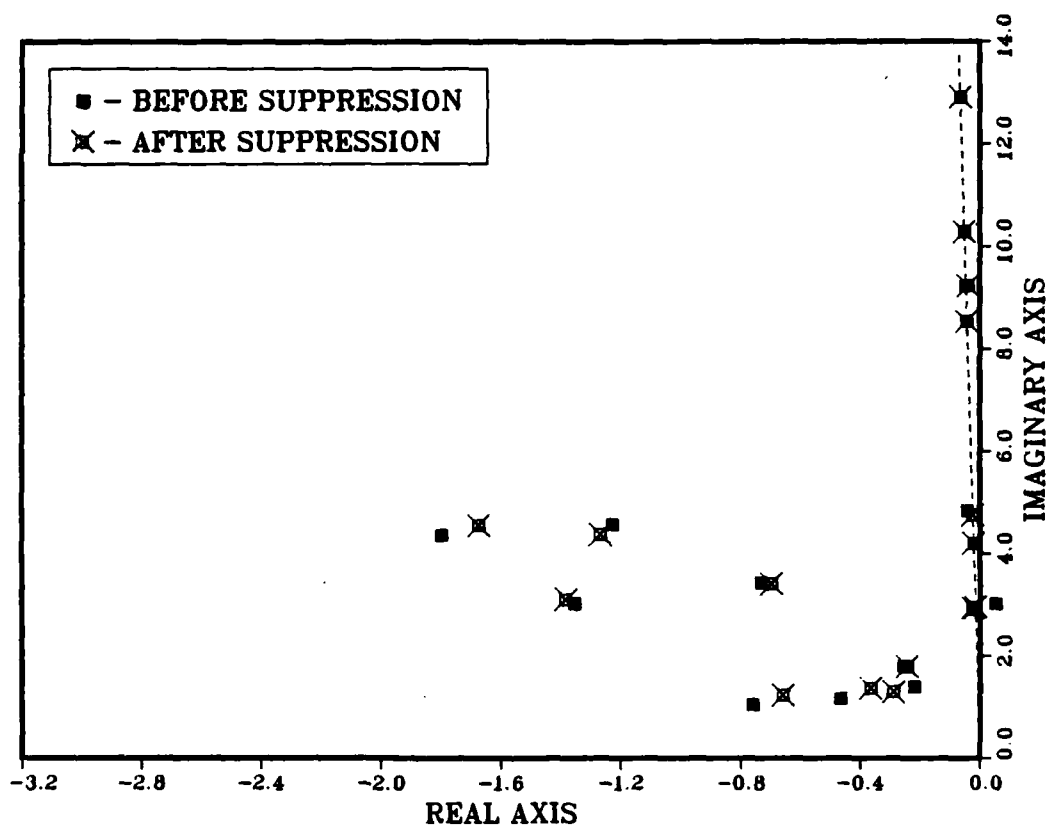


FIGURE 26. Extended scale time response for case 7

CONTROLLED SYSTEM EIGENVALUES (CASE 8)



CONTROLLED MODES : 1 2 5 7

SUPPRESSED MODES : 4 8

RESIDUAL MODES : 3 6 9 10 11 12

ZETA = 0.005

WEIGHTING = 20.00

FIGURE 27. Internal Balancing, CSDL I, 3/6 act sen
4 controlled - 2 suppressed modes

NODE ONE TIME RESPONSE (CASE 8)

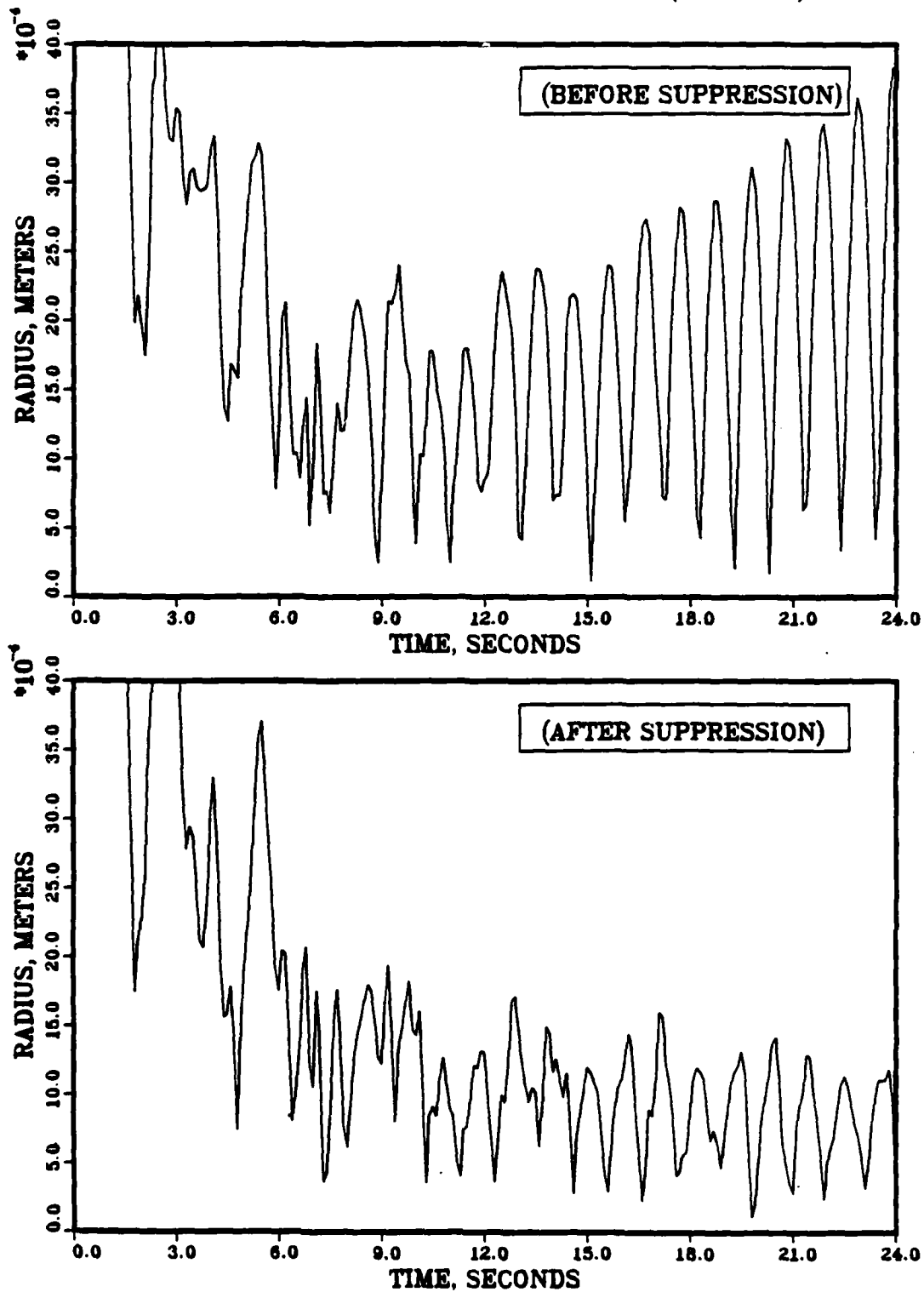
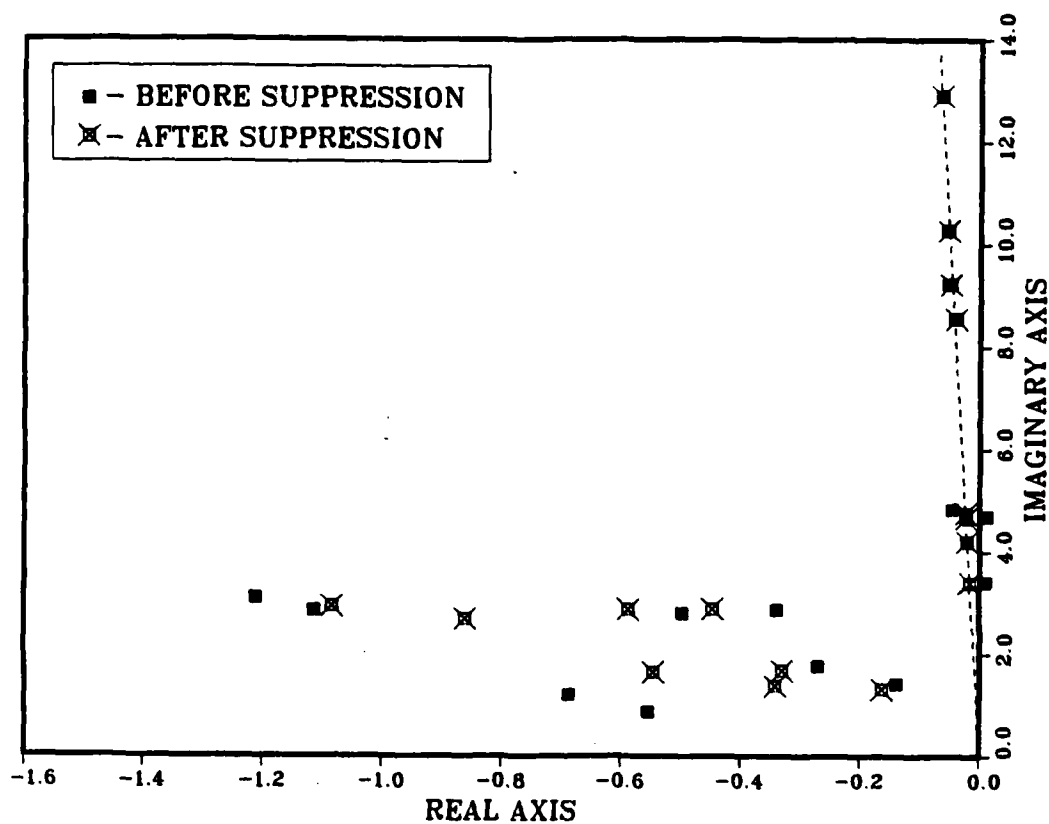


FIGURE 28. Time Response - Internal Balancing, CSDL I
4 controlled - 2 suppressed modes; 3/6 act/sen

CONTROLLED SYSTEM EIGENVALUES (CASE 9)



CONTROLLED MODES : 1 2 3 4
 SUPPRESSED MODES : 5 6 7 8
 RESIDUAL MODES : 9 10 11 12

ZETA = 0.005
 WEIGHTING = 20.00

FIGURE 29. Frequency Truncation, CSDL I, 3/6 act/sen
 4 controlled - 4 suppressed modes

NODE ONE TIME RESPONSE (CASE 9)

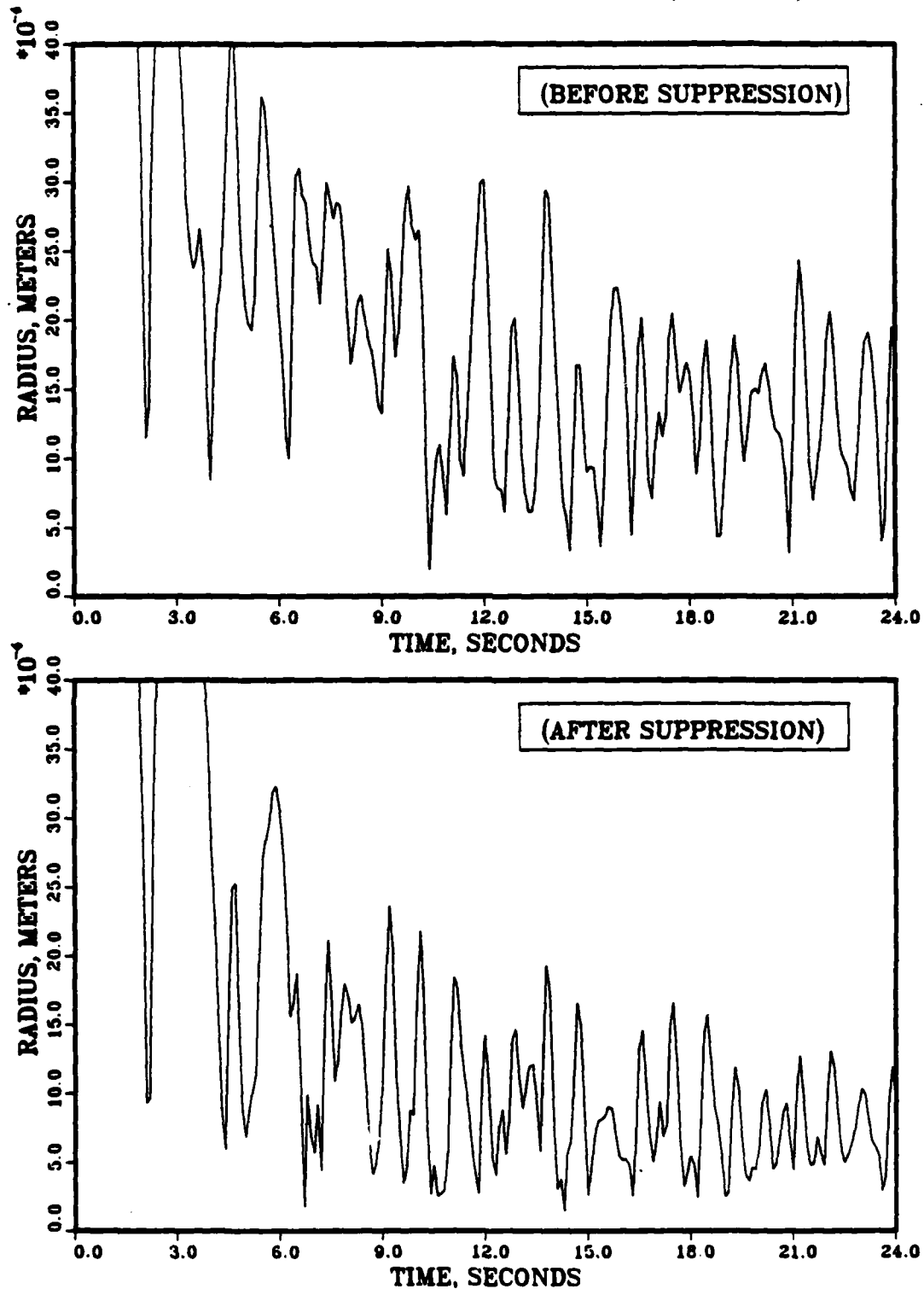


FIGURE 30. Time Response - Frequency Truncation, CSDL I
4 controlled - 4 suppressed modes; 3/6 act/sen

NODE ONE TIME RESPONSE (CASE 9)

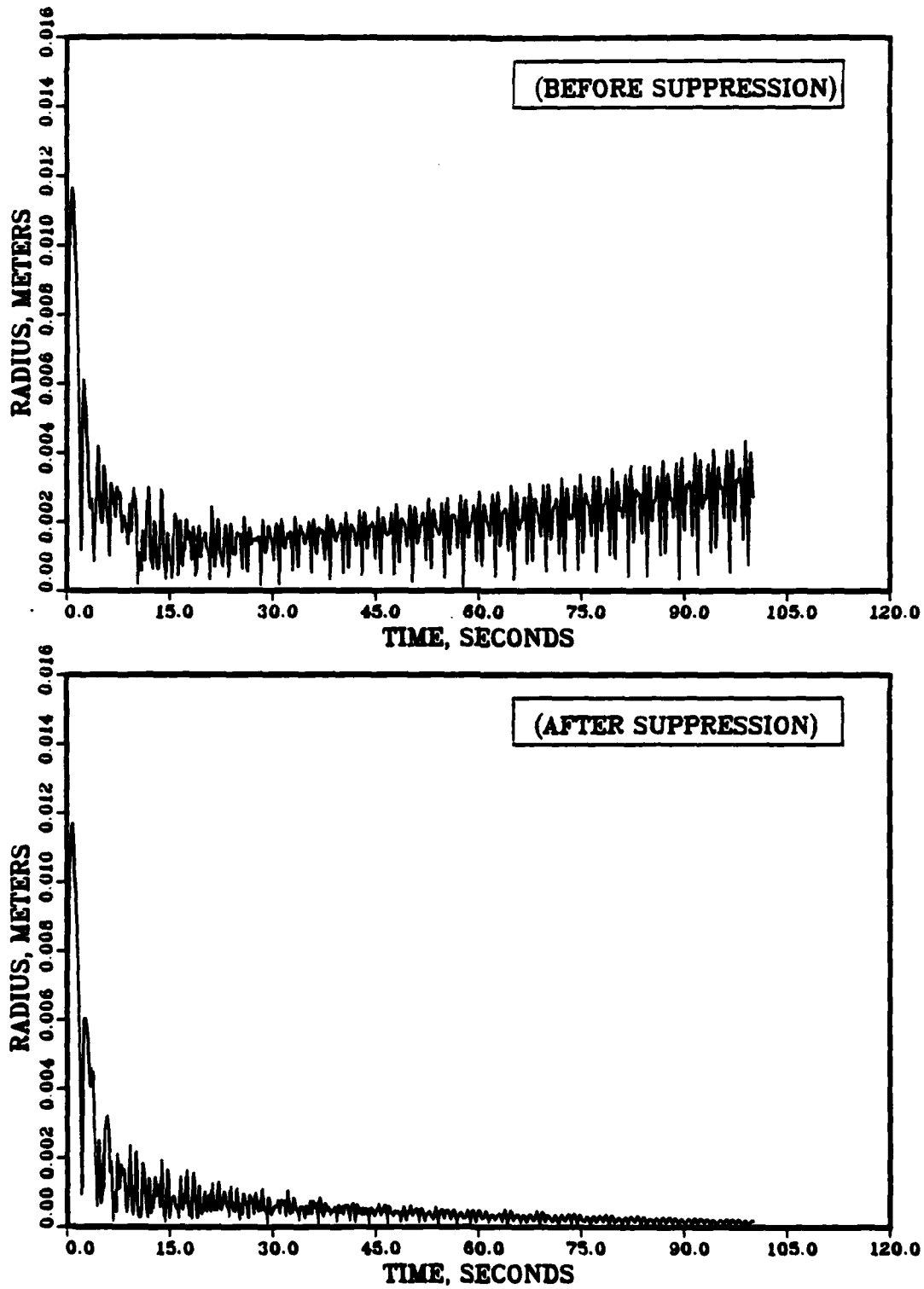
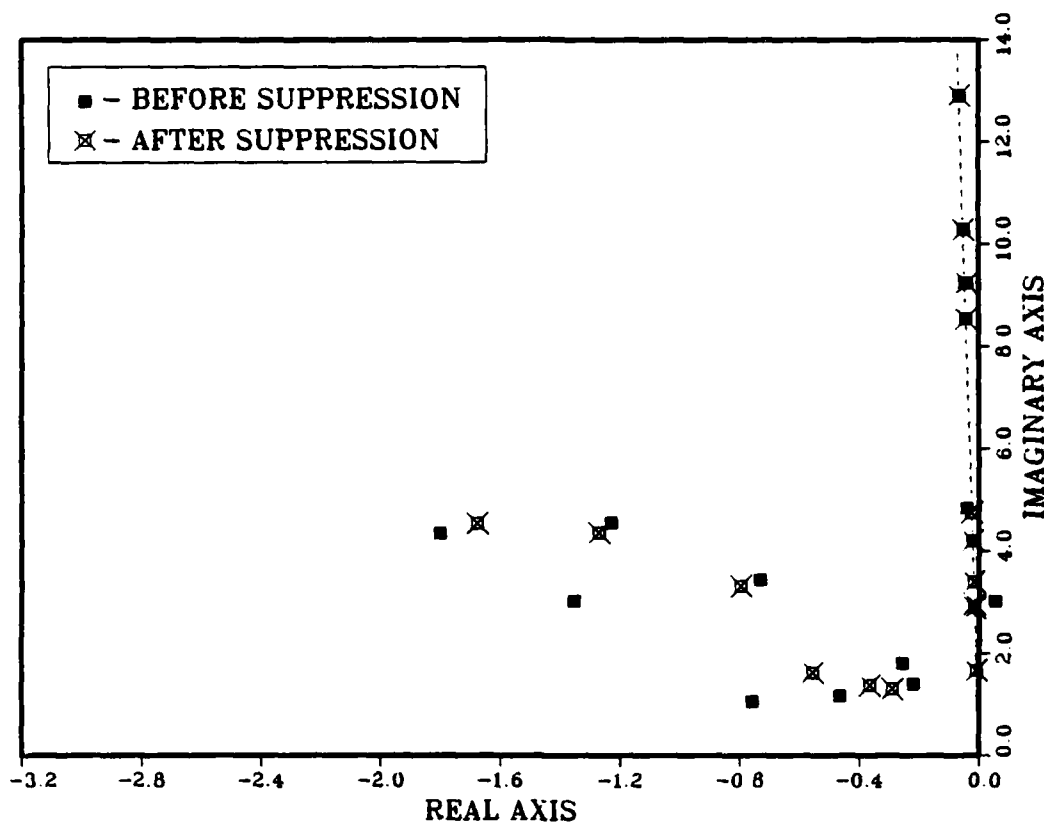


FIGURE 31. Extended scale time response for case 9

CONTROLLED SYSTEM EIGENVALUES (CASE 10)



CONTROLLED MODES : 1 2 5 7
 SUPPRESSED MODES : 4 8 3 11
 RESIDUAL MODES : 9 12 10 6

ZETA = 0.005
 WEIGHTING = 20.00

FIGURE 32. Internal Balancing, CSDL I, 3/6 act/sen
 4 controlled - 4 suppressed modes

NODE ONE TIME RESPONSE (CASE 10)

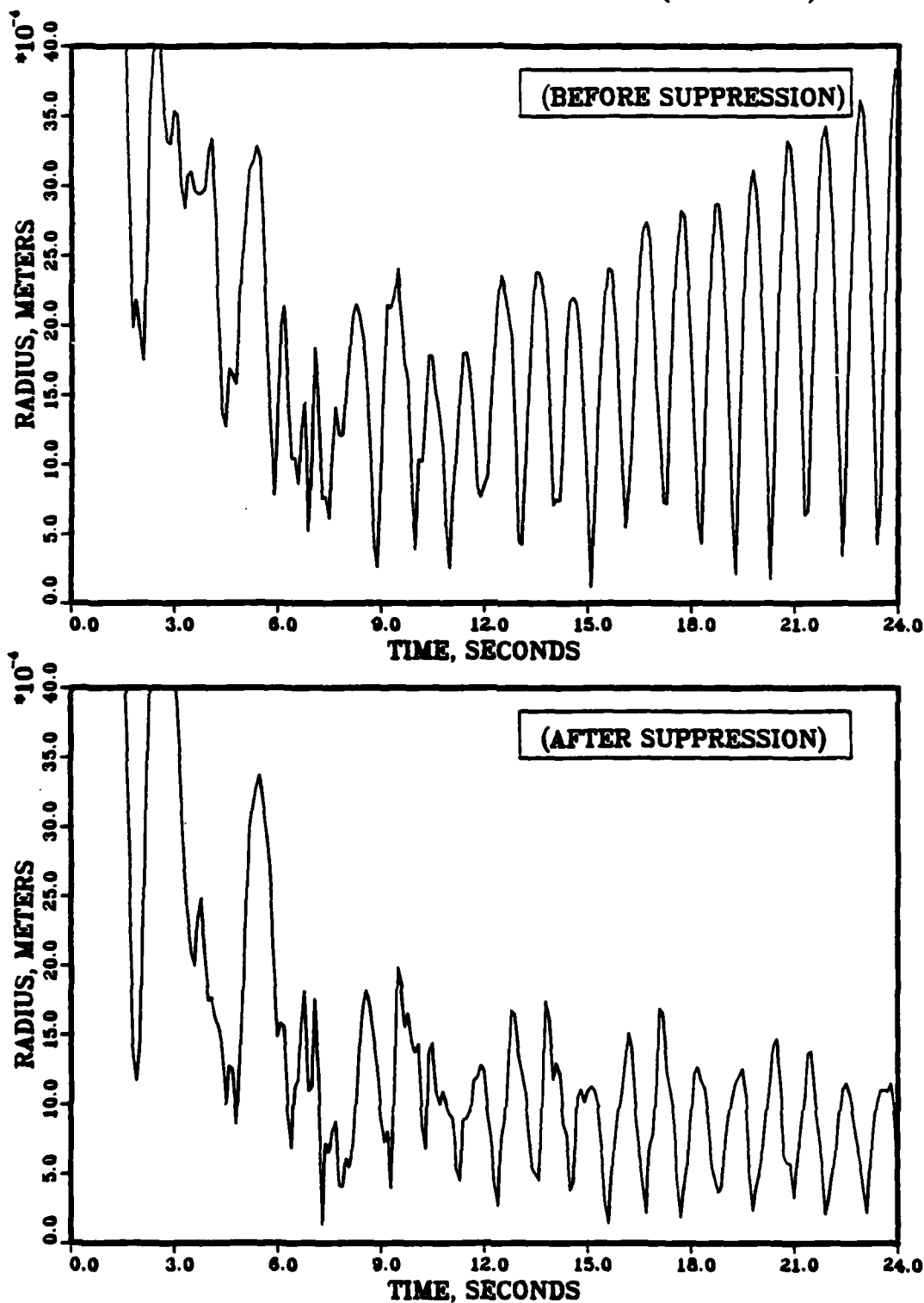


FIGURE 33. Time Response - Internal Balancing, CSDL I
4 controlled - 4 suppressed modes; 3/6 act/sen

MODAL RANKINGS, ACTUATOR/OUTPUT

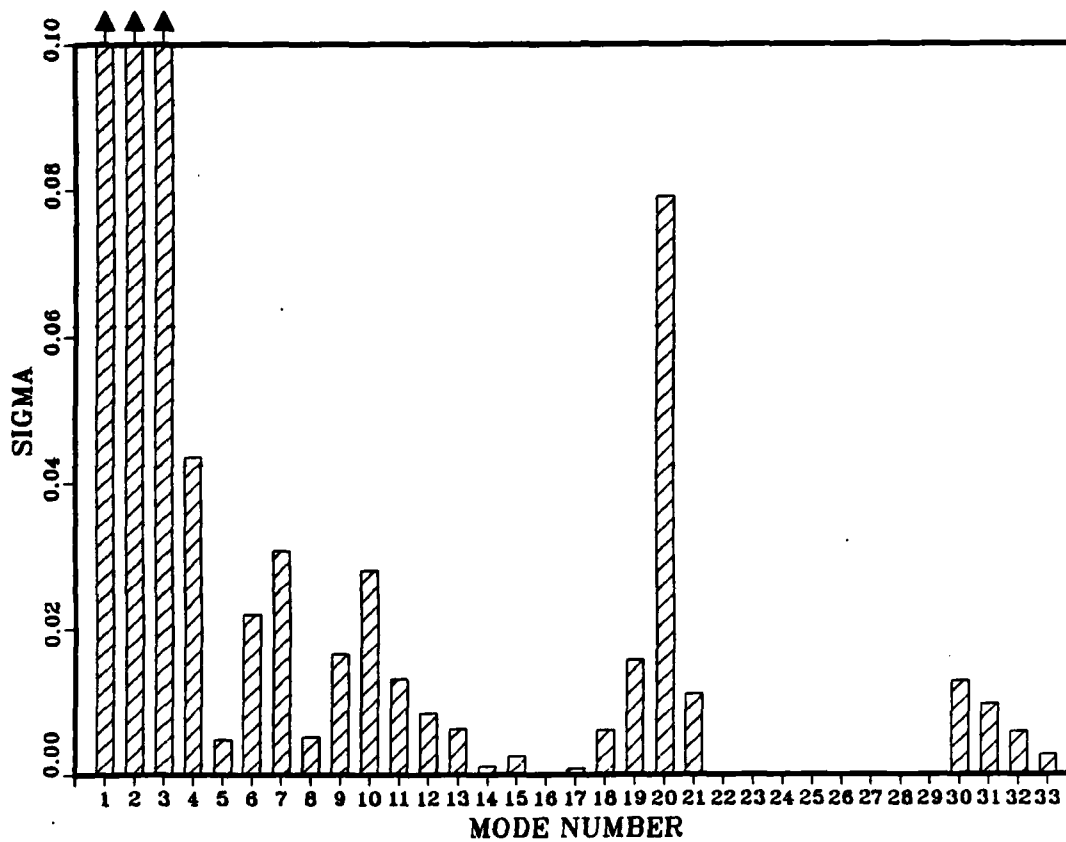


FIGURE 34. Internal Balancing Rankings, σ_{BC}
CSDL II, 21/21 act/sen

MODAL RANKINGS, ACTUATOR/SENSOR

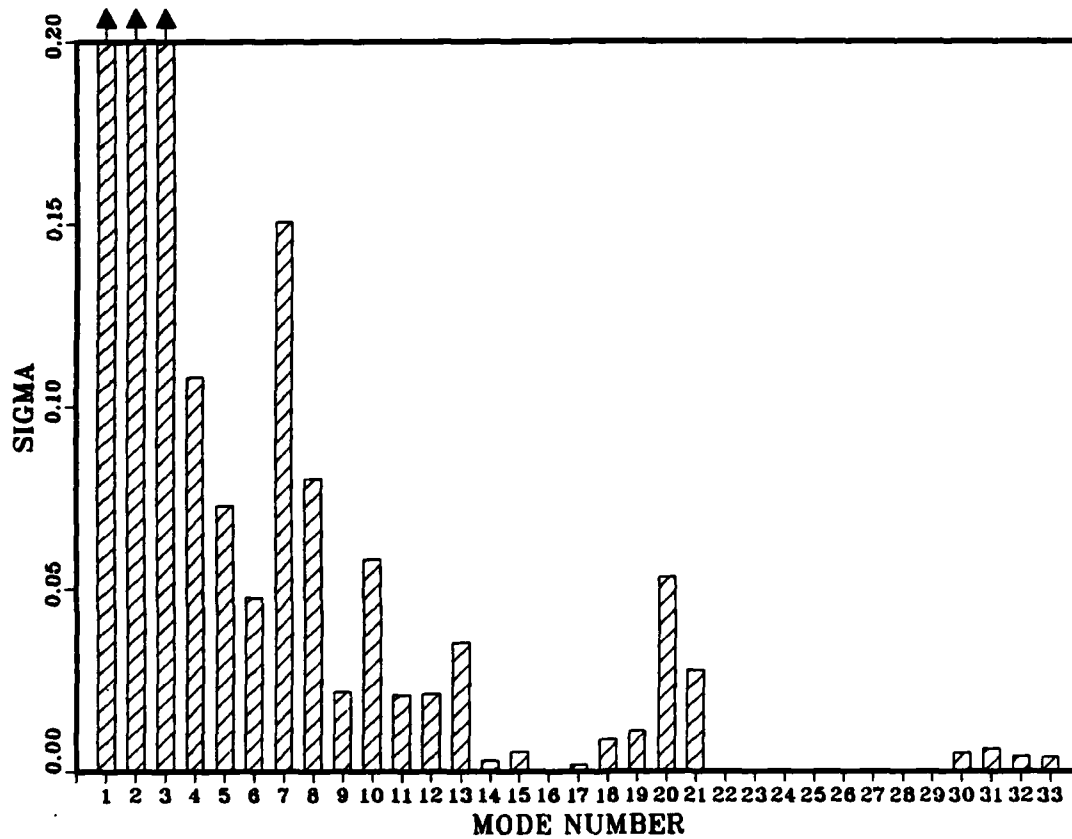


FIGURE 35. Internal Balancing Rankings, σ_{BH}
CSDL II, 21/21 act/sen

MODAL COST

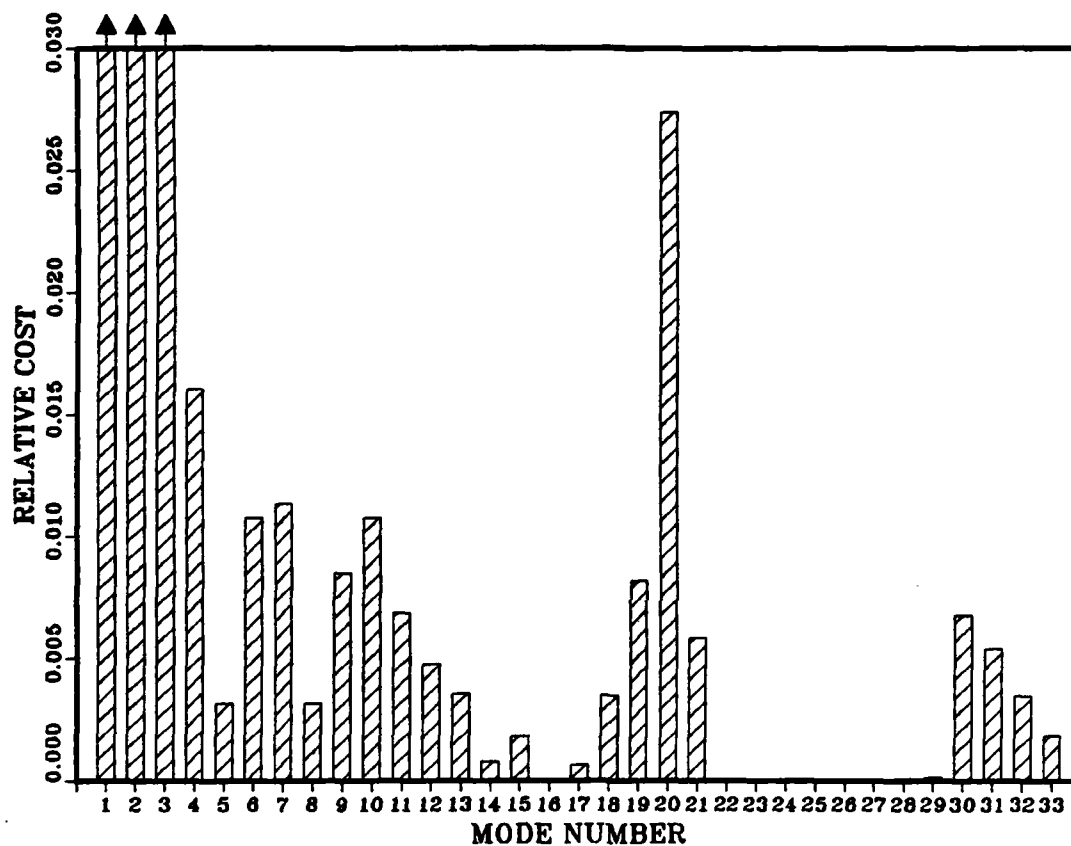


FIGURE 36. Modal Cost Rankings, CSDL II, 21/21 act/sen

<u>Mode i</u>	<u>Mode j</u>	<u>Approximation Test (Eq 66)</u>
5	6	.28
12	13	.60
14	15	3.95
14	16	.49
22	23	2.70
24	25	.92
26	27	.68
27	28	.31

TABLE 1. CSDL II Modes Not Satisfying Approximate Internal Balancing Test.

VII. CONCLUSIONS

The approximate internal balancing method offers a conceptually sound method for the choice of a reduced order control model. This method utilizes information about the sensor/actuator configuration in the mode selection process; modal cost analysis does not. In the CSDL I test cases it was not possible to demonstrate a clear superiority of one method, since the modes most critical to the performance objective (1 and 2) were contained in all reduced models. However, the improvement in time response seen in Figure 18 would seem to suggest the use of the internally balanced model for that case.

The 3 actuator/6 sensor test cases indicate that comparable performance may be achieved by a reduction in the number of actuators on CSDL I. However, spillover suppression must be applied to eliminate instabilities.

Application of the methods to the CSDL II model generated modal rankings that are significantly different from a simple frequency truncation. The internal balancing method reveals modal contributions to the system performance that are not otherwise obvious, and indicates the ability of the sensor/actuator configuration to influence these modes.

VIII. RECOMMENDATIONS

The following recommendations are suggested for follow-on research:

- 1). The effect of the reduced order model on the stability and time response of the CSDL II should be investigated.
- 2). It was assumed here that ideal sensor/actuators existed. The validity of this assumption could be investigated by modeling the actuator/sensors as noisy devices and approaching the control problem from a stochastic viewpoint.
- 3). Durability will be of concern in an actual system. It would be useful to examine the control system robustness in the face of sensor/actuator failures.
- 4). As selection of a reduced order model and controller design is so dependent on the accuracy of the structural model, it would be productive to investigate an adaptive control law that would account for modeling inaccuracies and changes in the structure from earth to space environments. The choice of modes to be controlled and suppressed could possibly be made on-line.

BIBLIOGRAPHY

1. Aldridge, E.S. Decentralized Control of a Large Space Structure as Applied to the CSDL 2 Model. MS Thesis. Wright-Patterson AFB, Ohio: School of Engineering, Air Force Institute of Technology, December 1982.
2. Balas, M.J. "Trends in Large Space Structure Control Theory: Fondest Hopes, Wildest Dreams," IEEE Trans. Auto. Control, Vol. AC-27, No.3, 1982.
3. Baker, R.G. Investigation of Multiple Controller System Efficiency as Applied to the CSDL I Model. MS Thesis. Wright-Patterson AFB, Ohio: School of Engineering, Air Force Institute of Technology, March 1984.
4. Gregory, C.Z. "Reduction of Large Flexible Spacecraft Models Using Internal Balancing Theory," AIAA Guidance and Control Conference, Gatlinberg, Tenn., 1983.
5. Hablani, H.B. "Synthesis of a Modern/Classical Controller for Large Space Structures," AIAA Guidance and Control Conference, San Diego, Ca., 1982.
6. Hanks, B.R. and Skelton, R.E. "Designing Structures for Reduced Response by Modern Control Theory," Proceedings of AIAA/ASME/ASCE/AHS 24th Structures, Structural Dynamics, and Materials Conference, Lake Tahoe, Nevada, 1983.
7. Hughes, P.C. and Skelton, R.E. "Controllability and Observability for Flexible Spacecraft," AIAA Journal of Guidance and Control. Vol. 3, No.5, 1980.
8. Janiszewski, A.M. Modern Optimal Control Methods Applied in Active Control of a Tetrahedron. MS Thesis. Wright Patterson AFB, Ohio: School of Engineering, Air Force Institute of Technology, December 1980.
9. Jonckheere, E.A. and Silverman, L.E. "Singular Value Analysis of Deformable Systems," Proceedings of IEEE Conference on Decision and Control, San Diego, Ca., December 1981, pp. 660-668.
10. Kwakernaak, H., and Sivan, R. Linear Optimal Control Systems. New York: John Wiley & Sons Inc., 1972.
11. Laub, A.J. "Computation of 'Balancing' Transformations," Proceedings of Joint Automatic Control Conference, San Francisco, Ca., August 1980.

12. Meirovitch, L. Elements of Vibration Analysis. New York: McGraw-Hill Book Company, 1975.
13. Moore, B.C. "Singular Value Analysis of Linear Systems," Proceedings of IEEE Decision and Control Conference, 1978.
14. Moore, B.C. "Principal Component Analysis in Linear Systems: Controllability, Observability, and Model Reduction," IEEE Trans. Auto. Control, Vol. AC-26, No.1, February 1981.
15. Pernebo, L. and Silverman, L.M. "Model Reduction via Balanced State Space Representations," IEEE Trans. Auto. Control, Vol. AC-27, No.2, April 1982.
16. RADC-TR-82-21. ACOSS FIVE (Active Control of Space Structures) Phase IA. Study conducted by Lockheed Missiles and Space Company, Inc. for the Rome Air Development Center, March 1982 (ADAl16655).
17. Reid, J.G. Linear System Fundamentals. New York: McGraw-Hill Book Company, 1983.
18. Skelton, R.E. "Cost Decomposition of Linear Systems With Application to Model Reduction," International Journal of Control, Vol. 32, No.6, 1980.
19. Skelton, R.E. and Gregory, C.Z. "Measurement Feedback and Model Reduction by Modal Cost Analysis," Proceedings, Joint Automatic Control Conference, Denver, Colorado, 1979.
20. Skelton, R.E. and Hughes, P.C. "Modal Cost Analysis for Linear Matrix-Second-Order Systems," Journal of Dynamic Systems, Measurement, and Control, Vol. 102/151, September 1980.
21. Skelton, R.E. and Hughes, P.C. and Hablani, H.B. "Order Reduction for Models of Space Structures Using Modal Cost Analysis," Journal Guidance, Control, and Dynamics, Vol. 5, No.4, July-August 1982.
22. Stewart, G.W. Introduction to Matrix Computations. New York: Academic Press, Inc., 1973.
23. Thyfault, D.V. Decentralized Control of a Large Space Structure Using Direct Output Feedback. MS Thesis. Wright-Patterson AFB, Ohio: School of Engineering, Air Force Institute of Technology, December 1983.

AD-A151 784

MODEL REDUCTION TECHNIQUES APPLIED TO THE CONTROL OF
LARGE SPACE STRUCTURES(U) AIR FORCE INST OF TECH
WRIGHT-PATTERSON AFB OH SCHOOL OF ENGI.. D W VARHOLA

2/2

UNCLASSIFIED DEC 84 AFIT/GA/RA/84D-11

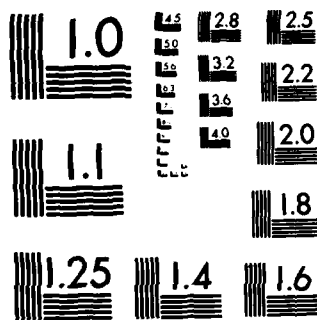
F/G 14/2

NL

END

FILMED

DTIC



MICROCOPY RESOLUTION TEST CHART
NATIONAL BUREAU OF STANDARDS-1963 A

Appendix A
CSDL I and CSDL II Data

CSDL I Node Coordinates

<u>Node</u>	<u>X</u>	<u>Y</u>	<u>Z</u>
1	0.0	0.0	10.165
2	-5.0	-2.887	2.0
3	5.0	-2.887	2.0
4	0.0	5.7735	2.0
5	-6.0	-1.1547	0.0
6	-4.0	-4.6188	0.0
7	4.0	-4.6188	0.0
8	6.0	-1.1547	0.0
9	2.0	5.7735	0.0
10	-2.0	5.7735	0.0

CSDL I Initial Conditions

<u>Mode</u>	<u>Displacement (η)</u>	<u>Velocity ($\dot{\eta}$)</u>
1	-.001	-.003
2	.006	.01
3	.001	.03
4	-.009	-.02
5	.008	.02
6	-.001	-.02
7	-.002	-.003
8	.002	.004
9	.0	.0
10	.0	.0
11	.0	.0
12	.0	.0

CSDL I D Matrix (Actuator Map)

- 6 Actuator Case -

0.0	0.0	0.0	0.0	0.0	0.0
0.0	0.0	0.0	0.0	0.0	0.0
0.0	0.0	0.0	0.0	0.0	0.0
0.3536	-0.3536	0.0	0.0	0.0	0.0
-0.6124	0.6124	0.0	0.0	0.0	0.0
0.7071	0.7071	0.0	0.0	0.0	0.0
0.0	0.0	0.3536	-0.3536	0.0	0.0
0.0	0.0	0.6124	-0.6124	0.0	0.0
0.0	0.0	0.7071	0.7071	0.0	0.0
0.0	0.0	0.0	0.0	-0.7071	0.7071
0.0	0.0	0.0	0.0	0.0	0.0
0.0	0.0	0.0	0.0	0.7071	0.7071

Note: $\underline{H}^T = \underline{D}$ for co-located sensors.

CSDL I D Matrix

- 3 Actuator Case -

0.0	0.0	0.0
0.0	0.0	0.0
0.0	0.0	0.0
0.4999	0.0	0.0
0.2887	0.0	0.0
0.8165	0.0	0.0
0.0	-0.4999	0.0
0.0	0.2887	0.0
0.0	0.8165	0.0
0.0	0.0	0.0
0.0	0.0	-0.5773
0.0	0.0	0.8165

NASTRAN Eigenvalue Analysis Results for CSDL I (Nominal)

<u>Mode</u>	<u>Generalized Mass</u>	<u>Generalized Stiffness</u>	$\omega \frac{\text{rad}}{\text{sec}}$	$\Omega \frac{\text{rad}^2}{\text{sec}^2}$
1	1.0E+00	1.80E+00	1.342E+00	1.80E+00
2	1.0E+00	2.77E+00	1.665E+00	2.77E+00
3	1.0E+00	8.36E+00	2.891E+00	8.36E+00
4	1.0E+00	8.75E+00	2.957E+00	8.75E+00
5	1.0E+00	1.15E+01	3.398E+00	1.15E+01
6	1.0E+00	1.76E+01	4.208E+00	1.76E+01
7	1.0E+00	2.17E+01	4.662E+00	2.17E+01
8	1.0E+00	2.26E+01	4.755E+00	2.26E+01
9	1.0E+00	7.29E+01	8.539E+00	7.29E+01
10	1.0E+00	8.56E+01	9.250E+00	8.56E+01
11	1.0E+00	1.05E+02	1.029E+01	1.05E+02
12	1.0E+00	1.67E+02	1.291E+01	1.67E+02

CSDL II Node Coordinates (Meters)

<u>Node</u>	<u>X</u>	<u>Y</u>	<u>Z</u>	<u>Node</u>	<u>X</u>	<u>Y</u>	<u>Z</u>
1	-7.0	0.0	0.0	37	-4.0	-3.0	24.0
2	-4.0	5.0	0.0	38	4.0	3.0	24.0
3	-4.0	-5.0	0.0	39	4.0	-3.0	24.0
4	0.0	5.0	0.0	40	0.0	2.5	2.0
5	4.0	5.0	0.0	42	0.0	5.0	-3.0
6	4.0	-5.0	0.0	43	-2.0	0.0	-1.3
7	7.0	0.0	0.0	44	0.0	-1.7	-1.3
8	-7.0	0.0	2.0	45	2.0	0.0	-1.3
9	-4.0	5.0	2.0	46	-4.0	-5.0	-0.3
10	-4.0	-5.0	2.0	47	4.0	-5.0	-0.3
11	4.0	5.0	2.0	48	-26.0	0.0	-1.3
12	4.0	-5.0	2.0	49	21.0	0.0	-1.3
13	7.0	0.0	2.0	50	16.0	0.0	-1.3
14	-6.0	0.0	12.0	51	-11.0	0.0	-1.3
15	-4.0	4.0	12.0	52	-6.0	0.0	-1.3
16	-4.0	-4.0	12.0	53	6.0	0.0	-1.3
17	4.0	4.0	12.0	54	11.0	0.0	-1.3
18	4.0	-4.0	12.0	55	16.0	0.0	-1.3
19	6.0	0.0	12.0	56	21.0	0.0	-1.3
26	-5.0	0.0	22.0	57	26.0	0.0	-1.3
27	-4.0	3.0	22.0	100	0.0	0.0	0.0
28	-4.0	-3.0	22.0	910	-4.0	-2.5	2.0
29	4.0	3.0	22.0	1001	0.0	-6.5	22.0
30	4.0	-3.0	22.0	1002	0.0	0.0	2.0
31	5.0	0.0	22.0	1003	0.0	6.5	22.0
32	-4.0	10.0	22.0	1004	0.0	4.0	2.0
33	4.0	10.0	22.0	1112	4.0	-2.5	2.0
34	-4.0	-10.0	22.0	2830	0.0	-3.0	22.0
35	4.0	-10.0	22.0	3233	0.0	10.0	22.0
35	-4.0	3.0	24.0				

CSDL II Lumped Mass Distribution

<u>Node</u>	<u>Mass (kg)</u>	<u>Node</u>	<u>Mass (kg)</u>
9	67.4	44	3500
10	67.4	48	81.9
11	67.4	50	1,638
12	67.4	52	73.8
27	69.5	53	73.8
28	6.74	55	163.8
29	69.5	57	81.9
30	6.74	1001	1000
32	6.74	1002	800
33	6.74	1003	1200
34	69.5	1004	600
35	69.5		

CSDL II Sensor/Actuator Locations and Orientations (x,y,z in direction cosines)

<u>Pair</u>	<u>Node</u>	<u>x</u>	<u>y</u>	<u>z</u>
1	9	0	1	0
2	9	0	0	1
3	10	0	0	1
4	11	1	0	0
5	11	0	1	0
6	11	0	0	1
7	12	0	0	1
8	27	1	0	0
9	27	0	1	0
10	27	0	0	1
11	28	0	0	1
12	29	0	1	0
13	29	0	0	1
14	30	0	0	1
15	32	0	0	1
16	33	0	0	1
17	34	1	0	0
18	34	0	1	0
19	34	0	0	1
20	35	0	1	0
21	35	0	0	1

NASTRAN Eigenvalue Analysis Results for CSDL II (Nominal)

Mode	Generalized Mass	Generalized Stiffness	ω $\frac{\text{rad}}{\text{sec}}$	Ω $\frac{\text{rad}^2}{\text{sec}^2}$
1-6	1.00E+00	0.0	0.0	0.0
7	1.00E+00	5.128E-01	7.161E-01	5.128E-01
8	1.00E+00	8.521E-01	9.231E-01	8.521E-01
9	1.00E+00	8.835E-01	9.399E-01	8.835E-01
10	1.00E+00	1.212E+00	1.101E+00	1.212E+00
11	1.00E+00	8.819E+00	2.862E+00	8.189E+00
12	1.00E+00	1.266E+01	3.502E+00	1.226E+01
13	1.00E+00	1.403E+01	3.746E+00	1.403E+01
14	1.00E+00	1.492E+01	3.863E+00	1.492E+01
15	1.00E+00	1.599E+01	3.998E+00	1.599E+01
16	1.00E+00	1.625E+01	4.032E+00	1.625E+01
17	1.00E+00	2.623E+01	5.122E+00	2.623E+01
18	1.00E+00	2.630E+01	5.128E+00	2.630E+01
19	1.00E+00	2.677E+01	5.174E+00	2.677E+01
20	1.00E+00	3.310E+01	5.753E+00	3.310E+01
21	1.00E+00	3.730E+01	6.197E+00	3.730E+01
22	1.00E+00	5.301E+01	7.281E+00	5.301E+01
23	1.00E+00	9.489E+01	9.746E+00	9.498E+01
24	1.00E+00	1.241E+02	1.114E+01	1.241E+02
25	1.00E+00	1.999E+02	1.414E+01	1.999E+02
26	1.00E+00	2.001E+02	1.416E+01	2.001E+02
27	1.00E+00	4.654E+02	2.157E+01	4.654E+02
28	1.00E+00	4.705E+02	2.169E+01	4.705E+02
29	1.00E+00	6.182E+02	2.468E+01	6.182E+02
30	1.00E+00	6.276E+02	2.505E+01	6.275E+02
31	1.00E+00	6.481E+02	2.546E+01	6.481E+02
32	1.00E+00	7.428E+02	2.725E+01	7.428E+02
33	1.00E+00	1.700E+03	4.123E+01	1.700E+03
34	1.00E+00	2.568E+03	5.067E+01	2.568E+03
35	1.00E+00	2.821E+03	5.311E+01	2.821E+03
36	1.00E+00	3.095E+03	5.563E+01	3.095E+03

CSDL II $[C_p \phi]^T$ Matrix

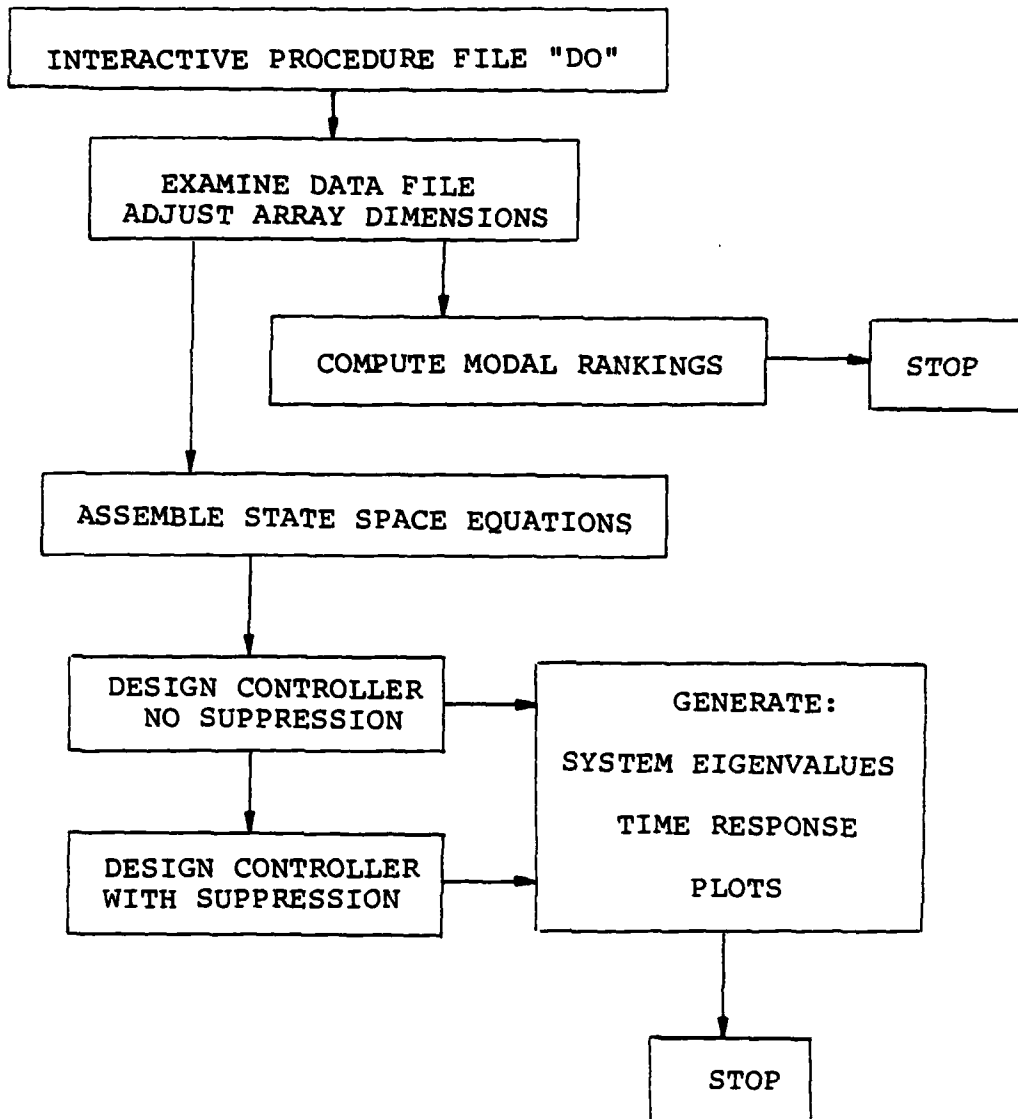
$$\underline{y} = [C_p \phi] \underline{\eta} \quad \underline{y} = \begin{bmatrix} XLOS \\ YLOS \\ ZLOS \end{bmatrix} \quad \underline{\eta} \equiv \text{modal coordinates*}$$

-.6234E-13	.7492E-02	.1045E-08
-.7284E-05	.1051E-05	.1453E-12
-.5364E-03	.8123E-07	.1103E-13
.1777E-02	-.1218E-05	-.3412E-05
-.1880E-05	-.4005E-04	.3185E-05
-.7555E-08	-.1351E-02	-.8232E-06
-.9693E-03	-.1106E-04	.1901E-05
-.5472E-04	-.8429E-04	.8500E-04
.6169E-02	.2150E-04	.1431E-04
.7284E-07	-.7115E-02	-.8065E-04
-.4461E-02	-.5071E-04	.3427E-05
.2215E-04	-.1870E-02	-.6674E-04
-.6301E-03	.6725E-04	-.1256E-04
-.1051E-04	-.2819E-03	.7612E-05
.4947E-05	-.8486E-03	-.2771E-04
-.7761E-15	-.2288E-12	-.1626E-15
-.2869E-04	-.2736E-03	.3586E-04
-.3600E-02	-.8429E-04	.1385E-04
-.2285E-01	-.1862E-05	-.4502E-04
.1621E+00	.1772E-03	.2510E-03
.6871E-02	.3786E-03	-.1182E-03
-.2481E-14	-.8148E-12	-.3790E-16
.4950E-06	.2705E-04	-.3122E-05
.2719E-13	-.3934E-11	.2880E-17
-.1781E-05	-.4463E-04	.5171E-05
-.1051E-05	-.5921E-04	-.1644E-04
.3466E-05	.1669E-04	-.2214E-04
-.3195E-03	.6525E-05	.2638E-06
-.1086E-02	.1486E-05	-.2936E-06
-.4526E-03	-.1765E+00	-.6466E-01
.1047E+00	.9565E-02	-.6518E-02
.1313E-01	.1605E-01	.5918E-01
-.7264E-02	-.1778E-02	.1289E-01

* here, 3 attitude rigid body modes and
30 flexible modes

Appendix B
Source Code Listing

PROGRAM FLOW



99

100

101


```

CALL EIGRF(ARC,NC12,NCOL,O,M1,TEN,NCOL,STOR,IER)
WRITE(0,*) IER = 'IER
DO 402 I=1,NC12
  WRITE(0,*) 'M1(I)
  WRITE(0,*) '(/)
C
  EIGENVALUES OF THE A SUPPRESSED MATRIX
  DO 404 I=1,NC2
    DO 404 J=1,NC2
      AS1(I,J) = AS1(I,J)
    CALL EIGRF(AS1,NC2,NCOL,O,M1,TEN,NCOL,STOR,IER)
    WRITE(0,*) IER = 'IER
  DO 408 I=1,NC2
    WRITE(0,*) 'M1(I)
    WRITE(0,*) '(/)
  IF (NR.EQ.0) THEN
    WRITE(0,*) NO RESIDUAL TERM EIGENVALUES
    GOTO 410
  ELSE
C
    EIGENVALUES OF THE A RESIDUAL MATRIX
    DO 408 I=1,NC2
      DO 408 J=1,NC2
        AR1(I,J) = AR1(I,J)
      CALL EIGRF(AR1,NC2,NCOL,O,M1,TEN,NCOL,STOR,IER)
      WRITE(0,*) IER = 'IER
    DO 408 I=1,NC2
      WRITE(0,*) 'M1(I)
      WRITE(0,*) '(/)
C
  410 CONTINUE
  IF (ZZ.EQ.1) GOTO 800
C
  IF (WHAT.EQ.0) THEN
    WRITE(0,*) '(/)
    WRITE(0,*) 'YOU ONLY WANTED THE UNSUPPRESSED Z MATRIX, SO THERE TIS.
    WRITE(0,*) '(/)
    GOTO 700
  ENDIF
C
  THIS SECTION FORMS THE TRANSFORMATION MATRICES.
  TO GET MAJN IN LOWER TRIANGULAR FORM, IT IS
  NECESSARY TO DRIVE THE KSC TERMS TO ZERO.
C
  AFTER THE TRANSFORMATION IS COMPLETE,
  THE ONE CONTROLLER MAJN (WITH RESIDUAL TERMS) WILL LOOK LIKE:
  ....
  AC-BG  BCG  O  O  O
  O  AC-KCC  O  KCR  O
  BSG  BSG  AS  O  O
  BRG  BRG  O  AR  ....

```

```

WHERE THE NON-ZERO TERMS INCLUDE THE
TRANSFORMATION MATRICES.
C
ON WITH THE TRANSFORMATION MATRICES!
FIRST THE OBSERVER GAIN MATRIX, K
CALL TFRCT(CS,NSEN,NS2,1,2)
DO 802 I=1,NS
  DO 802 J=1,NSEN
    V(I,J) = CT(I,J)
  NV = NS
  WRITE(0,*) 'V (CS) IS
  CALL LSVDF(V,NCOL,NV,NSEN,TEN,NCOL,-1,SING,STOR,IER)
  WRITE(0,*) 'LSVDF I IER = 'IER
  WRITE(0,*) '(/)
  CALL PRNT(V,NSEN,NSEN)
  P1 = NSEN - NV
  IF (P1.LT.1) THEN
    DO 803 I=1,NSEN
      GAMMA(I,1) = V(I,NSEN)
    P1 = 1
  ELSE
    DO 804 I=1,NSEN
      DO 804 J=1,P1
        GAMMA(I,J) = V(I,J+NV)
      ENDIF
    WRITE(0,*) 'TRANSFORMATION MATRIX GAMMA1
    CALL PRNT(GAMMA1,NSEN,P1)
C
  CHECK TO SEE THAT GAMMA1 IS ORTHOGONAL TO CS
  NOTE:  ARC IN THIS SECTION IS JUST A WORK AREA TO TEST
        THE ORTHOGONALITY OF CT = TR. IN ALL CASES IT
        SHOULD BE A BLOCK ZERO MATRIX.
  CALL TFRCT(CS,NSEN,NS2,1,2)
  CALL MMUL(CT,GAMMA1,NS2,NSEN,P1,ARC)
  WRITE(0,*) 'CST = GAMMA1
  CALL PRNT(ARC,NS2,P1)
  WRITE(0,*) 'CS SINGULAR VALUES
  CALL PRNT(SING,NV,1)
  CALL TFRCT(GAMMA1,NSEN,P1,1,2)
  CALL MMUL(TRY,GAMMA1,P1,NSEN,P1,ARC)
  CALL GRINV(P1,P1,ARC,NC1,J,TAPE)
  CALL TFRCT(CT,NSEN,NC12,1,2)
  CALL MMUL(TRY,CT,P1,NSEN,NC12,ARC)
  CALL MMUL(CT,GAMMA1,NC12,NSEN,P1,KOB1)
  CALL MMUL(KOB1,ARC,NC12,P1,STOR)
  CALL MMUL(STOR,ARC,NC12,P1,NC12,CTCC1)
C
  THIS CTCC1 WILL BE SUBSTITUTED BACK INTO MRIC
  SYSTEM 1 TO GET A NEW K1.
C

```



```

107
      AT(I,ICN) = 1.0
      A(I,NI,1) = -(W(NI)**2)
2    CONTINUE
      RETURN
      END
      SUBROUTINE FORMB(G,PHI,N,N2,NACT,IC)
      COMMON/NAIMB/NCOL
      REAL B(NCOL,NCOL),PHI(NCOL,NCOL)
      INTEGER IC(N),NACT,N,N2,I,J
      DO 1 I=1,N2
      DO 1 J=1,NACT
      B(I,J) = 0.0
1    CONTINUE
      DO 2 I=1,N
      N = IC(I)
      DO 2 J=1,NACT
      B(I,N2+J) = PHI(N,J)
2    CONTINUE
      RETURN
      END
      SUBROUTINE FORMC(C,PHIS,N,N2,NSEN,IC)
      COMMON/NAIMB/NCOL
      REAL C(NCOL,NCOL),PHIS(NCOL,NCOL)
      INTEGER IC(N),N,NSEN,N,N2,I,J
      DO 1 I=1,NSEN
      DO 1 J=1,N2
      C(I,J) = 0.0
1    CONTINUE
      DO 2 I=1,NSEN
      N = IC(I)
      DO 2 J=1,N
      C(I,J) = PHIS(N,I)
2    CONTINUE
      RETURN
      END
      SUBROUTINE FORMPHI(FEE,PHI,N,NC,IC)
      COMMON/NAIMB/NCOL
      REAL FEE(NCOL,NC),PHI(NCOL,NCOL)
      INTEGER IC(NC),N,N,NC,I,J
      DO 3 J=1,NC
      N = IC(J)
      DO 3 I=1,N
      FEE(I,J) = PHI(I,N)
3    CONTINUE
      RETURN
      END
      SUBROUTINE FORMQ(CLOS,C,N1,NACT,N2,QA,WORK)
      REAL CLOS(N1,NACT),C(NACT,N2),QA(NACT,NACT),WORK(NACT,NACT)
      INTEGER N1,N2,NACT
      CALL MNU(CLOS,C,N1,NACT,N2,NACT,QA,NACT,IER)
      RETURN
      END
      SUBROUTINE FORMQ1(Q,A,N,IC)
      COMMON/NAIMB/NCOL
      REAL A(NCOL),Q(NCOL,NCOL)
      INTEGER I,J,K,N,N2,IC(NCOL)
      N2 = N + 2
      DO 1 I=1,N2
      DO 1 J=1,N2
      Q(I,J) = 0.0
1    CONTINUE
      DO 2 I=1,N
      J = I
      N = IC(I)

```

```

      DO 3 K=1,I
      Q(I,K,J,K) = A(N)
3    CONTINUE
      RETURN
      END
      SUBROUTINE GRINV(MR,NC,A,U,MR,MT)
      DIMENSION A(1),U(1)
      COMMON/NAIMB/NCOL,NCOL1
      COMMON/INOUT/ICOUT
      TOL=1.E-12
      MR=NC
      MR=MR-1
      TOL=1.E-20
      JJ=1
      DO 100 J=1,NC
      FAC=DOT(MR,A(JJ),A(JJ))
      JJ=J+1
      JMH=JJ+MR-1
      JCH=JJ+JMH
      DO 30 I=JJ,JCH
      U(I)=0
      U(JCH)=1.0
      IF (J.EQ.1) GO TO 54
      KK=1
      DO 30 K=1,JMH
      IF (S(K).EQ.1.0) GO TO 50
      TEMP=DOT(MR,A(JJ),A(KK))
      CALL VADD(K,TEMP,U(JJ),U(KK))
      KK=KK+NCOL
      DO 50 I=1,2
      KK=1
      DO 50 K=1,JMH
      IF (S(K).EQ.0.) GO TO 50
      TEMP=DOT(MR,A(JJ),A(KK))
      CALL VADD(K,TEMP,U(JJ),U(KK))
      KK=KK+NCOL
      TOL1=TOL/FAC
      FAC=DOT(MR,A(JJ),A(JJ))
      IF (FAC.GT.TOL1) GO TO 70
      DO 55 I=JJ,JMH
      A(I)=0.
      S(J)=0.
      KK=1
      DO 55 K=1,JMH
      IF (S(K).EQ.0.) GO TO 55
      TEMP=DOT(K,U(KK),U(JJ))
      CALL VADD(MR,TEMP,A(JJ),A(KK))
      KK=KK+NCOL
      FAC=DOT(J,U(JJ),U(JJ))
      MR=MR-1
      GO TO 75
      S(J)=1.0
      KK=1
      DO 72 K=1,JMH
      IF (S(K).EQ.1.) GO TO 72
      TEMP=DOT(MR,A(JJ),A(KK))
      CALL VADD(K,TEMP,U(JJ),U(KK))
      KK=KK+NCOL
      FAC=1./SORT(FAC)
      DO 80 I=JJ,JMH
      A(I)=A(I)*FAC
      DO 85 I=JJ,JCH
      U(I)=U(I)*FAC
85

```

100	JJ=JJ*NCOL	100	FAC=DOT(J,U(JJ),U(JJ))
110	IF (MR.EQ.NR.OR.MR.EQ.NC) GO TO 120	70	MR=MR-1
120	FORMAT(13,1HX,12,5H N RANK,12)		GO TO 75
	JJ=1		S(J)=1.0
	DO 125 J=1,NC		KK=1
	DO 126 I=1,NR		DO 72 K=1,NM1
	11=1-J		IF (S(K).EQ.1.) GO TO 72
	S(I)=0.		TEMP=DOT(MR,A(JJ),A(KK))
125	S(I)=S(I)+A(IJ*KK)*U(KK)		CALL VADD(K,TEMP,U(JJ),U(KK))
	11=J		KK=KK+NDA
	DO 130 I=1,NR		FAC=1./SORT(FAC)
	U(IJ)=S(I)		DO 80 I=JJ,JM1
130	11=11+NCOL		A(I)=A(I)*FAC
135	JJ=JJ+NCOL		DO 85 I=JJ,JCH
	RETURN		U(I)=U(I)*FAC
	END		JJ=JJ+NDA
	SUBROUTINE GRINV1(MR,NC,A,U,MR,MT)		IF (MR.EQ.NR.OR.MR.EQ.NC) GO TO 120
	DIMENSION A(1),U(1)		IF (MT.NE.0) WRITE(KOUT,110)MR,NC,NR
	COMMON/MAIN1/ NM1,NDIM,S(1)		FORMAT(13,1HX,12,5H N RANK,12)
	COMMON/MAIN2/ NCOL,NDA1		JJ=1
	COMMON/INOUT/ KOUT		NEND=NC+NDA
	TOL=1.E-12		GO 125 J=1,NC
	MR=NC		DO 125 I=1,NR
	NM1=MR-1		11=1-J
	TOL=1.E-20		S(I)=0.
	JJ=1		DO 125 KK=JJ,NEND NDA
	DO 100 J=1,NC		S(I)=S(I)+A(IJ*KK)*U(KK)
	FAC=DOT(MR,A(JJ),A(JJ))		11=J
	JM1=J-1		DO 130 I=1,NR
	JCH=JJ+JM1		U(IJ)=S(I)
	DO 10 I=JJ,JM1		11=11+NCOL
20	U(I)=0.		JJ=JJ+NCOL
	U(JCH)=1.0		RETURN
	IF (U.EQ.1) GO TO 54		END
	KK=1		SUBROUTINE INTEG(A,C,S,T)
	DO 30 K=1,JM1		S=INTEGRAL EAC-SEA FROM 0 TO T
	IF (S(K).EQ.1.0) GO TO 30		C IS DESTROYED
	TEMP=DOT(MR,A(JJ),A(KK))		DIMENSION A(1),C(1),S(1)
	CALL VADD(K,TEMP,U(JJ),U(KK))		COMMON/MAIN1/ NM1,NDIM,X(1)
	KK=KK+NDA		COMMON/MAIN2/ NCOL,NCOL1
	DO 50 L=1,2		COMMON/MAIN2/ COEF(100)
	KK=1		NM1=N+NCOL
	DO 50 K=1,JM1		NM1=N-1
	IF (S(K).EQ.0.) GO TO 50		IND=0
	TEMP=DOT(MR,A(JJ),A(KK))		ANDRM=XNDRM(N,A)
	CALL VADD(M,TEMP,A(JJ),A(KK))		DT=1
	KK=KK+NDA		IF (ANDRM*ABS(DT).LE.0.5) GO TO 10
	TOL=1./FAC		DT=DT/2.
50	FAC=DOT(MR,A(JJ),A(JJ))		IND=IND+1
54	IF (FAC.GT.TOL) GO TO 70		GO TO 5
55	DO 55 I=JJ,JM1		DO 15 I=1,NM1
	A(I)=0.		J=1+NM1
	S(I)=0.		DO 15 JJ=1,J
	KK=1		S(JJ)=DT*C(JJ)
	DO 55 K=1,JM1		DO 25 IT=1,15
	IF (S(K).EQ.0.) GO TO 55		CALL MAUL(A,C,N,M,N,X)
	TEMP=DOT(K,U(KK),U(JJ))		DO 30 I=1,N
	CALL VADD(M,TEMP,A(JJ),A(KK))		11=11+1
55	KK=KK+NDA		DO 20 JJ=1,NM1
			11=11+1
			C(JJ)=C(JJ)+X(IJ)*T1
			S(JJ)=S(JJ)+C(JJ)
			T1=DT/COEF(IT)
			IF (IND.EQ.0) GO TO 100


```

30 COEF(11)=1.0
   DO 30 I=1,10
   II=11-I
   COEF(11)=DT*COEF(11+1)/FLOAT(11)
   DO 30 I=1,NN,NCOL
   J=I+NM1
   DO 35 JJ=1,J
   X(JJ)=A(JJ)*COEF(11)
   X(11)=X(11)+COEF(11)
40 II=11-NCOL
   DO 35 L=2,11
   CALL MMUL(A,X,N,M,C)
   II=1
   T1=COEF(11)
   DO 35 I=1,NN,NCOL
   J=I+NM1
   DO 50 JJ=1,J
   X(JJ)=C(JJ)
   X(11)=X(11)+T1
50 II=11-NCOL
   C=X*EXP(A*DT)
   L=0
60 L=L+1
   CALL MMUL(X,S,N,M,C)
   II=1
   DO 90 I=1,N
   J=11
   IF (1.EQ.1) GO TO 75
   DO 70 JJ=1,11,NCOL
   S(JJ)=S(JJ)
70 J=J+1
75 DO 85 JJ=1,N
   KK=JJ
   DO 80 K=1,NN,NCOL
   S(JJ)=S(JJ)+C(K)*X(KK)
80 J=J+NCOL
85 J=J+NCOL
   DO 87 JJ=1,NN,NCOL
   C(JJ)=X(JJ)
87 C(JJ)=X(JJ)
90 II=11-NCOL
   IF (1.EQ.IND) GO TO 100
   CALL MMUL(C,C,N,M,X)
   GO TO 80
100 CONTINUE
   RETURN
   END
   SUBROUTINE MEXP(N,A,T,EA)
   DIMENSION A(N),EA(N),C(10),D(11),E(110)
   COMMON/MAINT/NDIM,NDINT,TEN,X(1185)
   NN=N+2
   NP1=N+1
   IF (N.GT.1) GO TO 5
   EA(1)=EXP(T*A(1))
   RETURN
5 N=1.0
   DO 10 I=1,NN,N
   IL=I+NM1
   DO 10 J=1,1L
10 EA(J)=A(J)
   C1=X*NDIM(N,A)
   IND=0
   L=1
   T1=T

```

```

15 IF (ABS(T1-C1).LE.3.0) GO TO 20
   T1=T1/2
   IND=IND+1
   GO TO 15
20 C2=0
   DO 25 I=1,NN,NP1
   C2=C2+EA(1)
25 C2=C2+EA(1)/FLOAT(L)
   C(1)=C2
   D(1)=0.
   II=NM1-L
   E(11)=0
   II=1
   DO 35 I=1,NN,N
   IL=I+NM1
   DO 30 J=1,1L
30 X(JJ)=EA(J)
   X(11)=X(11)+C2
35 II=II+NP1
   IF (1.EQ.N) GO TO 40
   CALL MMUL(X,A,N,M,EA)
   N=NT1/FLOAT(L)
   L=L+1
   GO TO 20
40 CONTINUE
   C***** CAN CHECK X 0 FOR ACCURACY
   J=NM+3
   DO 45 L=N,J
   D(K)=(D(K+1)-W*C(K))*T1/FLOAT(L)
45 E(K)=E(K)+D(K)
80 W=D(1)
   II=1
   DO 60 I=1,NN,N
   IL=I+NM1
   DO 55 J=1,1L
55 EA(J)=E(1)+A(J)
   EA(11)=EA(11)+E(2)
60 II=II+NP1
   IF (N.EQ.2) GO TO 85
   DO 80 L=3,N
   CALL MMUL(EA,A,N,M,N,X)
   II=1
   C3=E(1)
   DO 75 I=1,NN,N
   IL=I+NM1
   DO 70 J=1,1L
70 EA(J)=X(J)
   EA(11)=EA(11)+C2
75 II=II+NP1
80 CONTINUE
85 IF (IND.EQ.0) RETURN
   DO 100 L=1,IND
   IL=I+NM1
   DO 90 J=1,1L
90 X(JJ)=EA(J)
100 CALL MMUL(X,X,N,M,N,EA)
   RETURN
   END
   SUBROUTINE MLINEQ(N,A,C,K,TOL,IER)
   SOLVES A*X+X+C=0
   A AND X CAN BE IN SAME LOCATION
   ANSWER RETURNED IN C AND X
   DIMENSION A(1),C(1),X(1)
   C
   C
   C

```

```

COMMON/MAIN2/P(1)
ADV-TOL=1.E-8
DT=1.0
MM=MMCOL
DO 5 I=1,MM,NCOL
  DT=DT+1.0
  X(J)=C(J)
  RETURN
END
SUBROUTINE AREA(X,Y,M1,M2,M3,Z)
COMMON/MAIN2/NCOL
DIMENSION X(NCOL),Y(NCOL),Z(NCOL)
DO 2 I=1,M2
  DO 3 J=1,M3
    Z=0
    DO 1 K=1,M1
      Z=Z+X(I,K)*Y(K,J)
    1 Z(J)=Z
    2 CONTINUE
  3
END
SUBROUTINE AREA1(X,Y,M1,M2,M3,Z)
REAL X(1),Y(1),Z(1)
COMMON/MAIN2/NCOL
MENDS=NCOL+M3
DO 1 I=1,M1
  DO 1 J=1,MENDS,NCOL
    TM=0
    KK=1
    KK=J-1
    KK=KK+1
    TM=TM+X(K)*Y(NK)
    K=K+NCOL
    IF (K.LE.MENDS) GO TO 5
    Z(J)=TM
    RETURN
  1
END
SUBROUTINE MRIC(N,A,S,Q,M,Z,TOL,IER)
DIMENSION A(1),S(1),Q(1),X(1),Z(1)
COMMON/MAIN2/NCOL,NCOL1
COMMON/MAIN2/TR(1)
ADV-TOL=1.E-8
MM=MMCOL
M1=M-1
M2=1
COUNT=0
IF (IER.EQ.1) COUNT=99
IF (IER.EQ.1) MM=M
IF (IER.EQ.1) GO TO 100
T1=1
CONTINUE
IER=0
COUNT=COUNT+1
DO 15 I=1,M
  DO 15 J=1,MM,NCOL
    Z(J)=S(I)
    CALL INTEGRAL(Z,Z,T1)
    CALL AFACOR(N,Z,Z,MR)
    IER=1
    IF (MR.LT.0) GO TO 200
    IER=0
    CALL GRINV(N,N,X,Z,MR,0)
    CALL TPA(TH,Z,N,M,1,2)
    CALL AREA(Z,TH,N,N,X)
    DO 15 I=1,MM,NCOL

```

```

SUBROUTINE PLOTXYZ,MM,SCALEB,ZETA,IC(1),5,10,MCT,MS,NM,SKIP,B)
INTEGER P
COMPLEX Z(48)
REAL HON(26),VERT(26),ZX(4),ZY(4),XSCALE(26)
DIMENSION IC(12),IS(12),IR(12)
COMMON/VALUES/XPLOT(303),YXPLOT(303),RADIUS(303),MCT,TIME(303)
CHARACTER*30 LAB(16)
LAB(1)='CONTROLLED SYSTEM EIGENVALUES'
LAB(2)='(BEFORE SUPPRESSION)'
LAB(3)='(AFTER SUPPRESSION)'
LAB(4)='REAL AXIS'
LAB(5)='IMAGINARY AXIS'
LAB(6)='ZETA'
LAB(7)='CONTROLLED MODES'
LAB(8)='SUPPRESSED MODES'
LAB(9)='RESIDUAL MODES'
LAB(10)='WEIGHTING'
LAB(11)='TIME, SECONDS'
LAB(12)='RADIUS, METERS'
LAB(13)='XLOS, METERS'
LAB(14)='YLOS, METERS'
LAB(15)='MODE 1 TIME RESPONSE'
K=0
L=0
DO 20 I=1,NM
  X = AIMAG(Z(I))
  IF(X .LT. 0) GO TO 20
  K = K+1
  VERT(K) = X
  HORIK = REAL(Z(I))
  IF(HORIK .GT. 0.) GO TO 20
  L=L+1
  XSCALE(L) = HOR(K)
20 CONTINUE
  WRITE(9, '/')
  WRITE(9, 'EIGENVALUES FOR PLOTTING :')
  WRITE(9, '/')
  DO 40 I=1,K
    40 WRITE(9, 'HOR = ',HOR(I), ' VERT = ',VERT(I))
  C COMPUTE VALUE TO GENERATE ZETA LINE
  C
  MMUM = (ZETA**2)/(14.0**2)
  MMUM = 1 - ZETA**2
  MMUM = SORT(MMUM/DEN)
  C ZX AND ZY ARE THE X & Y COORDINATES OF THE ZETA LINE
  C
  ZX(1) = 0.0
  ZY(1) = 0.0
  ZX(2) = -XC
  ZY(2) = 0.0
  ZY(3) = 14.0
  IF(MMUM.EQ.2) THEN
    CALL PLOT(0,3,5,-3)
    CALL FACTOR(7)
  ELSE
    CALL PLOT(20,0,0,0,-3)
  ENDIF
  IF(P.EQ.8)GO TO 80
  CALL SCALE(XSCALE,8,0,1,1)
  IF(TEST-XSCALE(L+1)/XSCALE(L+2)
  IF(7TEST.LT.8.0) XSCALE(L+1) = -8.0*XSCALE(L+2)
  CALL RECT(-825,-1.725,9.95,10.05,0.0,3)
  CALL RECT(-50,-1.70,9.10,0.0,0.0,3)
  CALL RECT(-125,8.80,1.0,8.225,0.0,3)
  CALL AXIS(0.0,LAB(4),-8.0,0.0,XSCALE(L+1),XSCALE(L+2))
  CALL AXIS(8.0,LAB(5),-14.7,80.0,0.2,1)

```

```

17 DO 17 J=11,NM,NCOL
18 X(J)=X(J)*X(I)/2
19 I=I+1
100 CONTINUE
10 CONTINUE
10 DO 10 I=1,N
  A=SK IS STABLE
  POSSIBLE UNCONTROLLABILITY IF MR.NE.N
  TOL=1-TOL/10.
  MAXIT=40
  DO 40 IT=1,MAXIT
    IF (IER.EQ.1) GO TO 101
    CALL MMUM(S,X,N,N,N,F)
    CALL MMUM(X,F,N,N,N,Z)
    DO 20 I=1,NM,NCOL
      II=I+NM
      DO 20 J=1,11
        X(J)=A(J)-F(J)
        Z(J)=Z(J)+Q(J)
    20 CONTINUE
    IER=0
    CALL MMUM(M,X,Z,X,TOL,IER)
    IF (IER.NE.0) GO TO 300
    L=0
    C1=0.0
    II=1
    DO 25 I=1,N
      IF (ABS(X(I)-TR(I)).LT.(ADV*TOL*X(I))) L=L+1
      TR(I)=X(I)
      II=II+NCOL
      C1=C1+TR(I)
    25 C1=C1+TR(I)
    IF (ABS(C1).GT.1.520) GO TO 80
    IF (I.NE.N) GO TO 40
    CALL MMUM(M,X,Z,F,MR,0)
    CALL MMUM(S,X,N,N,N,Z)
    DO 30 I=1,NM,NCOL
      II=I+NM
      DO 30 J=1,11
        Z(J)=A(J)-Z(J)
    30 CONTINUE
    IF (MR.NE.N) WRITE(KOUT,35)MR
    35 FORMAT(37HORICCATI SOLN IS PSD--RANK,13)
    GO TO 85
    40 CONTINUE
    45 WRITE(KOUT,45) MAXIT
    45 FORMAT(37HORICCATI NON-CONVERGENT IN,12,11H ITERATIONS)
    GO TO 80
    50 WRITE(KOUT,50)IT,T1
    55 FORMAT(30HORICCATI BLOW-UP AT ITERATION,12,12H INITIAL T=,F10.8)
    60 IER=1
    65 RETURN
    200 IF (END.EQ.2) GO TO 250
    IF (COUNT.GE.10.) RETURN
    T1=T1/(2.**COUNT)
    IND=2
    GO TO 300
    250 T1=T1*(2.**COUNT)
    IND=1
    GO TO 300
    END
  C

```

```

C THE FOLLOWING ARRAY ELEMENTS ARE REQUIRED BY THE PLOTTING ROUTINES
C
      ZI(3) = HOR(K+1) * XSCALE(L+1)
      ZI(4) = HOR(K+2) * XSCALE(L+2)
      VERT(K+1) = ZI(3) * 0.
      VERT(K+2) = ZI(4) * 2.
      CALL LINE(HOR, VERT, K, 1, -1, 8)
      CALL DASHLN(ZI, ZI, 2, 1)
      CALL SYMOL(0, 7, 5, 0, 21, LAB(1), 0, 28)
      CALL SYMOL(8, 7, 0, 0, 14, LAB(M), 0, 20)
      CALL PLOTID(LAB, ZETA, SCALES, NC1, IC1, NS, IS, NR, IR)
C THIS SECTION GENERATES THE TIME RESPONSE PLOTS
C
      IF(SKIP EQ, 2) GO TO 80
      CALL PLOT(20, 0, 0, -3)
      DO 80 RECT(1, 0.25, 1, 725, 10, 05, 0, 0, 3)
      CALL RECT(1, 0, 1, 70, 10, 2, 10, 0, 0, 3)
      CALL AXIS(0, 0, 1, LAB(1), 12, 0, 0, 0, 3, 0)
      CALL AXIS(0, 0, 1, LAB(12), 14, 0, 0, 0, 0, 0, 0008)
      TIME(NCT+1) = RADTUS(NCT+1) * 0.0
      RADTUS(NCT+2) = 3 * 0.0008
      CALL LINE(TIME, RADTUS, NCT, 1, 0, 4)
      CALL RECT(3, 8, 80, 1, 0, 4, 0, 3)
      CALL SYMOL(3, 828, 7, 8, 0, 21, LAB(18), 0, 20)
      CALL SYMOL(8, 128, 7, 0, 0, 14, LAB(M), 0, 20)
      CALL PLOTID(LAB, ZETA, SCALES, NC1, IC1, NS, IS, NR, IR)
      80 RETURN
C
      SUBROUTINE PLOTID(LAB, ZETA, SCALES, NC1, IC1, NS, IS, NR, IR)
      DIMENSION IC1(12), IS(12), IR(12)
      CHARACTER*30 LAB(18)
      CALL SYMOL(0, -1, 8, 0, 1, LAB(8), 0, 7)
      CALL NUMBER(898, 0, -1, 8, 0, 1, ZETA, 0, 3)
      CALL SYMOL(2, -1, 8, 0, 1, LAB(10), 0, 12)
      CALL NUMBER(898, 0, -1, 8, 0, 1, SCALES, 0, 1)
      CALL SYMOL(8, -1, 8, 0, 1, LAB(7), 0, 19)
      CALL WHERE(A, B, C)
      DO 80 I=1, NC1
      A=A+.3
      XMODE = IC1(I)
      80 CALL NUMBER(A, 8, 0, 1, XMODE, 0, -1)
      CALL SYMOL(8, -1, 2, 0, 1, LAB(6), 0, 18)
      CALL WHERE(A, B, C)
      DO 80 I=1, NS
      A=A+.3
      XMODE = IS(I)
      80 CALL NUMBER(A, 8, 0, 1, XMODE, 0, -1)
      CALL SYMOL(8, -1, 8, 0, 1, LAB(6), 0, 18)
      CALL WHERE(A, B, C)
      DO 70 I=1, NR
      A=A+.3
      XMODE = IR(I)
      70 CALL NUMBER(A, 8, 0, 1, XMODE, 0, -1)
      RETURN
      END
C
      SUBROUTINE PRINT(MAT, N, M)
      COMMON/MAINB/NCOL
      REAL MAT(NCOL, NCOL)
      INTEGER N, I, J, K, N

```

```

V = Y + NZ(K,1)*2
30 CONTINUE
IF(M(I).EQ.0.0) THEN
  SIG2(I) = RB
  RB = RB - 1
  GO TO 10
ENDIF
C = X*(V/M(I)+2)
SIG2(I) = SORT(C)/(4*ZETA*M(I))
10 CONTINUE
DO 40 I=1,M
  RMODE(I) = 1
40 CONTINUE
DO 50 J=1,(M-1)
  DO 60 J=(J+1),M
    X = SIG2(I)
    Y = SIG2(J)
    IF (Y GT X) THEN
      SIG2(I) = Y
      SIG2(J) = X
    ELSE
      RMODE(J) = 1
    ENDIF
  ENDIF
50 CONTINUE
60 CONTINUE
PRINT('///')
DO 70 I=1,M
  SIG2(I) = SORT(SIG2(I))
  PRINT('SIG=2 =',SIG2(I),' SIG =',SIG(I),' MODE =',RMODE(I))
70 CONTINUE
PRINT('///')
RETURN
END
SUBROUTINE TPR(X,A,M,K,I)
  I = 1
  1 GIVES X = A
  2 GIVES X = A'
  3 GIVES X = A AS A VECTOR
  4 GIVES A = X WHERE X WAS A VECTOR
  DIMENSION X(1),A(1)
  COMMON/MAINB/NCOL
  JS=(K-1)*NCOL+M
  JEND=M*NCOL
  DO 10 I=1,M
    DO 20 JJ=1,JEND,NCOL
      X(JJ)=A(JJ+JS)
      RETURN
    DO 40 II=1,N
      KK=(II-1)*NCOL
      DO 40 JJ=1,M
        LL=(JJ-1)*NCOL+II
        X(KK+JJ)=A(LL+JS)
      RETURN
    DO 60 II=1,JEND,NCOL
      LL=II*N-1
      DO 60 JJ=1,LL
        KK=KK+1
        X(KK)=A(JJ+JS)
      RETURN
    DO 80 II=1,N
      KK=KK+1
      X(KK)=A(JJ+JS)
      RETURN
    DO 80 II=1,N
      KK=KK+1
      X(KK)=A(JJ+JS)
      RETURN
  END

```

```

DO 80 II=1,M
  LL=(M-II)*NCOL+1
  DO 80 IJ=1,N
    KK=KK+1
    JJ=LL+N-IJ
    A(JJ+JS)=X(KK)
  RETURN
END
SUBROUTINE TIME(EAT2,MM,DT,XO,X1,XHAT,EAT)
  COMMON/MAINB/NCOL
  COMMON/INOUT/KOUT
  COMMON/VALUES/SPLOT(303),VPLOT(303),RADIUS(303),NCT,TIME(303)
  REAL A,Z,EAT2(MDA,MDA),EAT(MDA,MDA)
  REAL DT,XO(MDA),X1(MDA),XHAT(2,MDA),XLOS(2)
  A = 0
  Z = DT + 2
  WRITE(9,('(//'))
  WRITE(9,')',TIME,XLOS,RADIUS)
  CALL VMALFF(XHAT,XO,2,MDA,1,2,MDA,XLOS,2,IER)
  RAD=((XLOS(1)+2)+(XLOS(2)+2))*0.5
  WRITE(9,18)A,XLOS(1),XLOS(2),RAD
  FORMAT(2X,1F6.3,3(2X,1F10.8))
  NCT=NCT+1
  VPLOT(1)=XLOS(1)
  VPLOT(2)=XLOS(2)
  IF(RAD.GT.004)RAD=.004
  RADIUS(1)=RAD
  TIME(1)=0.0
  CONTINUE
20 N = 0
20 CONTINUE
CALL VMALFF(EAT2,XO,MM,MM,1,MDA,MDA,X1,MDA,IER)
DO 30 I=1,MM
  XO(I) = X(I)
  N = N + 1
  IF((M*DT).EQ.2) THEN
    A = A + Z
    CALL VMALFF(XHAT,XO,2,MDA,1,2,MDA,XLOS,2,IER)
    RAD=((XLOS(1)+2)+(XLOS(2)+2))*0.5
    WRITE(9,18)A,XLOS(1),XLOS(2),RAD
    NCT=NCT+1
    VPLOT(NCT)=XLOS(1)
    VPLOT(NCT)=XLOS(2)
    IF(RAD.GT.004)RAD=.004
    RADIUS(NCT)=RAD
    TIME(NCT)=A
    IF(A.GT.24.0) GOTO 80
    GOTO 20
  ELSE
    GOTO 30
  ENDIF
CONTINUE
RETURN
END
FUNCTION DOT(MR,A,B)
  DIMENSION A(1),B(1)
  DOT=0
  DO 1 I=1,MR
    DOT=DOT+A(I)*B(I)
  RETURN
END
SUBROUTINE VADD(M,C1,A,B)
  DIMENSION A(1),B(1)
  DO 1 I=1,N
    A(I)=A(I)+C1*B(I)
  1

```

```

C
END
FUNCTION XNORM(N,A)
COMPUTES AN APPROXIMATION TO NORM OF A -- NOT A BOUND
DIMENSION A(N,N)
NM=N*N
NP1=N+1
CI=0.
TR=A(1,1)
IF (N.EQ.1) GO TO 20
I=2
DO 10 II=NP1,NM,N
J=II
DO 5 JJ=J,II,N
CI=CI+ABS(A(J,J)*A(JJ))
J=JJ+1
TR=TR+A(J,J)
I=I+1
TR=TR/FLOAT(N)
DO 10 II=1,NM,NP1
CI=CI+(A(II)-TR)**2
END
XNORM1=ABS(TR)+SQRT(CI)
RETURN
END
FUNCTION XNORM(N,A)
COMPUTES AN APPROXIMATION TO NORM OF A -- NOT A BOUND
DIMENSION A(1)
COMMON/MAINB/NCOL,NCOL1
NM=N*NCOL
CI=0.
TR=A(1)
IF (N.EQ.1) GO TO 20
I=2
DO 10 II=NCOL1,NM,NCOL
J=II
DO 5 JJ=J,II,NCOL
CI=CI+ABS(A(J)*A(JJ))
J=JJ+1
TR=TR+A(J)
I=I+1
TR=TR/FLOAT(N)
DO 10 II=1,NM,NCOL1
CI=CI+(A(II)-TR)**2
END
XNORM1=ABS(TR)+SQRT(CI)
RETURN
END
SUBROUTINE VBAT(CLOS,NC1,NS,NR,NM,XHAT,PETA,CV,V,PHNEW)
COMMON/MAINB/NCOL,NCOL1
REAL CV(2,NCOL),V(NCOL,NCOL),PETA(NDA,NDA)
NMODE=NC1*NS*NR
CALL VMLF(CLOS,PHNEW,2,NMODE,NMODE,2,NCOL,CV,2,IER)
WRITE(6,*) 'THE CLOS * PHNEW PARTITION MATRIX IS '
DO 70 I=1,2
WRITE(6,/(I,12F10.8)/(CV(I,J),J=1,12)
DO 70 J=1,2
WRITE(6,/(I,12F10.8)/(V(I,J),J=1,12)
END
C
C GENERATE THE MATRIX PIETA) TO EXTRACT ETA
C FROM THE FULL STATE VECTOR Z
C
DO 60 I=1,NMODE
DO 60 J=1,NM

```

```

60 PETA(I,J)=0.0
DO 61 I=1,NC1
61 PETA(I,1)=1.0
K=NC1
KK=4*NC1
DO 62 I=1,NS
62 PETA(I*KK,I*KK)=1.0
K=K+NS
KK=KK+2*NS
DO 63 I=1,NR
63 PETA(I*KK,I*KK)=1.0
WRITE(6,*) 'THE MATRIX PIETA) IS '
CALL PMTIL(PETA,NMODE,NM)
DO 66 I=1,NMODE
66 WRITE(6,/(I,12F10.8)/(PETA(I,J),J=1,12)
C
C
DO 67 I=1,NMODE
67 WRITE(6,/(I,12F10.8)/(PETA(I,J),J=1,24)
C
C
DO 68 I=1,NMODE
68 WRITE(6,/(I,12F10.8)/(PETA(I,J),J=25,36)
C
C
DO 69 I=1,NMODE
69 WRITE(6,/(I,12F10.8)/(PETA(I,J),J=37,48)
C
C
CALL VMLF(CV,PETA,2,NMODE,NM,2,NDA,XHAT,2,IER)
DO 70 I=1,NDA
WRITE(6,*) 'XHAT'
70 WRITE(6,/(I,2F10.8)/(XHAT(J,1),J=1,2)
C
C
C XHAT = CLOS * PHNEW * P(ETA)
C
RETURN
END
SUBROUTINE TANGEL(FIEA,N,NACT,PMAG,ANG)
REAL FIEA(N,NACT),ANG(N,N),PMAG(N)
REAL CDOOT,MAGI,CANG
INTEGER I,J,K,N,NACT
C
C COMPUTE MAGNITUDE OF EACH VECTOR
DO 2 I=1,N
MAGI=0.0
DO 1 J=1,NACT
MAGI=MAGI+(FIEA(I,J)**2)
1 CONTINUE
PMAG(I)=MAGI**0.5
2 CONTINUE
C
C COMPUTE DOT PRODUCTS
DO 3 I=1,N
DO 4 J=1,N
CDOOT=0.0
DO 3 K=1,NACT
CDOOT=CDOOT+FIEA(I,K)*FIEA(J,K)
3 CONTINUE
ANG(I,J)=CDOOT
4 CONTINUE
5 CONTINUE
C
C COMPUTE THE ANGLES
DO 7 J=1,N
DO 6 I=1,N
CANG=ANG(I,1)/(PMAG(I)*PMAG(J))
C

```


VITA

Dennis William Varhola is a native of Pennsylvania. He received his Bachelor of Science in Mechanical Engineering from Drexel University in 1971, and worked as a design and development engineer for Ford Motor Company, Dearborn, Michigan, until 1974. He then moved to Portland, Oregon where he pursued an interest in live theatre. He received his commission in January, 1983 from Officer Training School, USAF, and entered the masters degree program in Astronautical Engineering, Air Force Institute of Technology, in June, 1983.

Permanent address: P.O. Box 3524
Portland,
Oregon 97208

UNCLASSIFIED

SECURITY CLASSIFICATION OF THIS PAGE

REPORT DOCUMENTATION PAGE

1a. REPORT SECURITY CLASSIFICATION UNCLASSIFIED		1b. RESTRICTIVE MARKINGS										
2a. SECURITY CLASSIFICATION AUTHORITY		3. DISTRIBUTION/AVAILABILITY OF REPORT Approved for Public Release; Distribution Unlimited.										
2b. DECLASSIFICATION/DOWNGRADING SCHEDULE												
4. PERFORMING ORGANIZATION REPORT NUMBER(S) AFIT/GA/AA/84D-11		5. MONITORING ORGANIZATION REPORT NUMBER(S)										
6a. NAME OF PERFORMING ORGANIZATION School of Engineering	6b. OFFICE SYMBOL (If applicable) AFIT/EN	7a. NAME OF MONITORING ORGANIZATION										
6c. ADDRESS (City, State and ZIP Code) Air Force Institute of Technology Wright-Patterson AFB, Ohio 45433		7b. ADDRESS (City, State and ZIP Code)										
8a. NAME OF FUNDING/SPONSORING ORGANIZATION	8b. OFFICE SYMBOL (If applicable)	9. PROCUREMENT INSTRUMENT IDENTIFICATION NUMBER										
8c. ADDRESS (City, State and ZIP Code)		10. SOURCE OF FUNDING NOS. <table border="1"><tr><td>PROGRAM ELEMENT NO.</td><td>PROJECT NO.</td><td>TASK NO.</td><td>WORK UNIT NO.</td></tr><tr><td></td><td></td><td></td><td></td></tr></table>		PROGRAM ELEMENT NO.	PROJECT NO.	TASK NO.	WORK UNIT NO.					
PROGRAM ELEMENT NO.	PROJECT NO.	TASK NO.	WORK UNIT NO.									
11. TITLE (Include Security Classification) See Box 19												
12. PERSONAL AUTHOR(S) Dennis W. Varhola, 2Lt, USAF												
13a. TYPE OF REPORT MS Thesis	13b. TIME COVERED FROM _____ TO _____	14. DATE OF REPORT (Yr., Mo., Day) 1984 December	15. PAGE COUNT 123									
16. SUPPLEMENTARY NOTATION												
17. COSATI CODES <table border="1"><tr><th>FIELD</th><th>GROUP</th><th>SUB. GR.</th></tr><tr><td>22</td><td>02</td><td></td></tr><tr><td></td><td></td><td></td></tr></table>		FIELD	GROUP	SUB. GR.	22	02					18. SUBJECT TERMS (Continue on reverse if necessary and identify by block number) Flexible Space Structures, Control, Model Reduction, Modal Analysis.	
FIELD	GROUP	SUB. GR.										
22	02											
19. ABSTRACT (Continue on reverse if necessary and identify by block number) Title: MODEL REDUCTION TECHNIQUES APPLIED TO THE CONTROL OF LARGE SPACE STRUCTURES Thesis Advisor: Dr. Robert A. Calico <div style="text-align: right;"><small>RECEIVED BY THE AIR FORCE RESEARCH AND DEVELOPMENT COMMAND AFIT/EN/AA/84D-11 1984 DEC 17 10 11 33 AFIT/EN/AA/84D-11 1984 DEC 17 10 11 33 AFIT/EN/AA/84D-11 1984 DEC 17 10 11 33</small></div>												
20. DISTRIBUTION/AVAILABILITY OF ABSTRACT UNCLASSIFIED/UNLIMITED <input checked="" type="checkbox"/> SAME AS RPT. <input type="checkbox"/> DTIC USERS <input type="checkbox"/>		21. ABSTRACT SECURITY CLASSIFICATION UNCLASSIFIED										
22a. NAME OF RESPONSIBLE INDIVIDUAL Dr. Robert A. Calico	22b. TELEPHONE NUMBER (Include Area Code) 513-255-5533	22c. OFFICE SYMBOL AFIT/ENY										

UNCLASSIFIED

SECURITY CLASSIFICATION OF THIS PAGE

Three model reduction techniques are examined for their applicability to large lightly damped systems. Frequency truncation, modal cost analysis, and approximate internal balancing methods are applied to the CSDL I and II models. Two actuator/sensor configurations are investigated on the CSDL I. Control of the CSDL I model is implemented through the use of steady state optimal regulator theory, and the effect of various reduced order control models on the structure's time response is detailed. Modal cost analysis and internal balancing yield essentially equivalent results for the cases chosen, although the internal balancing technique provides more information concerning actuator/sensor effectiveness. These methods provide more effective reduced order models for higher order systems than simple frequency truncation.

Insert Keywords include:

Page 1 of 2

UNCLASSIFIED

SECURITY CLASSIFICATION OF THIS PAGE

END

FILMED

4-85

DTIC